The role of the core autophagy gene ATG3 in leukemia cell survival and metabolism

Dissertation

zur Erlangung des Doktorgrades

der Naturwissenschaften

vorgelegt beim Fachbereich

Biowissenschaften

der Johann Wolfgang Goethe-Universität

in Frankfurt am Main

von

Fatima Mariam Baker

aus Stuttgart

Frankfurt (2022)

(D 30)

vom Fachbereich Biowissenschaften der
Johann Wolfgang Goethe-Universität als Dissertation angenommen.

Dekan:	Prof. Dr. Sven Klimpel
Gutachter:	Prof. Dr. Heinz D. Osiewacz
	Prof. Dr. med. Christian H. Brandts

Datum der Disputation: 16.12.2022

Most of the data and results, interpretations of data, suggestions and conclusions presented in this dissertation were published in the journal article cited below.

Fatima Baker, Ibrahim H. Polat, Khalil Abou-El-Ardat, Islam Alshamleh, Marlyn Thoelken, Daniel Hymon, Andrea Gubas, Sebastian E. Koschade, Jonas B. Vischedyk, Manuel Kaulich, Harald Schwalbe, Shabnam Shaid*, and Christian H. Brandts* (6 December 2021) '**Metabolic Rewiring Is Essential for AML Cell Survival to Overcome Autophagy Inhibition by Loss of ATG3**', Cancers 13(23):6142. doi: 10.3390/cancers13236142.

* Corresponding authors

Table of Contents

Table of Contents I

1. Introduction 1

1.1. Acute myeloid leukemia 1
1.1.1. Treatment options for acute myeloid leukemia 2

1.2. Autophagy 4
1.2.1. The autophagy machinery 4
1.2.2. Autophagy in cancer 6

1.3. Metabolism in cancer 8
1.3.1. Glycolysis 10
1.3.2. Glutamine and glutathione metabolism 11
1.3.3. TCA cycle and OXPHOS 12
1.3.4. Autophagy and metabolism in cancer 14
1.3.5. ATG3 15

2. Aims of the thesis 18

3. Materials and Methods 19

3.1. Materials 19
3.1.1. Reagents, cell culture media, and kits 19
3.1.2. Antibodies 21
3.1.3. Instruments, incubators, and microscopes 22

3.2. Methods 23
3.2.1. Cell culture 23
3.2.2. CRISPR/Cas9 proliferation screen 23
3.2.3. Generation of stable ATG3 knockdown cells and CRISPR/Cas9-mediated ATG3 knockout cells by lentiviral transduction 25
3.2.4. Cell growth analysis and colony formation assay 25
3.2.5. Flow cytometry measurements of apoptosis, cell cycle, total intracellular ROS, mitochondrial superoxide, mitochondrial membrane potential, and mitochondrial mass 26
3.2.6. Western Blot 27
3.2.7. Autophagy and mitophagy flux measurements 27
3.2.8. Immunofluorescence staining 28
3.2.9. Analysis of mitochondrial activity 28
3.2.10. NMR spectroscopy 29
3.2.11. Colorimetric assays for glucose, glutamine, and lactate production 30
3.2.12. Statistical analysis 31

4. Results 32

4.1. CRISPR/Cas9 dropout screen identifies autophagy genes important for leukemia cell proliferation 32
4.1.1. Certain autophagy genes are important for AML cell survival 32

4.2. Loss of ATG3 impairs proliferation and blocks autophagy in leukemia cells 38
4.2.1. CRISPR/Cas9-meditated loss of ATG3 reduces proliferation and autophagy 38
4.2.2. ATG3 depletion by shRNA impairs proliferation and autophagy 40
4.2.3. Loss of ATG3 increases apoptosis while retaining cell survival 43

4.3. Mitochondrial homeostasis is not altered by loss of ATG3 45
4.3.1. Mitochondrial degradation by mitophagy is not altered in ATG3-depleted cells 46
4.3.2. Mitochondrial membrane potential is not changed upon ATG3 loss 47
4.3.3. ATG3 depletion does not alter mitochondrial mass 48

4.4. Mitochondrial activity is upregulated upon loss of ATG3 49

4.4.1. Loss of ATG3 increases reactive oxygen species 49
4.4.2. Loss of ATG3 increases ATP production by oxidative phosphorylation 52
4.5. Rewiring of the central carbon metabolism in ATG3-deficient AML cells 54
4.5.1. ATG3 depletion increases glucose and glutamine consumption 54
4.5.2. ATG3 depletion alters central carbon metabolism in leukemia cells 54
4.6. ATG3 depletion upregulates the glycolytic pathway in leukemia cells 55
4.6.1. Loss of ATG3 increases glucose uptake and utilization 56
4.6.2. Lactate is retained intracellularly in ATG3-depleted AML cells 57
4.7. ATG3-depleted AML cells depend on OXPHOS for cell survival 60
4.7.1. Loss of ATG3 activates TCA cycle and increases glutathione production 60
4.7.2. ATG3 depletion sensitizes leukemia cells to inhibition of mitochondrial metabolism 62
5. Discussion 64
5.1. The role of autophagy in acute myeloid leukemia 64
5.2. The role of autophagy and ATG3 in mitochondrial homeostasis 66
5.3. Metabolic rewiring in leukemia 68
5.3.1. Alterations of the glycolytic pathway 68
5.3.2. Alterations of mitochondrial metabolism 69
5.3.3. The diversity of metabolic reprogramming in leukemia cells 70
5.4. Mitochondrial dependence of AML cells 71
5.5. Conclusion 72
6. Outlook 74
6.1. Molecular mechanisms of the metabolic alterations upon loss of ATG3 74
6.2. Relation of ATG3's enzymatic activity to the proliferation and metabolic phenotypes in ATG3-depleted AML cells 75
6.3. Causes for apoptosis induction upon loss of ATG3 75
7. Zusammenfassung 77
8. References 83
9. Appendix 95
9.1. Figures 95
9.2. Tables 98
10. Abbreviations 101
11. List of Figures 105
12. List of Tables 107
13. Publications and conferences 108
13.1. Publications 108
13.2. Conferences including talks and poster contributions 108

1. Introduction

1.1. Acute myeloid leukemia

Hematopoiesis is an essential process in the bone marrow in which the various blood cells are continuously formed to replenish the blood system. In the process of normal hematopoiesis, progenitor cells are constantly produced by hematopoietic stem cells (HSCs) using their self-renewal capacity.[1] These progenitor cells proliferate and differentiate into the various blood and immune cell lineages in a hierarchical order.[2,3] Leukemogenesis is initiated by transformation events that allow HSCs to proliferate or myeloid progenitor cells to self-renew resulting in leukemia stem cells (LSCs). The mutations that drive leukemogenesis are diverse, and therefore leukemias are genetically very heterogenous diseases.[4]

Among the different leukemia subtypes, acute myeloid leukemia (AML) has the highest incidence worldwide.[5] The median age of AML patients is 64 years,[6] and develops due to prior cancer therapy, primary hematologic diseases, or predominantly *de novo* in previously healthy individuals.[7] The clinical picture is defined by uncontrolled clonal expansion of undifferentiated progenitor cells leading to an accumulation of immature blasts that are non-functional and impair normal hematopoiesis (**Figure 1**).[8] Consequently, patients suffer from a deficiency of white blood cells (leukopenia), an abnormally low red blood cell count (anemia), and a greatly reduced platelet count (thrombocytopenia), resulting in fatigue, dizziness, weakness, increased susceptibility to infection, and fever.[9]

The World Health Organization classifies AML into the following groups based on clinical features, immunophenotype, cyto- and molecular genetics, and morphology: AML with recurrent genetic abnormalities, therapy-related myeloid neoplasms, AML with myelodysplasia-related changes, AML not otherwise specified, myeloid sarcoma, and myeloid proliferations of Down syndrome.[10] In addition, three prognostic risk groups predictive of response to standard therapy and patient survival are defined based on cytogenetics and molecular subset: favorable, intermediate, and adverse. When analyzing patient survival during 5 years after initial diagnosis or start of treatment, the so-called 5-year overall survival rate is 65% for the favorable risk group. The overall survival at 5 years for intermediate and adverse risk groups is 41% and 11%, respectively.[11]

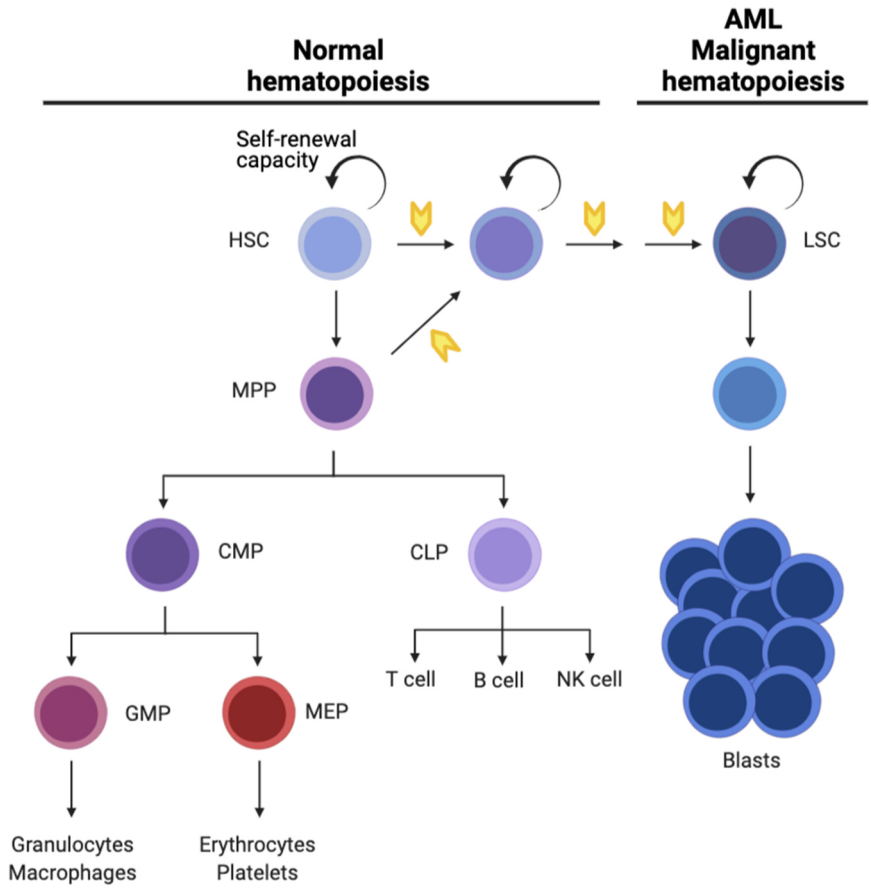

Figure 1. Schematic description of normal and malignant hematopoiesis. In normal hematopoiesis HSCs differentiate into different progenitor cells that subsequently differentiate into the various cell types of the blood. To become an LSC, HSCs or MPPs acquire mutations for unlimited self-renewal capacity and proliferation (yellow arrows). The LSCs give rise to leukemic blasts by mimicking normal hematopoiesis. These blasts cannot terminally differentiate and have lost self-renewal capacity resulting in non-functional blood cells. CLP, common lymphoid progenitor; CMP, common myeloid progenitor; GMP, granulocyte macrophage progenitor; HSC, hematopoietic stem cell; MEP, megakaryocyte erythrocyte progenitor; MPP, multipotent progenitor. Figure was adapted from Chopra and Bohlander, 2019,[4] and created using Biorender.com.

1.1.1. Treatment options for acute myeloid leukemia

As AML is a very fast-progressing disease, newly diagnosed patients have a life expectancy of 3 to 34.7 months and AML accounts for 47% of leukemia-associated deaths.[12,13] Although a cure is achieved in 35-40% of patients by age 60 with chemotherapy, the majority of patients is over 60 years old. In these patients, a maximum cure of 15% is achieved resulting in a poor prognosis for most patients.[14] However, the basic structure of standard chemotherapy remained unchanged for the past 50 years and consists of an initial induction therapy with cytarabine and an anthracycline. Cytarabine, also known as AraC (arabinosylcytosine) is a pyrimidine analog, which is incorporated into the DNA instead of cytidine. Consequently, the DNA replication of fast dividing cells during S-phase of the cell cycle is terminated leading to cancer cell death.[15] Anthracyclines are antibiotics from *Streptomyces* spp. that are known to

inhibit DNA and RNA synthesis, induce ROS generation, and interact with topoisomerase-II, resulting in a blocked DNA repair thereby exerting their antitumor effect.[16] After therapy with cytarabine and an anthracycline, the rates of complete remission (CR), in which no symptoms and clinical markers are detectable, are determined. High CR rates are reported in patients younger than 60 years with up to 85%, but are significantly lower in patients over 60 years, with a maximum of 60%.[14] Furthermore, patients with an adverse risk disease achieve only 40% of CR rate with standard chemotherapy.[17] Importantly, without further treatment, all patients who achieved CR will relapse.[18] Therefore, a post-remission therapy follows initial induction therapy to prevent relapse by applying conventional chemotherapy or hematopoietic stem cell transplantation.[17] Nevertheless, further relapses after post-remission therapy are common in up to 50% of patients resulting in an unmet medical need for new therapeutic options to treat AML.[19]

In recent years, significant progress has been made in the genetic profiling and biological understanding of AML, resulting in the generation of several novel therapies that entered clinical trials or are already approved. These new therapeutic approaches include advanced chemotherapy, cell cycle checkpoint inhibitors, and pro-apoptotic agents like venetoclax, amongst others.[17,20] Furthermore, inhibitors targeting certain common patient mutations, like the driver mutation internal tandem duplication of the FMS-like tyrosine kinase 3 (FLT3-ITD) and mutations of isocitrate dehydrogenase 1 and 2 (IDH), have been developed.[17,20]

Moreover, for targeted therapy, options targeting essential signaling pathways in AML, such as the catabolic degradation pathway, known as autophagy, have been investigated.[21,22] However, in pancreatic cancer cells monotherapy with the autophagy inhibitor hydroxychloroquine (HCQ) showed a poor therapeutic efficacy in clinical trials.[23] But in combination with other therapies, autophagy inhibition achieved encouraging antitumor effects. A combination of the lysosomal inhibitor chloroquine (CQ) and the alkylating agent temozolomide resulted in a partial response or stable disease in around 40% of melanoma patients.[24,25] Furthermore, the treatment of CQ, radiation and temozolomide increased the median survival of glioblastoma patients three times compared to control patients.[25,26] Also, in brain tumors with BRAF(V600E) mutations combining the BRAF inhibitor vemurafenib and CQ synergistically decreased cancer cell survival.[27] Although these initial combination studies were promising, clinical trials have also shown less convincing results.[25] For instance, upon CQ treatment inherent and acquired resistance to inhibition of autophagy were observed, causing further cancer cell growth after the initial clinical benefit from treatment with CQ.[24,28] Thus, the role of autophagy in cancers, including AML, is highly intricate and requires further and a more detailed investigation.

1.2. Autophagy

1.2.1. The autophagy machinery

The catabolic degradation process by which cytosolic components are delivered to lysosomal digestion was named 'autophagy' (Greek for 'self-eating') in 1963 by Christian de Duve.[29] Autophagy is an evolutionary conserved pathway among eukaryotes and is classified into three groups, namely macroautophagy, microautophagy, and chaperone-mediated autophagy, based on the entry mechanism of the cytosolic components (cargos) into the lysosome.[30,31] In microautophagy and chaperone-mediated autophagy the cargos are directly incorporated into lysosomes and degraded afterwards.[30] Macroautophagy (referred to as autophagy hereafter) is defined by the bulk sequestration of non-specific cytosolic material in double-membrane vesicles called autophagosomes, which later fuse with lysosomes to form the autolysosome. The cargos are then degraded in the autolysosome.[32] The intracellular cargos can also be degraded via autophagy in a highly selective way. For selective autophagy, selective autophagy receptors are additionally needed that label the specific cargo for degradation by ubiquitination. Selective autophagy degrades cargos including mitochondria (mitophagy), protein aggregates (aggrephagy), ribosomes (ribophagy), peroxisomes (pexophagy), nucleus (nucleophagy), endoplasmic reticulum (ER-phagy), lipids (lipophagy), and invasive bacteria (xenophagy).[33]

The autophagy machinery is a multistep process, which consists of different phases: initiation, nucleation, elongation, maturation, fusion, and degradation (**Figure 2**).[34] The autophagy process is hierarchically controlled by numerous proteins and protein complexes of autophagy-related genes (ATG). Autophagy induction occurs upon different stress stimuli, like nutrient starvation including amino acids and serum depletion, hypoxia, oxidative stress, mitochondrial damage, protein aggregation, and pathogen invasion.[35] Under nutrient-rich conditions, the mammalian target of rapamycin (mTOR) complex mTORC1, a key regulator of autophagy, phosphorylates ATG13 and ULK1 thereby inhibiting autophagy initiation.[36] The AMP-activated protein kinase (AMPK), an antagonist of mTORC1, is activated upon ATP deprivation and inhibits mTORC1 activity, leading to the stimulation of autophagy induction. In addition, AMPK directly activates various autophagy proteins such as ULK1, Beclin1, and VPS34 by phosphorylation.[37,38] When autophagy is induced, mTORC1 is inactive, and consequently ULK1 activates ATG13 and FIP200. As a result, the ULK1 complex is built (consisting of ATG13, ULK1, ATG101, and FIP200) at the site of autophagosome formation, the phagophore assembly site (PAS), thereby initiating the nucleation process.[39] Upon initiation, ULK1 recruits the PI3K complex with VPS34, VPS15, Beclin1, and ATG14 by phosphorylating Beclin1.[40,41] ULK1 further activates ATG9A, which forms a complex with ATG2, and WIPI2, and this

complex is then recruited to the PAS for ongoing autophagosome formation and engulfment of cytoplasmic material.[42] The next phases of autophagy, namely phagophore elongation and maturation of the autophagosome, are facilitated by two ubiquitin-like ATG conjugating systems, the ATG12-conjugating system and the LC3-conjugating system, which act sequentially.[43,44] The ATG12-conjugating system has similarities to an E1-E2-E3 conjugating system. Firstly, as an E1-like enzyme, ATG7 activates ATG12, which is afterwards transferred to ATG10 (E2-like enzyme), and in a third step conjugated to ATG5. ATG12-ATG5 then forms a complex with ATG16L thereby functioning as an E3-like enzyme in the ligation of LC3 to phosphatidylethanolamine (PE), which also involves the E2-like enzyme ATG3.[33,45] Initially, Pro-LC3 is cleaved by ATG4B to LC3-I, and subsequently lipidation of LC3 catalyzed by ATG7 and ATG3 results in the formation of membrane bound LC3-II.[45] Afterwards, for the formation of an autophagolysosome, the outer membrane of the mature autophagosome immediately fuses with a lysosome.[34] In the final step of the autophagy process the inner membrane of the autophagosome and the cytoplasmic components are decomposed by lysosomal enzymes, including hydrolases, within the autolysosome. The cytoplasmic components are broken down into macromolecules like amino acids, nucleotides, fatty acids, and sugars that can be released into the cytosol via lysosomal transporters.[46]

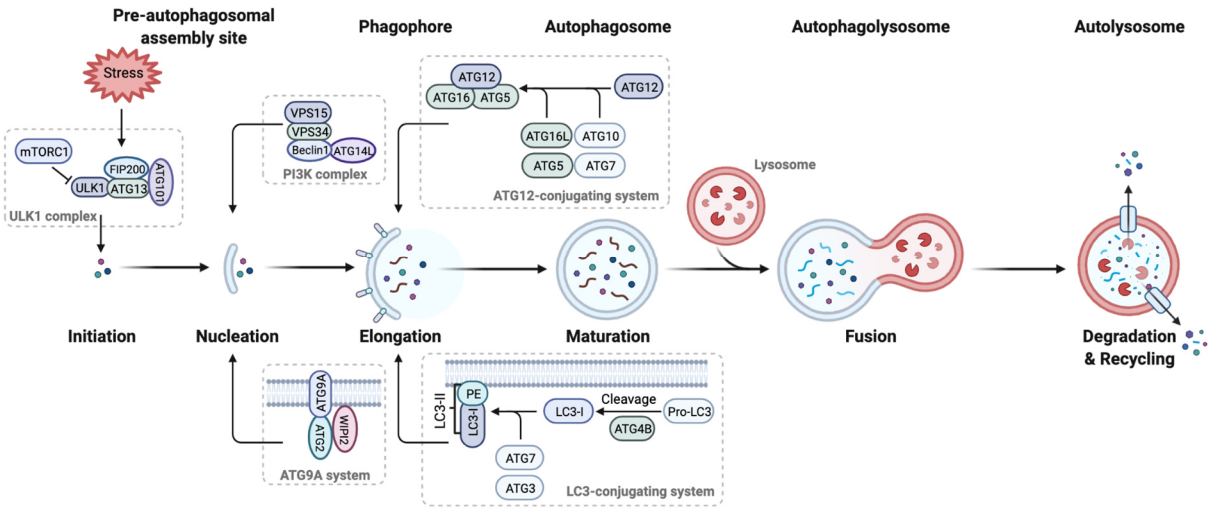

Figure 2. Schematic description of autophagy. Upon autophagy induction by cellular stress (starvation, oxidative stress, protein aggregation, hypoxia, or pathogen invasion) mTORC1 is inactive resulting in the activation of the ULK1 complex at the phagophore assembly site (PAS). ULK1 activates Beclin1 thereby recruiting the PI3K complex to the PAS. Additionally, the ATG9A complex is recruited to the PAS at the nucleation step. For phagophore elongation and maturation the ATG12 and LC3-conjugating systems are required by which LC3 is conjugated to phosphatidylethanolamine (PE) at the membrane of the autophagosome. Afterwards, the mature autophagosome fuses with a lysosome, resulting in an autolysosome in which the cytosolic components are degraded for recycling. Figure was modified from Li, He and Ma, 2020,[34] and created using Biorender.com.

1.2.2. Autophagy in cancer

Autophagy plays an important role in the maintenance of cellular homeostasis and is tightly regulated. Therefore, dysregulation of the autophagy machinery contributes to tumorigenesis (**Figure 3**).[47] Autophagy has a tumor suppressive function and protects healthy cells from malignant transformation and genotoxic stress by removing damaged mitochondria that produce high amounts of reactive oxygen species (ROS), and by preventing DNA damage, amongst others.[47,48] However, in established tumors, it can promote tumor progression and cancer cell survival by sustaining energy levels. Furthermore, autophagy can promote resistance to cancer therapy.[47]

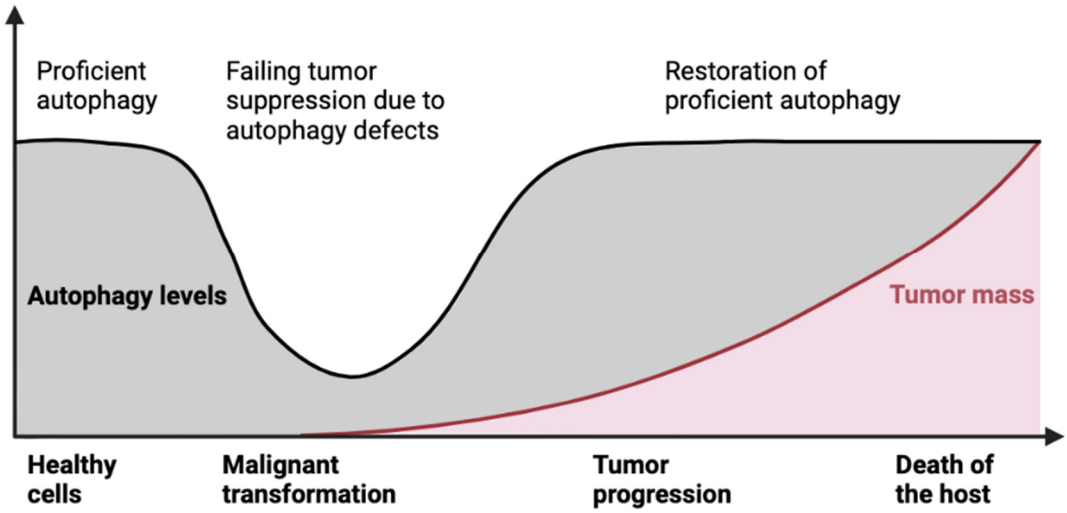

Figure 3. Potential role of autophagy in malignant transformation and tumor progression. A temporary loss of proficient autophagy due to autophagy defects might facilitate malignant transformation of healthy cells. Once malignancy is established, autophagy may support survival and proliferation of tumor cells. Figure was adapted from Galluzzi *et al.*, 2015,[47] and created using Biorender.com.

The tumor suppressive role of autophagy in cancer has been demonstrated by several studies. In the first studies the autophagy gene Beclin1 was identified as a negative regulator of human breast carcinoma growth and cancer cells showed reduced expression of Beclin1 compared to healthy epithelial cells.[49] Also, the development of lymphomas, liver cancer, and lung cancer were observed in mice upon heterozygous loss of Beclin1.[50] Additionally, the core autophagy genes ATG5 and ATG7 play a prominent role in tumorigenesis. For example, it was shown that loss of ATG5 and ATG7 resulted in multiple liver tumors caused by damaged mitochondria and oxidative stress.[51] Similarly, in leukemia, loss of ATG5 and ATG7 supported cell proliferation *in vitro*, which was dependent on glycolytic metabolism, and promoted leukemia progression in an MLL-ENL mouse model.[52] The tumor suppressive role of autophagy is also supported by the fact that primary AML blasts showed reduced expression levels of several

autophagy-related genes involved in autophagosome formation (initiation, nucleation, and elongation) when compared to healthy granulocytes.[53] Interestingly, Rao *et al*. investigated the dual role of autophagy in a $KRas^{G12D}$-driven lung cancer mouse model.[34,48] In this model, knockout of ATG5 resulted in prolonged overall survival of mice due to impaired mitophagy and impaired mitochondrial function. Importantly, at 6 weeks of ATG5 knockout, mice had an increased tumor burden whereas the number of tumors in the lung was significantly reduced after 12 and 18 weeks of knockout, demonstrating increased tumor initiation but reduced tumor progression upon impaired autophagy.[48]

As a tumor-promoting pathway, autophagy contributes to the aggressiveness of more advanced tumors that have to cope with stresses (nutrient deprivation and hypoxia) by maintaining mitochondrial homeostasis and tumor cell metabolism.[25] Several studies showed that pharmacological inhibition of autophagy-related genes significantly reduced tumor growth and increased survival of mice. For example, in pancreatic ductal adenocarcinomas (PDAC) loss of ATG5 and treatment with the autophagy inhibitors CQ or bafilomycin A1 (Baf) resulted in ROS production, DNA damage, and defective energy homeostasis by impaired oxidative phosphorylation leading to reduced tumor growth *in vitro*.[54] Also, PDAC xenograft mice models showed prolonged survival upon CQ treatment.[54] Furthermore, genetic deletion of autophagy-related genes impaired cancer cell proliferation. In a human breast cancer mouse model deletion of FIP200 impaired cancer progression by reduced proliferation and by enhanced immune surveillance.[55] Deletion of ATG5 and ATG7 showed promising results in a melanoma study in which autophagy inhibition by loss of ATG5 or ATG7 led to the depletion of arginine levels in mice, which suppressed tumor growth thereby identifying a metabolic vulnerability of cancer cells.[56] Encouraging data were also found in an MLL-ENL murine leukemia mouse model in which loss of ATG5 and ATG7 impaired clearance of defective mitochondria resulting in increased cell death and elevated oxidative stress in LICs (leukemia-initiating cells) and delayed leukemia progression.[57] In accordance with this, Guo *et al*. found autophagy to be important for maintaining Ras-driven tumor metabolism, especially for mitochondrial homeostasis. Defective autophagy resulted in an accumulation of abnormal mitochondria, impaired oxygen consumption, depleted energy levels, and reduced tricarboxylic acid (TCA) cycle metabolite concentrations upon starvation.[58] Starvation of autophagy-deficient Ras-driven tumor cells was overcome by glutamine or glutamate supply, which fuel the TCA cycle, thereby restoring the nucleotide pools.[59] In addition, ATG7 depletion increased sensitivity of leukemia cells to cytarabine, describing a promoting function of autophagy in therapy resistance.[60] Therefore, autophagy can contribute to the survival of cancer cells and inhibition of autophagy may be a promising therapeutic option for the treatment of AML.

However, cancer cells depend on autophagy in varying degrees, with some being very sensitive to autophagy inhibition resulting in impaired growth, while others are not affected by impaired autophagy. The reasons for driving autophagy dependence are not well studied but for some solid cancers it may be connected to the RAS-RAF-MEK-ERK pathway activation or constitutively active BRAF(V600E) mutations as growth of these cancer types is severely impaired by inhibition of autophagy. Also, p53 status of cancer cells may determine the dependence on autophagy.[25]

Since autophagy-related genes have been associated with different types of cancer, studying the occurrence of mutations in these genes is of particular interest in this context. The analysis of the frequency of somatic point mutations in TCGA datasets revealed that the genes of the core autophagy machinery are rarely affected by these mutations. Only a small number of single-nucleotide mutations with very rare frequency and limitation to cancer type were found in FIP200, ATG4C, ULK4, and ATG7,[61] indicating that the core autophagy machinery is generally not mutated in AML and other tumors.[62,63] Contributing to this conclusion is the observation of a largely invariant gene expression of ATGs, suggesting that the core autophagy machinery may be protected from changes in transcriptional expression.[62] These findings suggest that the autophagy process contributes to the proliferation and maintenance of cancer cells.[63]

1.3. Metabolism in cancer

Cancer cells share certain essential abilities to regulate tumorigenesis, known as the “hallmarks of cancer”. Among those, metabolic reprogramming is emerging as a hallmark of cancer.[64] The metabolic pathways in cancer cells are activated or upregulated to sustain cell survival and promote proliferation by using available nutrients and oxygen to meet energy requirements for biosynthesis, and to maintain redox homeostasis.[65] Therefore, nutrients like carbohydrates, proteins, and fatty acids are either converted into energy and smaller end products such as lactate and CO_2 in the process of catabolism, or these nutrients are used during biosynthesis/ anabolism to build more complex molecules like lipids, polysaccharides, nucleic acids, and proteins (**Figure 4**).[65]

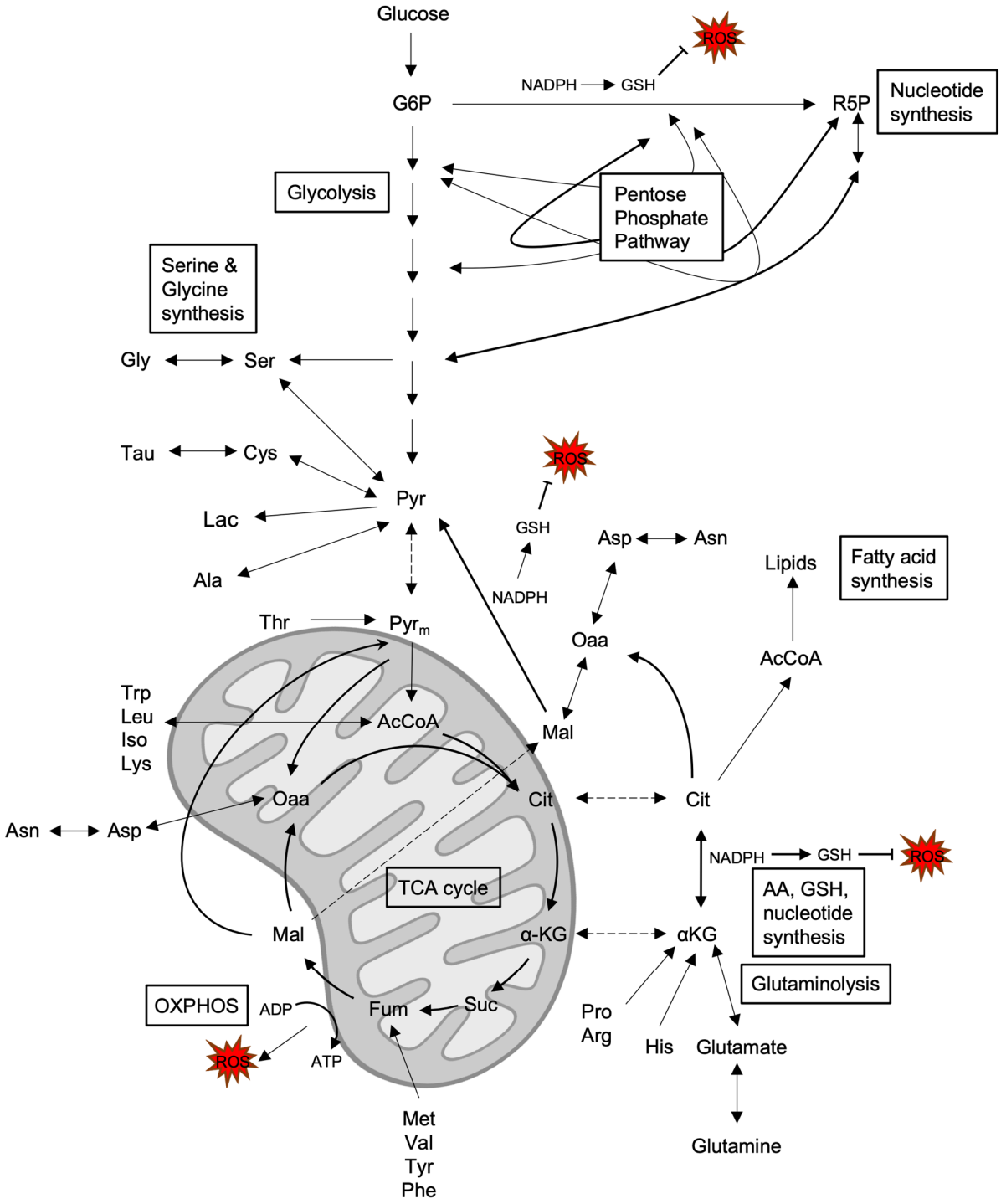

Figure 4. Overview of main metabolic pathways involved in metabolic rewiring. The main metabolic pathways for macromolecule synthesis are depicted here. AA, amino acid; Ac-CoA, acetyl coenzyme A; Ala, alanine; Arg, arginine; Asn, asparagine; Asp, aspartate; Cit, citrate; Cys, cysteine; Fum, fumarate; Gly, glycine; GSH, glutathione; G6P, glucose-6-phosphate; His, Histidine; Iso, Isoleucine; α-KG, α-Ketoglutarate; Lac, lactate; Leu, leucine; Lys, lysine; Mal, malate; Met, methionine; Oaa, oxaloacetate; Phe, phenylalanine; Pro, proline; Pyr, pyruvate; R5P, ribose-5-phosphate; ROS, reactive oxygen species; Ser, serine; Suc, succinate; Tau, taurine; Thr, threonine; Trp, tryptophane; Tyr, tyrosine; Val, valine.

Metabolic rewiring alters the cellular metabolism to satisfy the demands of energy and macromolecules of cancer cells in the form of building blocks and ATP. The most striking changes of metabolism include upregulated glycolysis and glutamine metabolism, increased amino acid and lipid metabolism, enhanced pentose phosphate pathway, increased mitochondrial biogenesis, and macromolecule biosynthesis.[66,67] Similarly, AML cells display a high metabolic plasticity for cellular maintenance by altering their glucose metabolism and mitochondrial metabolism consisting of oxidative phosphorylation (OXPHOS) and the TCA cycle. Furthermore, changes in amino acid metabolism and fatty acid metabolism were linked to AML proliferation.[68]

1.3.1. Glycolysis

AML cells display an increased glucose consumption and a high dependence on glycolysis.[68] During glycolysis, glucose is taken up by cells via glucose transporters (GLUT) and is further decomposed to pyruvate in 10 sequential steps with different enzymes involved.[69,70] One fate of the generated pyruvate is to enter the TCA cycle afterwards and to fuel OXPHOS.[71] Pyruvate can also be converted to lactate by lactate dehydrogenase (LDH) without producing ATP.[69] With an increased production of lactate, glycolytic cancer cells upregulate their lactate export in order to prevent intracellular acidification, which would otherwise result in cell death.[72] Glycolysis is a rapid process with an overexpression of glycolytic genes in more than 70% of cancer;[73] however it is an inefficient energy producing process with a generation of two ATPs per glucose molecule. Additionally, glycolysis supplies building blocks in the form of lipids, nucleotides, and amino acids.[74] Of note, upregulated glycolysis is not unique to cancer cells as non-cancerous cells like murine fibroblasts, human and mouse lymphocytes, thymocytes, as well as chick embryonic cells enhance glycolysis during rapid proliferation.[74]

Interfering with glucose metabolism showed an effective disturbance of cancer cell survival. Prostate cancer cells were shown to overexpress the GLUT1 transporter. Consequently, knockdown of GLUT1 impaired glycolysis and prostate cancer cell survival.[75] Also, transgenic breast cancer models demonstrated that glycolysis inhibition delayed breast cancer growth.[76] Notably, in AML cells, Chen *et al*. observed a distinct glycolytic signature resulting in significant alterations in six different metabolites originating from glucose, among those lactate and pyruvate, which were negatively associated with the overall survival of patients. This glucose metabolism signature was found independently of AML subtypes, suggesting that it may be a consistent characteristic of AML.[68,77] Furthermore, glycolysis inhibition by 2-deoxyglucose (2-DG) was shown to induce apoptosis and cell cycle arrest in different AML cell lines,[78] decreased pancreatic cancer cell survival and sensitized chemotherapy-resistant pancreatic cancer cells to the cytostatic gemcitabine.[79] In summary, since cancer cells increase glycolysis

to achieve an efficient supply of energy, disrupting glycolysis and glucose utilization is a valid anticancer strategy.[80]

1.3.2. Glutamine and glutathione metabolism

As glucose and glutamine are two important carbon sources of cancer cells,[65] glutamine metabolism is also known to be upregulated in cancer. Glutamine has the highest concentration of all amino acids in human plasma. It is either synthesized *de novo* by cancer cells, taken up via glutamine transporters (SLC1A5 and SLC7A5), or recycled after lysosomal degradation. As it contributes to energy production, redox homeostasis, and synthesis of macromolecules, glutamine is firstly converted to glutamate by the enzyme glutaminase (GLS), which is further converted to α-Ketoglutarate (α-KG), known as the process of glutaminolysis. Afterwards, α-KG enters the TCA cycle, or it is utilized as a carbon donor for fatty acid synthesis or for the production of the main ROS scavenger glutathione, amongst others.[68] On the other hand, after several deamination reactions glutamate can be used to produce amino acids and nucleotides, or for the synthesis of glutathione.[81]

Glutathione is used as one essential redox buffering system to maintain ROS homeostasis and control oxidative stress in mitochondria.[82] In general, reactive oxygen species (ROS) are formed as byproducts in different enzymatic reactions and in different cell compartments and organelles or are specifically produced by NADPH oxidases as signaling molecules.[83] Particularly the electron transport chain in mitochondria, which is used to produce ATP, is a major source of ROS.[84] For signaling, ROS are important in normal cellular processes but high ROS levels induce an imbalance, leading to oxidative stress and subsequently to metabolic dysfunction.[83,84]

A study by Gregory *et al*. demonstrated that redox homeostasis by glutathione is critical for AML cell survival, since inhibition of GLS reduced glutathione levels and enhanced mitochondrial superoxide levels accompanied by increased apoptosis in different AML cell lines independently of their FLT3 status. Replenishment of glutathione successfully reduced ROS levels and impaired apoptosis induction in GLS-inhibited AML cells.[85] Other studies have also identified glutamine metabolism as a promising target to impair leukemogenesis.[66,86] Genetic and pharmacological inhibition of glutaminolysis decreased OXPHOS activity thereby impairing AML cell proliferation.[86] Furthermore, glutamine uptake was altered in different cancers. In lung cancer, the glutamine importer SLC1A5 was found to be overexpressed, which regulated the reliance of lung cancer cells on glutamine, and consequently glutamine deprivation resulted in impaired cancer growth.[87] Inhibition of SLC1A5 further induced apoptosis and oxidative stress thereby decreasing tumorigenesis of non-small lung cancer

cells.[88] Moreover in melanoma, glutamine transport was identified as a critical process for cancer progression.[89] Therefore, targeting glutamine metabolism alters ROS homeostasis and metabolism in cancer cells and thus represents an attractive anticancer approach.

1.3.3. TCA cycle and OXPHOS

Although numerous cancers are highly dependent on glycolysis for energy production, inhibition of glucose metabolism is often not sufficient to eliminate cancer cells. In fact, many cancer cells have the ability to switch their metabolism from glycolysis to OXPHOS and to increase their mitochondrial activity by upregulating glutamine entry into the TCA cycle in response to changing environmental conditions.[90] In cells, glucose is broken down to energy and CO_2 in the process of oxidative decarboxylation that occurs in the TCA cycle, also called Krebs cycle or citric acid cycle, within mitochondria. As various substrates can feed the TCA cycle, it is very important in cellular metabolism. In the TCA cycle, acetyl-CoA (consisting of two carbon atoms), originating from pyruvate oxidation, fatty acids, or amino acids, and oxaloacetate (OAA, four carbon atoms) are initially used to form citrate, a six-carbon molecule, which is then converted to isocitrate. Afterwards, during oxidative decarboxylation, α-KG (consisting of five carbons) is generated, which is subsequently converted to succinyl-CoA (four carbons) and releases two CO_2 molecules. Succinyl-CoA is afterwards converted to succinate by which GTP/ ATP is generated. Oxidation of succinate to fumarate by succinate dehydrogenase releases two hydrogen atoms, which are transferred to FAD resulting in $FADH_2$. Subsequently, fumarate is converted into malate and afterwards into OAA, and a new cycle begins. Per cycle three $NADH^+$ molecules and one $FADH_2$ are produced, which transfer their electrons to the electron transport chain (ETC). Therefore, TCA cycle and OXPHOS are directly linked to ensure the generation of energy within mitochondria (**Figure 5**).[91] During OXPHOS, which requires the presence of oxygen, energy is produced in the form of ATP by respiratory enzymes, which oxidize nutrients within mitochondria. The ETC consists of several protein complexes (complex I to IV) in the inner mitochondrial membrane. Electrons are transferred through the protein complexes thereby increasing the reduction potential and creating a proton gradient. $NADH^+$ is re-oxidized at complex I of the ETC, whereas $FADH_2$ is re-oxidized at complex II and the released electrons are then shuffled to coenzyme (CoQ), and subsequently to complex III, cytochrome C, and complex IV. In a last step the electrons are shuffled to O_2 as the final electron acceptor, which results in the production of H_2O. The proton gradient is generated by pumping protons into the inner mitochondrial membrane space. This proton gradient is then used by the ATPase (complex V) to produce ATP (**Figure 5**).[91–93]

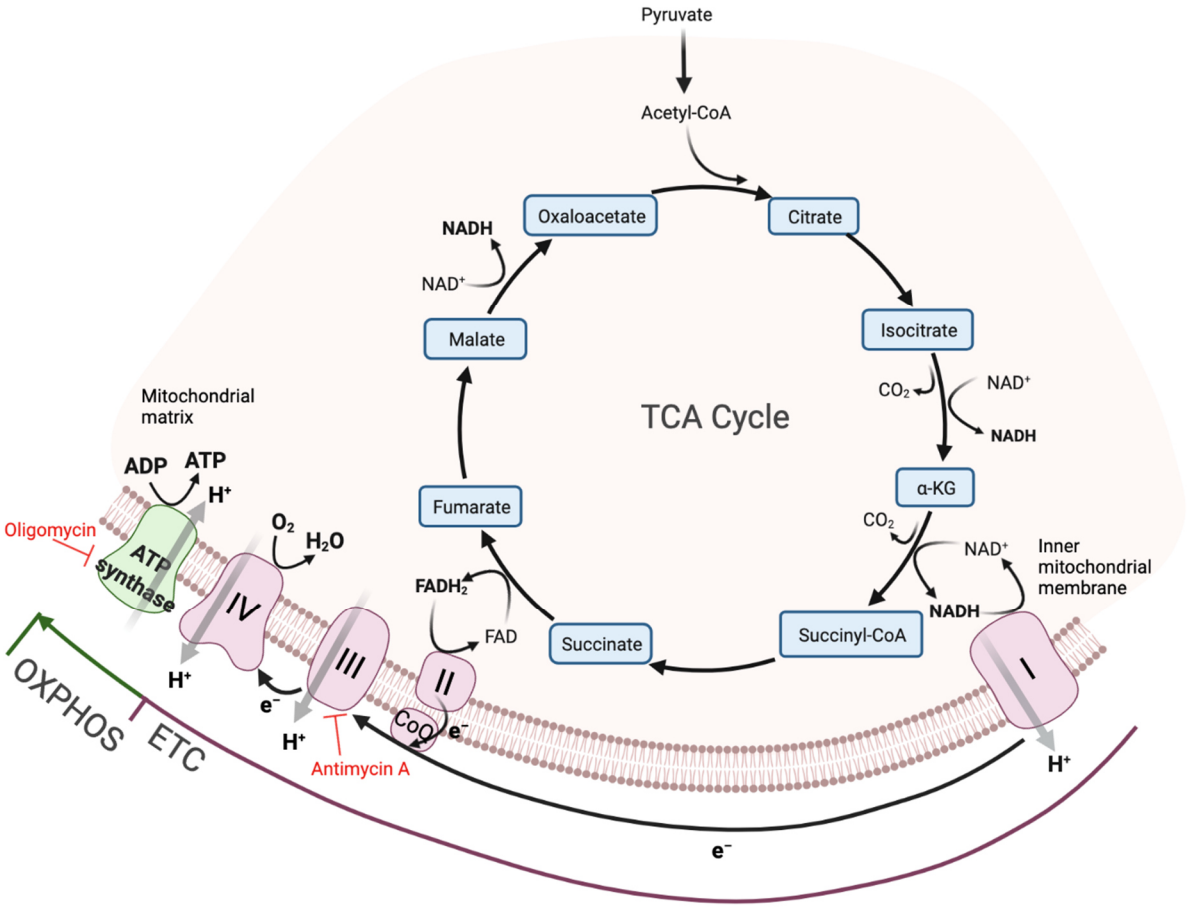

Figure 5. TCA cycle and OXPHOS are directly linked within mitochondria. In the TCA cycle NADH and $FADH_2$ molecules are generated, which are needed for the transfer of electrons (e^-) at the electron transport chain (ETC). The electron transfer through the complexes I-IV of the ETC and proton transport (H^+) generates a membrane potential, which is used for ATP production. The production of ATP further requires O_2 and is therefore called oxidative phosphorylation (OXPHOS). In red: Inhibitors targeting the different complexes of the ETC that are used in this study. α-KG, α-Ketoglutarate. Figure was adapted from Martínez-Reyes and Chandel, 2020,[91] and created using Biorender.com.

Abnormalities in OXPHOS and in certain TCA cycle enzymes were linked to different types of cancer. Primitive CML cells showed higher oxidative phosphorylation compared to normal hematopoietic cells.[94] Furthermore, chemotherapy resistance seems to be generally coupled to increased OXPHOS, as an upregulation of OXPHOS was found in resistant breast cancer, melanoma, and AML cells.[95–97] Also the expression and function of different TCA cycle enzymes were found to be altered in cancer. Citrate synthase, which catalyzes the generation of citrate, is a rate limiting enzyme of the TCA cycle and was shown to be overexpressed in different cancers like pancreatic, renal, and ovarian cancer.[98] Moreover, loss of citrate synthase reduced cell proliferation of ovarian cancer cells *in vitro*.[99] Also, mutations in isocitrate dehydrogenase are frequently found in various cancers including AML. Particularly, mutations in the cytosolic and mitochondrial isoforms of isocitrate dehydrogenase (IDH1 and IDH2) cause the formation of the oncometabolite 2-hydroxyglutarate resulting in changes of the epigenetic

landscape of AML cells.[100] In addition, mutations in the succinate dehydrogenase complex mediating the conversion of succinate to fumarate in the TCA cycle have been associated with hereditary paragangliomas, pheochromocytomas, melanoma, and sarcoma, amongst others. Mutations of succinate dehydrogenase result in an accumulation of succinate and increases ROS levels thereby inducing genomic instability and promoting tumorigenesis.[98,101] Furthermore, the next step of the TCA cycle that converts fumarate to malate can be impaired by mutations in the fumarate hydratase leading to an accumulation of fumarate, which can also function as an oncometabolite and may be involved in the pathogenesis of renal, breast, and bladder cancer.[102] In summary, numerous studies have demonstrated the relevance of mitochondrial metabolism, OXPHOS and the TCA cycle, in the initiation and maintenance of cancer.

1.3.4. Autophagy and metabolism in cancer

Cancer cells benefit from altered autophagy and metabolism, and several studies have underlined the complex relation of autophagy and metabolism in cancer. Glucose deprivation, which results in an impaired synthesis of ATP and a subsequent accumulation of AMP leading to reduced energy levels, activates AMPK. The activation of AMPK further results in the phosphorylation of autophagy genes and autophagy induction.[103] As a master regulator of metabolism, AMPK inhibits mTORC1, which additionally to its role as a negative autophagy regulator controls anabolic pathways.[104] Autophagy induction is further triggered by an accumulation of NAD^+, since NAD is an important substrate of glycolysis, TCA cycle, and OXPHOS amongst others. Also, a depletion of amino acids and reduced cytosolic acetyl-CoA levels activate autophagy, since depletion of acetyl-CoA results in impaired activity of acetyl transferases that regulate proteins of the autophagy process.[104]

Furthermore, lipids are known to induce autophagy through different pathways.[104] Autophagy deficiency by ATG7 loss resulted in an aberrant lipid metabolism caused by a defective mitochondrial fatty acid oxidation in K-Ras driven p53-deficient lung cancer cells.[105] Therefore, autophagy is needed to maintain the pool of functional mitochondria. Depletion of ATG7 further resulted in increased sensitivity towards starvation and glutamine deprivation in lung cancer suggesting that autophagy also provides amino acids to maintain mitochondrial metabolism and survival.[105,106] This is in line with a study by Bhatt *et al*., in which autophagy deficiency by ATG7 deletion altered lipid metabolism and impaired the supply of amino acids to mitochondria resulting in an energy crisis in $Kras^{G12D}$;$Lkb1^{-/-}$ lung cancer.[107] Moreover, it was shown that during starvation recycling of several metabolites was impaired upon autophagy inhibition by ATG7 loss leading to substrate limitations in mitochondrial metabolism.[59]

Glycolysis is known to regulate autophagy as well as inhibition of the glycolytic metabolism by 2-DG induces autophagy.[69] Upon glycolysis inhibition autophagy was increased and rescued the energy crisis by driving OXPHOS in leukemia cells to sustain cell survival.[108] Moreover, Ye *et al*. highlighted the activation of autophagy upon glucose deprivation and suggested a combinatory treatment of glycolysis inhibition and autophagy inhibition for the treatment of lung cancer.[109] Thus, autophagy and metabolism are tightly connected as autophagy is regulated by metabolism and in turn profoundly influences metabolism.[104]

1.3.5. ATG3

ATG3 is one of the more than 40 identified autophagy-related genes and belongs to the core autophagy genes that are needed for autophagosome formation.[110,111] ATG3 functions as an E2-like conjugating enzyme and is crucial for the lipidation of LC3/GABARAP, known as ATG8 proteins, by interacting with the autophagosomal membrane, ATG8, ATG7, and ATG12.[111,112] In detail, after the initial step of LC3 cleavage by ATG4 for LC3 conjugation, LC3 is activated by ATG7 forming an LC3-ATG7 thioester intermediate and is subsequently transferred to ATG3 to form an LC3-ATG3 thioester intermediate. In a last step, LC3 is conjugated to PE by an amide bond between the C-terminal glycine of LC3 and the amino group of PE.[113] This reaction is promoted by the ATG5-ATG12-ATG16L complex.[114] Additionally to the interaction with the autophagosomal membrane, ATG3 increases the local PE concentration to support LC3 conjugation (**Figure 6A**).[113]

By analyzing the crystal structure of ATG3, it was found to be a dynamic protein without a rigid structure. The structure is a hammer with a head region, the core, and a handle region (HR), which is important for binding ATG8 proteins.[115] Between the core and the HR, a flexible region (FR) is inserted and within the FR, the binding sites for ATG12 (RIA 12) and ATG7 (RIA 7) are located, which overlap partially (AA 157-170) (**Figure 6B**).[116,117]

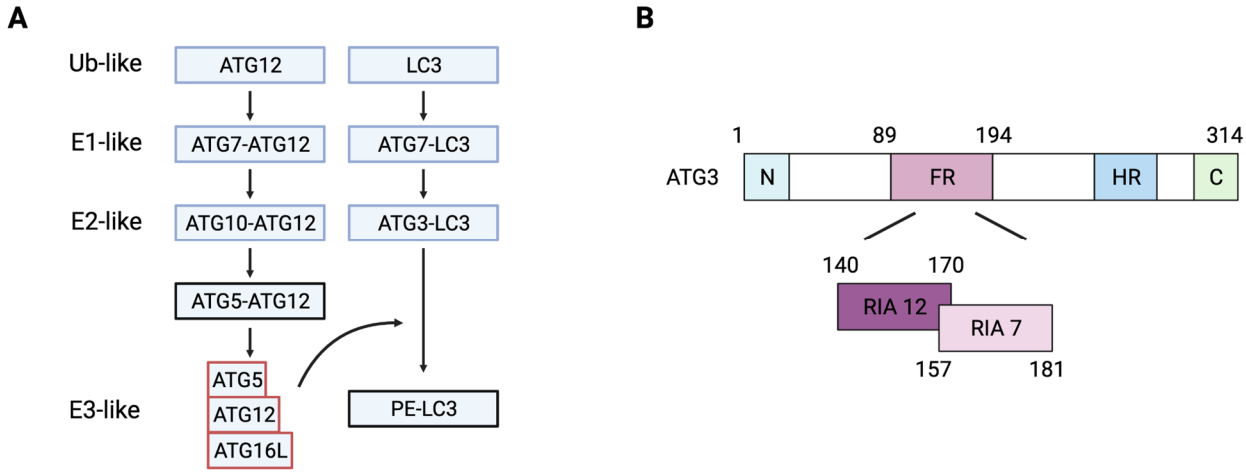

Figure 6. Function and structure of ATG3. (A) The ubiquitin-like system of the LC3-lipidation mechanism is shown. ATG7 plays a role as an E1-like enzyme, ATG3 functions as an E2-like enzyme, and ATG5-ATG12-ATG16L functions as an E3-like enzyme in the conjugation reaction of LC3 with the substrate PE. PE, Phosphatidylethanolamine; Ub, Ubiquitin. Figure was adapted from Shaid *et al*., 2013.[33] (B) Structure of ATG3 is depicted. Numbers describe the amino acid position. C, C-terminus; FR, flexible region; HR, handle region; RIA 7, interaction region with ATG7; RIA 12, interaction region with ATG12; N, N-terminus. Figure was modified from Zheng *et al*., 2019,[114] and created using Biorender.com.

The effects of loss of ATG3 were analyzed in ATG3 knockout mice. Phenotypic analyses of ATG3$^{-/-}$ mice revealed that ATG3 knockout mice die within one day after birth similar to ATG5- and ATG7-deficient mice. In ATG3-deficient mice, ATG8 conjugation was defective as well as autophagosome formation including elongation and maturation of autophagosomes. Furthermore, the formation of the ATG12-ATG5 complex was impaired upon loss of ATG3.[118] The findings from Sou *et al*. suggest that ATG3 not only plays a fundamental role in autophagy but is also important for maintaining cellular homeostasis by supplying amino acids necessary for survival of new-born mice during the neonate starvation period.[118]

Given the crucial role of ATG3 in autophagy, several studies have highlighted the contribution of ATG3 in cancer progression. In CML, loss of ATG3 impaired autophagy and resulted in increased apoptosis of BCR-Abl positive leukemia cells thereby suppressing leukemogenesis.[119] Also, in cervical cancer loss of ATG3-mediated autophagy together with an oncolytic viral infection induced apoptosis.[120] Moreover, higher expression levels of ATG3 were shown to favor cancer cell growth. Upregulated ATG3 expression was linked to cisplatin resistance in non-small cell lung cancer cells,[121] and to the induction of colon cancer cell proliferation and invasion.[122] In addition, the investigation of ATG3 expression in hepatocellular carcinoma revealed upregulated ATG3 levels resulting in a poor prognosis.[123] However, in another study ATG3 was reported as positive prognostic value in gastric cancer and upregulated ATG3 expression favored overall survival of patients.[124] This is in line with a study in myelodysplastic syndrome, a pro-leukemic state, which showed that overexpression

of ATG3 impaired SKM-1 cell growth and increased cell death.[125] These different studies and outcomes of ATG3 loss suggest that ATG3 might have distinct functions at different stages of tumorigenesis and/ or in various tumors.[111]

In a few studies, ATG3 was also linked to autophagy-independent pathways, especially LC3-associated phagocytosis, cell proliferation, and secretion/ exocytosis.[126] Ma *et al*. showed that ATG3 phosphorylation, induced by PTK2 (protein tyrosine kinase 2), is important for maintaining cell viability upon DNA damage in colon cancer.[127] Also, loss of ATG3 impaired cell survival of innate lymphocytes.[128] Furthermore, independently of its autophagy function ATG3 was shown to play a role in LC3-associated phagocytosis, which is induced by phagocytosis of particles via toll-like receptors (TLR) followed by the degradation of engulfed pathogens.[129] In addition, the interaction of ATG12-ATG3 with Alix, a protein involved in endocytosis amongst others, was found to control late endosome distribution and exosome biogenesis which is distinct from ATG3's canonical autophagy function.[130] Therefore, ATG3 may further be involved in other cellular pathways beyond autophagy.

2. Aims of the thesis

Autophagy is an important survival mechanism of leukemia cells that allows recycling of nutrients and degradation of damaged organelles thereby contributing to AML proliferation. Several studies have highlighted the role of autophagy in AML development and maintenance and presented autophagy inhibition as a promising therapeutical approach to treat AML. However, monotherapy with autophagy inhibitors achieved only modest efficacy in clinical trials. One possible explanation for this observation may be the development of mechanisms to compensate for autophagy inhibition in leukemia. To date, little is known about these mechanisms by which autophagy-dependent AML cells can overcome autophagy inhibition.

This work aims to elucidate the role of autophagy and autophagy inhibition in AML cell proliferation and to study the compensatory mechanisms that may arise from autophagy inhibition in AML cells. Firstly, a focused CRISPR/Cas9 proliferation screen was performed to identify a suitable autophagy-related gene to investigate the effects of impaired autophagy. Secondly, by use of shRNA-mediated depletion of the identified autophagy gene ATG3, the function of ATG3 in mitochondrial homeostasis and cellular metabolism was analyzed in two AML cell lines in order to identify potential metabolic vulnerabilities that may arise upon autophagy inhibition.

3. Materials and Methods

3.1. Materials

3.1.1. Reagents, cell culture media, and kits

Reagents, cell culture media, and kits	Manufacturer
7-Aminoactinomycin D (7AAD)	BD Biosciences
Annexin V	BD Biosciences
Bafilomycin A1	Selleck Chemicals
Bovine serum albumin (BSA)	Sigma-Aldrich
BrdU Flow Kit	BD Biosciences
BlockAid solution	Invitrogen
CellTiter-Glo®	Promega
Chloroform	Sigma-Aldrich
Distilled water (DNase/RNase free)	Gibco, Thermo Fisher Scientific
Dialyzed fetal bovine serum (FBS)	Sigma-Aldrich
Deferiprone (DFP)	Sigma-Aldrich
D-Glucose U-$^{13}C_6$	Sigma-Aldrich
DMEM medium	Gibco, Thermo Fisher Scientific
Ethanol	Carl Roth
Ethylenediaminetetraacetic acid (EDTA)	Sigma-Aldrich
Glucose	Sigma-Aldrich
Glutamine	Gibco, Thermo Fisher Scientific
Glycine	Sigma-Aldrich
Image-IT FX Signal Enhancer	Life Technologies
MethoCult M3231	STEMCELL Technologies

MitoProbe JC-1	Thermo Fisher Scientific
MitoSOX™ Red mitochondrial superoxide indicator	Life Technologies
MitoTracker™ Green FM	Cell Signaling
MES SDS Running Buffer (20x)	Life Technologies
Methanol	Sigma-Aldrich
Milk powder	Carl Roth
MiSeq Reagent Kit v3 (150 cycles)	Illumina
NaCl	Sigma-Aldrich
NaF	Sigma-Aldrich
Next High-Fidelity 2x PCR Master Mix	New England Biolabs
NP40	Sigma-Aldrich
PCR Clean-up kit	Macherey-Nagel
Pentra Glucose HK CP	Axonlab
Phosphate buffered saline (PBS)	Gibco, Thermo Fisher Scientific
Penicillin and streptomycin (Pen/Strep)	Sigma-Aldrich
Phenylmethylsulfonylfluoride (PMSF)	Sigma-Aldrich
Polybrene	Sigma-Aldrich
Polyethylenimine (PEI)	Sigma-Aldrich
Proteinase K	Carl Roth
Prolong Diamond Antifade Mountant	Life Technologies
Protease inhibitor cocktail	Roche
Puromycin	Sigma-Aldrich
Pyruvate	Gibco, Thermo Fisher Scientific
RPMI 1640 Medium	Gibco, Thermo Fisher Scientific
Seahorse XF Cell Mito Stress Test Kit	Agilent

Sodium dodecyl sulfate (SDS)	Sigma-Aldrich
Sodium orthovanadate	Sigma-Aldrich
SuperSignal™ West Femto	Thermo Fisher Scientific
SYBR Safe DNA gel stain	Invitrogen
SYTOX Green nucleic acid stain	Thermo Fisher Scientific
Tris	Sigma-Aldrich
Tween ® 20	Applichem
Trypan Blue	Sigma-Aldrich
2-Deoxy-D-glucose (2-DG)	Sigma-Aldrich

Table 1. List of reagents, cell culture media, and kits

3.1.2. Antibodies

Antibodies for Western Blot

Antibodies	Species	Dilution	Type	Manufacturer
Anti-ß-actin	Mouse	1:10000	Primary	Sigma-Aldrich, #A2228
Anti-ATG3	Mouse	1:500	Primary	Santa Cruz, #sc-393660
Anti-Caspase 3	Rabbit	1:1000	Primary	Cell Signaling, #14220
Anti-cleaved Caspase 3	Rabbit	1:1000	Primary	Cell Signaling, #9664
Anti-COXIV	Rabbit	1:1000	Primary	Cell Signaling, #4844
Anti-LC3	Rabbit	1:1000	Primary	Novus Biologicals, #NB100-2220
Anti-PARP	Rabbit	1:1000	Primary	Cell Signaling, #9542
Anti-mouse IgG-HRP	Goat	1:10000	Secondary	Jackson ImmunoResearch, #115-030-003
Anti-rabbit IgG-HRP	Goat	1:10000	Secondary	Jackson ImmunoResearch, #111-036-047

Table 2. List of used antibodies for western blot

Antibodies for immunofluorescence

Antibodies	Species	Dilution	Type	Manufacturer
Anti-LC3	Mouse	1:50	Primary	MBL Life science, #M152-3
Anti-mouse IgG-AF594	Goat	1:300	Secondary	Thermo Fisher Scientific, #A-11005

Table 3. List of used antibodies for immunofluorescence

3.1.3. Instruments, incubators, and microscopes

Instruments, incubators, and microscopes	Manufacturer
BD FACSAria III	BD Biosciences
BD LSRFortessa™	BD Biosciences
BD FACSCelesta™	BD Biosciences
Cell Culture Microplate	Agilent
Cytospin 4 Centrifuge	Thermo Fisher Scientific
Heracell 150i incubator	Thermo Fisher Scientific
Infinite Pro 200	Tecan
Leica TCS SP5 II	Leica Microsystems
Mastercycler pro	Eppendorf
NanoDrop 2000c Specrophotometer	Thermo Fisher Scientific
Odyssey FC imaging system	Li-COR Biosciences
Seahorse XFe96 Extracellular Flux Analyzer	Agilent
XCell SureLock™ Mini-Cell Electrophoresis System	Invitrogen
Biometra Compact S agarose gel electrophoresis	Analytik Jena

Table 4. List of instruments, incubators, and microscopes

3.2. Methods

3.2.1. Cell culture

The human AML cell lines THP-1, MV4-11, Molm13, HL-60, and HEL276 (purchased from Leibniz-Institut DSMZ-Deutsche Sammlung von Mikroorganismen und Zellkulturen GmbH, Braunschweig, Germany) were cultured in RPMI 1640 Medium supplemented with 10% FBS, 2 mM glutamine, and 1% penicillin/streptomycin. HEK293T cells (DSMZ) were cultured in DMEM medium containing 10% FBS, and 1% penicillin/streptomycin. The cell lines were cultured in a humidified Heracell 150i incubator at 37°C with 5% CO_2.[63]

3.2.2. CRISPR/Cas9 proliferation screen

For the proliferation screen a library with 876 guide RNAs against 192 autophagy-related genes including 4% non-targeting controls was used. The sgRNA autophagy library was provided by the Frankfurt CRISPR/Cas Screening Center (FCSC, Dr. Manuel Kaulich and Dr. Ivan Dikic, Goethe University Frankfurt). Virus production was performed by co-transfecting the autophagy library together with the packaging vectors pMD2.G and psPAX2 into HEK293T cells using 4.5 µg/mL Polyethylenimine (PEI). 16 h following transfection, the medium was changed from 10% FBS to DMEM supplemented with 5% FBS, and the produced lentivirus was collected 48 h afterwards by filtering the medium supernatant of the HEK cells. To find the virus concentration (virus titer) resulting in an MOI of ~0.3, stable Cas 9-expressing THP-1 and MV4-11 cells were transduced with the virus of the autophagy-library by spinfection with serial dilutions of the virus. After transduction a first medium change was performed after 24 h, then the medium was changed 24 h later a second time to start selection with 2 µg/mL puromycin. Cells were selected for 3 days, and the percentage of successfully transduced cells was assessed by quantifying the live/dead ratio with flow cytometry. Virus titer was calculated as followed: virus titer [TU/mL] = $\frac{\text{number of transduced cells x \% of successfully transduced cells}/100}{\text{volume of virus supernatant [mL]}}$. To determine the number of cells needed for transduction aiming a coverage of 1000 and a transduction efficiency (MOI) of 0.3, the following formula was used: number of needed cells = $\frac{\text{guides x desired coverage}}{\text{transduction efficiecy}} = \frac{876 \text{ x } 100}{0.3} = 2{,}92\text{x}10^6$. Therefore, for transduction around 3x10^6 THP-1 and MV4-11 cells constantly expressing Cas9 were used for each replicate and condition. Cells were incubated with 5 µg/mL polybrene for 30 min and afterwards the virus was added to the cells. Then, spinfection was performed for one hour at 34°C and 1000xg. After a medium change 24 h later, cells were selected with 2 µg/mL puromycin for the whole duration of the screen. Samples were taken on the second day after transduction before starting puromycin selection as

timepoint day 0 and as an endpoint after 34 days counted from day 0. On both days 3-5x10^6 cells were centrifuged by 1000xg, washed with PBS, and cell pellets were frozen at -80°C and stored until isolation of genomic DNA.[63]

To isolate genomic DNA, cells were lysed overnight at 37°C in 1 mL TEX buffer containing 10 mM Tris-HCl pH 7.5, 1 mM EDTA pH 7.9, and 0.5% SDS with the addition of 250 µg/mL proteinase K. For DNA precipitation, 350 µL 5M NaCl was added, vortexed briefly, and incubated at 4°C for 30 min. After a centrifugation step at 12.000xg at 4°C for 30 min the supernatant was mixed with 2 mL ice cold 100% ethanol. After vortexing the samples were incubated for one hour at -80°C. Afterwards, to finish DNA isolation, the samples were centrifuged at 5.000xg at 4°C for 45 min. The supernatant was discarded, and the DNA pellet was washed using 2 mL 70% ice-cold ethanol and centrifugation was repeated. The pellet was air dried, and DNA was dissolved in 200 µL DNase-free water.[63]

For sequencing of the isolated genomic DNA, two PCR reactions were performed. The first PCR was performed to amplify the desired sequences and the second PCR used Illumina specific primers for barcoding. The total amount of genomic DNA that was needed for the first PCR reaction was calculated as follows: amount of genomic DNA = $\frac{\text{number of guides x coverage}}{\text{transduction efficiency}} \text{x } 6.6 \text{ pg DNA} = \frac{876\text{x}1000}{0.3} \text{x } 6.6 \text{ pg DNA} = 19.3$ µg DNA per sample. For the first PCR reaction (PCR1) 45 ng of plasmid DNA as positive control or 2 µg of genomic DNA per PCR reaction was used. The final volume of 50 µL contained 25 µL Next High-Fidelity 2x PCR Master Mix, 2.5 µL of the 10 µM PCR1 forward primers and 2.5 µL of the 10 µM reverse primers. The protocol for the thermal cycler was set as follows: Initial denaturation for 2 min at 98°C followed by 15 cycles of 1) denaturation at 98°C for 2 min, 2) annealing at 60°C for 55 sec, and 3) extension at 72°C for 1 min, and the final extension for 10 min at 72°C. In a second PCR reaction (PCR2) 12.5 µL of PCR1 product were mixed with 25 µL 2x Next High-Fidelity 2x PCR Master Mix, and 2.5 µL of each 10 µM PCR2 forward and reverse primers containing Illumina adaptors and barcodes in a total volume of 50 µL. For PCR2 the protocol for the thermal cycler was set as follows: Initial denaturation at 98°C for 3 sec, then 15 cycles of 1) denaturation at 98°C for 1 min, 2) annealing for 55 sec at 68°C, and 3) extension for 55 sec at 72°C, and the final extension for 10 sec at 72°C. PCR2 products were run on a 2% agarose gel stained with SYBR Safe DNA gel stain at 70 V for 30 min, the PCR product at 660 bp was cut out and purified using the Nucleospin Gel and PCR Clean-up kit.[63]

For genomic DNA sequencing Illumina technology was used. The gel-purified PCR products of the screen samples were diluted according to Illumina guidelines. A final concentration of 2.6 pM in 2.2 mL was set with 15% PhiX control and loaded onto a MiSeq, NextSeq500

sequencer (Illumina) aiming a read counts (500- to 1,000-fold sequencing depth), according to the manufacturer's protocol. Paired end reads sequencing with 75 cycles plus 8 cycles of index reading was performed. MAGeCK with maximum likelihood estimation (version 0.5.9) was used for data analysis. Data of the different samples were normalized to d0.[63]

3.2.3. Generation of stable ATG3 knockdown cells and CRISPR/Cas9-mediated ATG3 knockout cells by lentiviral transduction

To generate ATG3 deficient cells, knockdown of ATG3 was performed by lentiviral transduction using pLKO.1-puro vector with shRNA targeting the 3'UTR of the human endogenous ATG3 (TRCN0000148120, Sigma-Aldrich, sequence: 5'-CCGGGATGTGACCATTGACCATATTCTCGAGAATATGGTCAATGGTCACATCTTTTTTG-3'). For knockdown of ATG5 and ATG7, the pLKO.1-puro vector was used with the shRNAs (TRCN0000330394, Sigma-Aldrich, 5'-CCGGCCTGAACAGAATCATCCTTAACTCGAGTTAAGGATGATTCTGTTCAGGTTTTTG-3'), and (TRCN0000377305, Sigma-Aldrich, CCGGGGCGTGAGACACATCACATTTCTCGAGAAATGTGATGTGTCTCACGCCTTTTTG), respectively. As control, a non-targeting shRNA (SHC002, Sigma-Aldrich, sequence: 5'-CCGGCAACAAGATGAAGAGCACCAACTC-3') was used. For ATG3 knockout, pKLV2.2-h7SKgRNA5(SapI)-hU6-gRNA5-PGKpuroBFP-W vector was used with gRNA against human ATG3 (5'-GTAGATACATATCACAACAC-3'), ATG9A (5'-TCAAGGCCGAGTACAAACGT-3'), ATG12 (5'-CTCCCCAGAAACAACCACCC-3') or a non-human-targeting control (gNHT) (5'-AACTATTTCCTTTTTGTTTA-3') inserted at the hU6gRNA cassette. The production of lentivirus was performed by transfection of HEK293T cells with shRNA-pLKO.1-puro or pKLV2.2-h7SKgRNA5(SapI)-hU6-gRNA5-PGKpuroBFP-W. For transduction, cells were incubated with 5 µg/mL polybrene for 30 min and afterwards lentiviruses were added in a 1:5 ratio. Spinfection was performed for one hour at 34°C and 1000xg. Selection of transduced cells was achieved in the presence of 2 µg/mL puromycin for at least 3 days.[63]

3.2.4. Cell growth analysis and colony formation assay

To analyze cell growth, expansion curves were performed for 7 days. $1x10^4$ cells were seeded in 100 µL growth medium in a 96 well plate on d0. At day 2, 4, and 7 absolute cell numbers were determined by counting and trypan blue exclusion. Fresh growth medium was added at day 2 (350 µL) and day 4 (500 µL) and cells were transferred to a bigger cell culture plate (48 well and 24 well plate).[63] For determining the colony formation capacity, 500 cells were

seeded in 1 mL methylcellulose MethoCult M3231 (STEMCELL Technologies) and colonies were counted after 7 days of incubation.[63]

3.2.5. Flow cytometry measurements of apoptosis, cell cycle, total intracellular ROS, mitochondrial superoxide, mitochondrial membrane potential, and mitochondrial mass

Apoptosis measurement was performed using the apoptotic markers annexin V (APC-conjugated annexin V) and 7AAD. $1x10^5$ cells were washed with PBS and resuspended in annexin V binding buffer (10 mM HEPES, pH 7.4, 140 mM NaCl, 2.5 mM $CaCl_2$). 1 µL of annexin V and 1 µL of 7AAD were added. Cells were shortly vortexed and incubated at room temperature for 15 min in the dark. 200 µL annexin V binding buffer was added, and cells were analyzed by flow cytometry.[63]

For cell cycle analysis $2x10^5$ cells were stained using the APC BrdU Flow Kit according to the manufacturer's instructions and measured by flow cytometry afterwards.[63]

Cellular ROS analysis was performed by staining $2x10^5$ cells with 1 µM Dihydrorhodamine 123 in the dark for 5 min at 37°C in PBS supplemented with 10 mM glucose and 4 mM glutamine. Cells were washed with PBS and measured by flow cytometry.

For analyzing mitochondrial superoxide levels, $1x10^5$ cells were incubated in medium with 5 µM MitoSOX™ Red Mitochondrial Superoxide Indicator at 37°C in the dark for 10 min. Cells were washed with PBS and afterwards measured by flow cytometry.[63]

Mitochondrial mass was determined by staining $1x10^5$ cells with 20 nM MitoTracker™ Green FM for 30 min at 37°C, washed with PBS and afterwards measured by flow cytometry.[63]

Mitochondrial membrane potential was analyzed with the MitoProbe JC-1. $2x10^5$ cells were stained with 2 µM JC-1 for 30 min at 37°C, washed with PBS and analyzed by flow cytometry using BD FACSCelesta.

The flow cytometer BD LSRFortessa was used for all measurements unless stated otherwise. Flow Jo software v10 (BD) was used to analyze the results.

3.2.6. Western Blot

For total protein extraction at least $1x10^6$ cells were lysed in NP40 lysis buffer (150 nM NaCl, 50 nM Tris (pH 7.5-7.8), 5 mM NaF, 0.5% NP40, 1x Protease Inhibitor Cocktail, 9.2 mM sodium orthovanadate, 0.1 mg/mL PMSF) by incubation for 30 minutes on ice. To clear cell lysates samples were centrifuged at 14000xg for 10 minutes at 4°C. Supernatant containing the proteins was mixed with 4x LDS and 10x reducing buffer and boiled at 80°C for 5 min. Proteins were separated by 4-12% Bis-Tris polyacrylamide gel electrophoresis for 2.5 h at 120 V and transferred onto nitrocellulose membranes for 2 h at 30 V. After blocking in 5% non-fat milk, membranes were probed with primary antibodies over night at 4°C shaking. Afterwards, membranes were washed three times with PBS-T for 5 min, incubated with secondary antibodies goat anti-mouse IgG-HRP or goat anti-rabbit IgG-HRP in PBS-T for one hour at room temperature. Membranes were washed again three times with PBS-T for 5 min and subsequently visualized via Odyssey FC imaging system using SuperSignal™ West Femto Maximum Sensitivity Substrate. For quantification densitometry analysis was performed with ImageJ Software (NIH) and signal intensities of all antibodies were normalized to the loading control ß-actin.[63]

3.2.7. Autophagy and mitophagy flux measurements

To measure autophagy and mitophagy flux, reporter cell lines were generated. For autophagy flux, the sequence of the autophagic probe GFP-ratLC3B-RFP was cloned into a pLentiCRISPv2-Hygromycin plasmid and positive clones were determined by sanger sequencing. Afterwards, virus was produced by transfecting HEK293T cells. THP-1 and MV4-11 cells were transduced with virus from pLentiCRISPRv2-GFP-rLC3B-RFP-Hygromycin or pLentiCRISPRv2-mt-mKEIMA (mitophagy flux) by spinfection for 1 hour at 34°C and 1000xg. Autophagy flux reporter cells were selected with 500 µg/mL hygromycin for THP-1 and 400 µg/mL hygromycin for MV4-11 cells for at least three days and the reporter expression was confirmed by flow cytometry. For mitophagy flux, mt-mKEIMA expressing cells positive for both pH4 and pH7 were sorted with BD FACSAria III according to manufacturer's instructions.

Then, $1x10^5$ GFP-rLC3B-RFP or mt-mKEIMA expressing cells were transduced with lentivirus and selected for three days with puromycin. As starvation condition, the autophagy flux reporter cells were incubated in PBS for 4 hours. For autophagy inhibition the cells were treated with 100 nM bafilomycin A1 for 4 hours and autophagy flux was measured afterwards. To inhibit glycolysis cells were incubated with 1 mM 2-deoxy glucose (2-DG) for 24 h and autophagy flux was measured afterwards. To induce mitophagy, transduced mt-mKEIMA expressing cells were treated with 400 µM deferiprone (DFP) for 16 hours or 10 µM oligomycin

plus 10 µM antimycin A (O/A) for 8 hours. GFP, RFP, or pH change of the cells were measured by flow cytometry using the flow cytometer BD LSRFortessa and results were analyzed with FlowJo software (BD).[63]

3.2.8. Immunofluorescence staining

Immunofluorescence staining was performed to analyze autophagosome formation. $1x10^5$ cells transduced with shCtrl or shATG3 were selected for three days with puromycin and were then treated with bafilomycin A1 for 4 hours, centrifuged at 1000xg for 5 min, and resuspended in PBS supplemented with 10% FCS. Cells were attached onto microscope slides by cytospins with 500xg for 10 min. Afterwards, cells were fixed in 4% paraformaldehyde for 15 min, washed with PBS three times for 5 min, and the cell membrane was permeabilized using 0.5% Triton X for 15 min. Then, cells were washed again three times with PBS for 5 min, and Image-iT FX signal enhancer was applied on the slides for 30 min. Afterwards, three washing steps and blocking with BlockAid Blocking solution for 1 h followed. Next, the blocking solution was removed, and primary antibody diluted in blocking solution was applied on the slides and incubated over night at 4°C. Slides were washed three times with PBS for 5 min and secondary antibody was applied for 1 hour at RT in the dark. After washing the slides, nuclear staining was performed by incubating the slides with 1 µM SYTOX Green nucleic acid stain for 8 minutes. Slides were washed 1x with PBS, and cells were mounted in ProLong Diamond Antifade Mountant and dried for at least 3 days at 4°C before confocal microscope images were captured using Leica TCS SP5 II (63x oil immersion objective) and LAS AF Software. Quantification of LC3 punctae was performed using ImageJ. Five z-sections with around 100 cells per replicate and condition were analyzed for LC3 signal intensity per cell after subtraction of SytoxGreen signal and background.[63]

3.2.9. Analysis of mitochondrial activity

For the determination of ATP levels produced per cell, the CellTiter-Glo® Luminescent Cell Viability Assay was performed three days after transduction. $1x10^4$ cells were seeded in 100 µL media in a 96 well plate and incubated at 37° for 72 h. Firstly, cells were counted using trypan Blue and secondly 25 µL CellTiter-Glo reagent was added to each well. After incubation for 10 min at RT, luminescence was measured using Tecan infinite M200 Pro plate reader. To calculate ATP/cell ratio luminescence signal was divided by the cell number in the corresponding well.[63]

Oxygen consumption rate (OCR) and extracellular acidification rate (ECAR) measurements were performed in real time using the Seahorse XFe96 Analyzer. Dulbecco's modified Eagle medium supplemented with 10 mM glucose, 2 mM glutamine, and 1 mM pyruvate was used for OCR, and ECAR was measured in Dulbecco's modified Eagle medium supplemented with 2 mM glutamine. $2x10^5$ cells were washed twice with basal medium, resuspended in the corresponding medium, and transferred in each well of a XF96 Polystyrene Cell Culture Microplate. Cells were incubated at 37°C for 1 h without CO_2 before measurement. OCR was measured in the presence of 2 µM oligomycin, 2 µM carbonyl cyanide 4-(trifluoromethoxy) phenylhydrazone (FCCP), and 2 µM antimycin plus 2 µM rotenone (from the XF Cell Mito Stress Test Kit). ECAR was measured in the presence of 10 mM glucose, 2 µM oligomycin, and 2 µM FCCP.[63]

3.2.10. NMR spectroscopy

Concentrations of different metabolites was measured by NMR spectroscopy. THP-1 and MV4-11 cells were transduced with shRNA against ATG3 or non-targeting control and selected for 4 days using 2 µg/mL puromycin. Cells were set at a density of $0.3x10^6$ cells/mL and for unlabeled NMR spectroscopy measurements $1x10^7$ THP-1 and $1.5x10^7$ MV4-11 cells were harvested after 24 h by centrifugation at 2000xg for 3 min at RT. Cells were then washed with 1 mL PBS and pelleted for 20 sec at 13000xg at 4°C. PBS was removed, 400 µL ice-cold methanol was added and cells were vortexed for 10 sec. Methanol was afterwards transferred to a glass vial, 325 µL ice-cold H_2O was added and 400 µL ice-cold chloroform. The glass vials were strongly vortexed for 40 sec and incubated on ice for 10 min. As a next step, samples were centrifuged at 4500xg for 10 min at RT in a swingout rotor centrifuge. 500 µL of upper polar phase were taken as well as 300 µL of unipolar phase below the protein layer and samples were stored at -80°C. Measurement of samples was performed in the group of Harald Schwalbe by Islam Alshamleh. Cell extracts were dried for 4 h at 4°C in a vacuum dryer and resuspended in 190 µL NMR phosphate buffer containing 100 mM sodium phosphate in 100% D_2O and the reference compound 0.5 mM trimethylsilylpropanoic acid (TMSP), pH 7). Samples were then sonicated for 10 min. The measurement was performed in NMR tubes using a Bruker AV600MHz spectrometer equipped with a nitrogen-cooled triple resonance probe head (5 mm TCI Prodigy, 1H, 13C, 15N Z-GRD). Tuning, matching, and shimming were performed, and for recording a NOESYGPPR1D pulse sequence at 25°C with 512 number of scans, 12 ppm spectral width (SW) and 32K TD was used.[63] Spectral processing was performed with the software NMRLab according to Ludwig *et al*., 2011.[63,131] For metabolite identification the Chenomx profiler software was used as described previously.[63,132] The quantification of metabolites was performed in NMRLab and intensities were normalized according to TMSP peak. The fold change of each metabolite was calculated relative to non-targeting control.[63]

For labeled NMR transduced AML cells were selected for four days and then medium was changed to glucose-free RPMI (10% FCS, 2 mM glutamine, 1% pen/strep) with the addition of 10 mM D-Glucose U-$^{13}C_6$. After 24 h $1x10^7$ THP-1 and $2.4x10^7$ MV4-11 cells were harvested and metabolites were extracted as described above. Measurement of samples was performed in the group of Harald Schwalbe by Islam Alshamleh and Daniel Hymon. The vacuum dried samples were resuspended in 40 µL NMR phosphate buffer, sonicated for 10 min, and loaded in NMR tubes. For measurements a Bruker AV600MHz spectrometer with a nitrogen-cooled triple resonance probe head (1.7 mm TCI MicroCryoProbe) was used. Tuning, matching, and shimming were performed, and for recording a HSQCCTPHPRSP pulse sequence at 25°C with 32 scans, 1428 points in the direct and 1468 points in the indirect dimension was used. For spectral processing the software TopSpin 4.0.2 was used. NMRFAM-Sparky and the Human Metabolome Database were used to identify and assign each metabolite. For intensity normalization the scaling factor in TopSpin was determined. Again, a fold change of the intensities of each metabolite was calculated relative to control samples.[63]

3.2.11. Colorimetric assays for glucose, glutamine, and lactate production

Glucose consumption was quantified using a colorimetric assay by which the decrease in the concentration of extracellular glucose was calculated after measurement of glucose concentration in the initial medium and in medium 72 h after cell cultivation. $1x10^5$ cells were incubated in 1 mL cell culture medium for 72 hours and medium was harvested by centrifugation at 2000xg for 5 min at 25°C. 150 µL of ABX Pentra Glucose HK CP was measured initially using Tecan plate reader Infinite 200 Pro at 340 nm. Afterwards 5 µL of sample medium was added and incubated for 10 min at 37°C before measuring final absorbance at 340 nm. The extracellular glucose concentration was measured by NAD(P)H concentration that changed by the conversion of glucose to glucose-6-phosphate by hexokinase, and conversion of glucose-6-phosphate into D-gluconate-6-phosphate by glucose-6-phosphate-dehydrogenase.[63]

For glutamine consumption firstly a glutaminase reaction was performed. 50 µL of medium was mixed with 50 µL of sodium acetate buffer (0.5 M, pH 4.9), 30 µL of GLS enzyme (1 kU/L), and 120 µL of water. The reaction was incubated for 30 min at 37°C. For determination of glutamine concentration, 160 µL of reagent R (0.5 M glycine, 0.6 M hydrazine, and 2 mM EDTA (pH 9), 3.75 mM ADP, and 6 mM NAD^+) was mixed with 20 µL medium, or glutaminase reaction, and incubated for 5 min at 37°C before measuring initial absorbance at 340 nm. 20 µL of reagent SR1 (1,9 U glutamate dehydrogenase in triethanolamine buffer) was added and samples were incubated for 30 min at 37°C in dark. Final absorbance was measured at 340 nm

to measure the change of NADH during conversion of glutamate to α-ketoglutarate by glutamate dehydrogenase.[63]

To determine lactate concentration the change in NADH concentration was measured from lactate dehydrogenase (LDH) activity. 170 µL of a reagent A solution consisting of 12 mM EDTA, pH 9, 0.2 M hydrazine, and 1.22 mg/mL NAD^+ were mixed with 10 µL of sample medium and incubated for 5 min at 37°C. Afterwards, initial absorbance was measured at 340 nm and 5 µL of reagent B (87.7 U/mL LDH and 2.1 µM $(NH_4)_2SO_4$, pH 6.5) was added. After 30 min incubation at 37°C, 14 µL of H_2O were added and final absorbance of NADH was measured at 340 nm.[63]

3.2.12. Statistical analysis

Each experiment (colony formation assay and NMR analyses excluded) was performed at least 3 times. Data are shown as mean ± standard error of the mean (SEM). Two-tailed paired Student's t-test was performed using GraphPad Prism 9 software. Statistical significance was assumed if a null hypothesis could be rejected when at least $p < 0.05$.[63]

4. Results

4.1. CRISPR/Cas9 dropout screen identifies autophagy genes important for leukemia cell proliferation

To identify a suitable candidate gene to study the role of autophagy inhibition in AML, I established a CRISPR/Cas9 knockout screen and performed it in the AML cell lines THP-1 and MV4-11. For gene knockout the extended single guide RNA (sgRNA) autophagy library was used, which was manufactured and provided by the Frankfurt CRISPR/Cas Screening Center (FCSC) and the group of Manuel Kaulich. This library targets 192 autophagy-related genes and contains autophagy-regulating transcription factors, core autophagy genes, ubiquitin-specific proteases, and autophagy receptors, amongst others.[63,133] It consists of 876 sgRNAs in total by containing four different sgRNAs per gene.[63] As an initial step of the screen, virus was generated by transfecting HEK-293T cells with the obtained autophagy library and stored at -80°C until further use. Afterwards, the virus titer was determined by flow cytometry and the volume of virus was calculated that was needed for the transduction of the AML cells. To guarantee that most cells receive only one copy of sgRNA, a 1000-fold library coverage and a multiplicity of infection (MOI) of ~0.3 for the lentiviral transduction of cells were aimed. The screen was then performed for 34 days after initial transduction and cells were cultivated in RPMI medium supplemented with puromycin with the help of Marlyn Thölken (AG Brandts). Cell samples were harvested 48 hours after transduction as day 0 and again 34 days later for the extraction of genomic DNA (illustrated in **Figure 7A**).[63] Afterwards, I performed the subsequent steps of DNA extraction and PCR reactions with initial support for protocol optimization from Andrea Gubas (group of Ivan Dikic) and Ibrahim Polat (AG Brandts). I isolated genomic DNA by a desalting method using sodium chloride and ethanol for precipitation. Subsequently, in a first PCR reaction a smaller template containing the sgRNA sequences was generated and the resulting PCR product was used in a second PCR reaction with primer sets containing different Illumina adapter sequences, barcodes, and staggers for each sample. After I purified the PCR products, the samples were then sequenced in collaboration with Khalil Abou-El-Ardat from the group of Sebastian Wagner at the University Hospital Frankfurt.

4.1.1. Certain autophagy genes are important for AML cell survival

To identify important dropout genes from the knockout screen a MAGeCK (model-based analysis of genome-wide CRISPR-Cas9 knockout) analysis was performed with the sequencing results of THP-1 and MV4-11 cells by Khalil Abou-El-Ardat (AG Wagner). Around 90% of sgRNAs could be detected in the sequencing analysis (percentage of mapped

reads) (**Table 5**).[63] Except for one sample all sgRNAs were represented with at least one read count (number of sgRNAs with 0 read counts). Furthermore, the sgRNA distribution was equal shown by a very low Gini Index,[63] since a small Gini Index value corresponds to a more equal distribution of read counts (**Table 5**).

Sample	Number of reads mapped to library	Percentage of mapped reads	Number of sgRNAs with 0 read counts	Gini Index
THP-1 d0 replicate 1	860984	92%	0	0.04
THP-1 d0 replicate 2	783130	92%	0	0.04
THP-1 d34 replicate 1	1157560	92%	0	0.05
THP-1 d34 replicate 2	1196487	92%	0	0.05
MV4-11 d0 replicate 1	123882	92%	0	0.06
MV4-11 d0 replicate 2	259081	87%	0	0.05
MV4-11 d34 replicate 1	45239	90%	0	0.12
MV4-11 d34 replicate 2	24760	71%	5	0.16

Table 5. MAGeCK count report of the CRISPR/Cas9 screen results in human AML cell lines. Duplicates of the samples from day 0 and day 34 were analyzed. Gini Index (of the read count distribution) can be used to measure the evenness of read counts and a smaller value corresponds to a more equal distribution of reads.

For the analysis of the results, all genes were ranked according to the smallest $\log_2$ fold change and plotted against their $-\log_{10}$ p-value (**Figure 7B**). As expected, the most depleted genes contained several known genes that are essential for cell proliferation in both cell lines (**Figure 7B**, **Table 6**).[63] To analyze the screen results in detail, I applied a significance threshold of $-\log_{10}$ p-value ≥ 2 and a dropout threshold of $\log_2$ fold change ≤ -0.2 to identify significantly depleted genes. I identified 74 significantly depleted genes in THP-1 and 44 genes in MV4-11 cells (**Figure 7C** red quadrant, **Table 6**).[63]

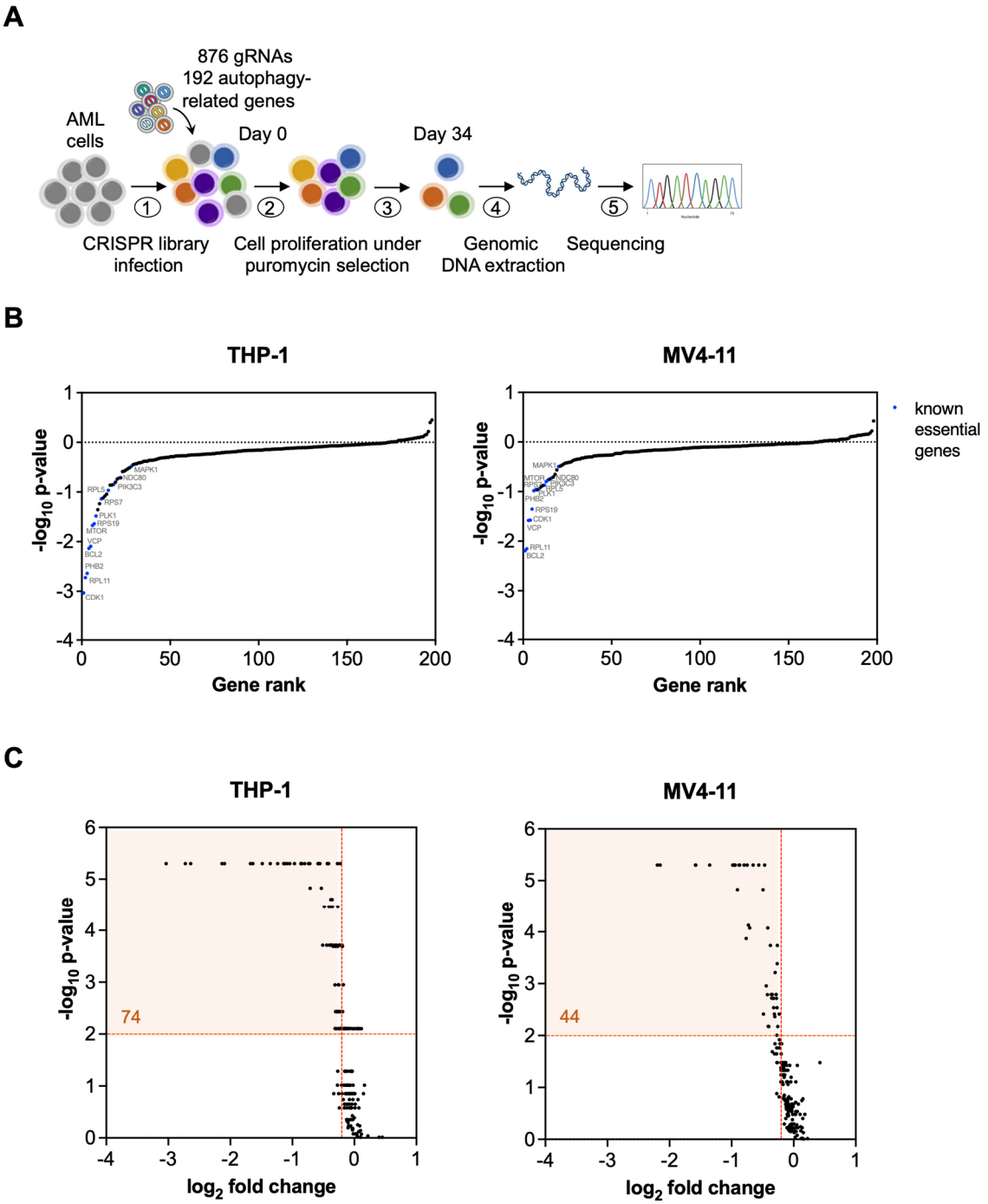

Figure 7. CRISPR/Cas9 dropout screen identifies certain autophagy genes that are important for leukemia cell proliferation. (A) Scheme of the CRISPR/Cas9 proliferation screen using an autophagy library in THP-1 and MV4-11 cells. (B) Gene ranks according to $\log_2$ fold change is plotted against $-\log_{10}$ p-value. Known essential genes are labeled in blue. (C) Scatter plot of all genes from the CRISPR/Cas9 screen. A significance threshold of $-\log_{10}$ p-value ≥ 2 and a dropout threshold of $\log_2$ fold change ≤ -0.2 were applied.[63] Figures (A, C) were modified from Baker *et al.*, 2021.

Cell line	THP-1	MV4-11	Known essential genes
Number of dropout genes	**74**	**44**	**13**
Genes	AMBRA1 ARF6 ATF4 ATG12 ATG16L2 ATG2A ATG3 ATG4C ATG4D ATG9A ATG9B BAG1 BCL2 BNIP3 CAMKK2 CDK1 CREB1 CUL3 CUL4A DDB1 DRAM2 EPG5 HDAC6 HSP90AB1 HSPA8 LGALS3 MAP1LC3A MAPK1 MTOR NDC80 NEDD4 NEDD4L OPTN PARK7 PEX13 PEX3 PHB2 PI4K2A PIK3C3 PINK1 PLK1 PRKAA1 RAB1A RAB24 RAB7A RB1CC1	AMBRA1 ARF6 ATF4 ATG101 ATG12 ATG16L2 ATG3 ATG9A BCL2 CDK1 CUL3 CUL4A DDB1 E2F1 GABARAP HSP90AB1 KEAP1 LAMP1 MAPK1 MTOR NDC80 PEX13 PHB2 PIK3C3 PLK1 RAB24 RAB7A RHEB RPL11 RPL5 RPS19 RPS7 SEC22B SNAPIN SPNS1 STUB1 TMEM41B ULK1 USP15 USP36 USP8 VCP WAC ZFYVE1	BCL2 CDK1 MAPK1 MTOR NDC80 PHB2 PIK3C3 PLK1 RPL11 RPL5 RPS19 RPS7 VCP

	RGS19 RHEB RPL11 RPL5 RPS19 RPS7 RUBCN SAR1A SEC22B SEC62 SNAPIN SPNS1 SREBF2 STUB1 STX8 TBC1D5 TECPR2 TFEB TRIM21 USP10 USP15 USP8 UVRAG VAMP8 VCP WAC WDR45B ZFYVE1		

Table 6. Significant dropout genes in THP-1 and MV4-11 cells from the focused CRISPR/Cas9 screen. A threshold of $-\log_{10}$ p-value ≥ 2 was defined for significance and a threshold of $\log_2$ fold change ≤ -0.2 was set for dropout hits. Known essential genes were defined as critical for cell survival.[63] Table was adapted from Baker *et al*., 2021.

To identify autophagy-related genes that impair AML proliferation, I compared the individual significant dropout hits of both cell lines and identified 23 common depleted genes (**Figure 8A**).[63] To analyze the reliability of the screen results, I compared my screen data with publicly available data from the integrated database of CRISPR Screens (iCSDB).[63,134] This database includes 24 different human leukemia cell lines and 40 performed dropout screens.[63] To standardize the distribution of sgRNAs and compare the screen results, z-scores of my results were calculated according to Li *et al*., 2019,[135] with the help of Jonas Vischedyk (AG Brandts). The comparison of z-scores revealed that 22 of the 23 genes showed similar depletion patterns indicating the reliability of the obtained screen data (**Figure 8B**).[63]

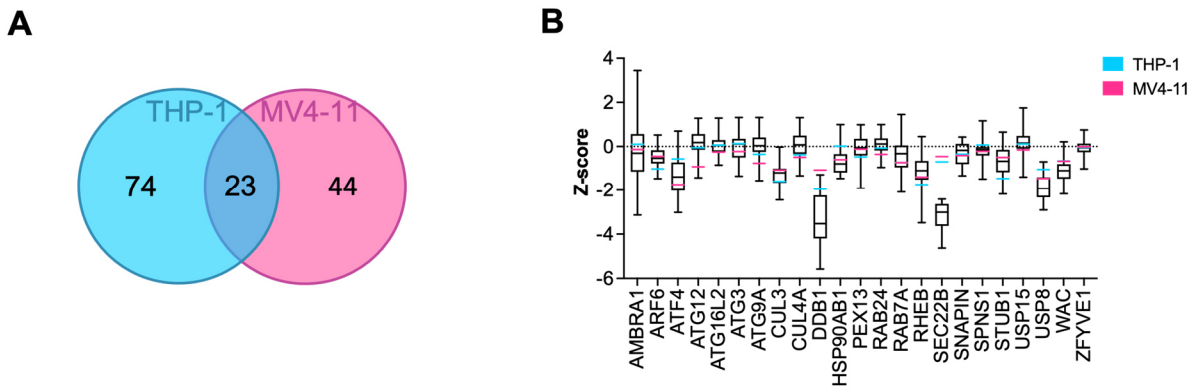

Figure 8. CRISPR/Cas9 proliferation screen identifies 23 common dropout genes in AML cell lines. (A) Venn diagram of significant dropout genes. (B) Z-scores of the common dropout hits of both AML cell lines are depicted in a box-whiskers plot (min–max). The calculated z-scores were compared to 40 CRISPR/Cas9 proliferation screens containing 24 human leukemia cell lines from the integrated database of CRISPR screens (iCSDB).[63,134] Figure (B) was modified from Baker *et al.*, 2021.

As a next step, I compared the fold change of depletion for each gene in both AML cell lines for the 23 common genes (**Figure 9A**, Appendix **Table 7**). The $\log_2$ fold change was similar for around 50% of the dropout hits ($\log_2$ fold change ± 0.15) in both cell lines (Appendix **Table 7**). The significance of the dropout hits in THP-1 and MV4-11 cells however differed for most genes (Appendix **Table 8**). I further assigned the function to each of the 23 hits (**Figure 9B**, Appendix **Table 9**). Among them were mainly core autophagy genes, E3-ligases involved in protein ubiquitination, and GTPases. The core autophagy genes are known to have a very low frequency of somatic single-nucleotide mutations in various cancers including AML and transcriptome analysis revealed a largely invariant ATG gene expression,[61,62] indicating their importance in cell survival for the majority of human cancers.[63] Therefore, I focused on three identified core autophagy genes in my screen: ATG3, ATG9A, and ATG12 (**Figure 9A, C**).[63,110] Also, the isoform ATG16L2 of the core autophagy gene ATG16L was significantly depleted. However, in contrast to ATG16L1, ATG16L2 functions unlike other genes of the canonical autophagy pathway and was found not to be involved in autophagosome formation thereby limiting the interpretation of its autophagy-related function.[63,136,137] Hence, I did not include ATG16L2 in my further validation experiments.[63]

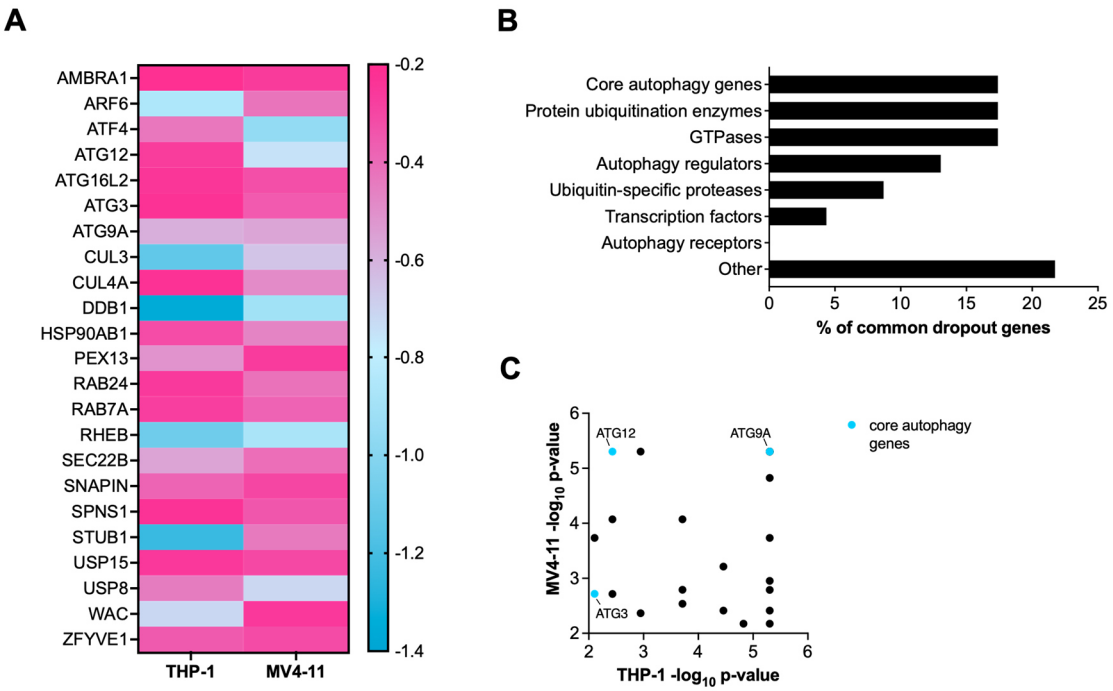

Figure 9. CRISPR/Cas9 proliferation screen identifies core autophagy genes as dropout genes in two AML cell lines. (A) Heat map depicting the scaled $\log_2$ fold change of the 23 common genes in THP-1 and MV4-11. (B) Common genes were assigned to their function and categorized into the indicated groups. (C) Scatter plot of significant genes with $-\log_{10}$ p-value ≥ 2. Chosen core autophagy genes are depicted in blue.[63] Figures (A, C) were modified from Baker *et al.*, 2021.

4.2. Loss of ATG3 impairs proliferation and blocks autophagy in leukemia cells

4.2.1. CRISPR/Cas9-meditated loss of ATG3 reduces proliferation and autophagy

To determine the impact of the three identified ATG genes on AML cell proliferation I created a CRISPR/Cas9-mediated knockout of ATG3, ATG9A, and ATG12 (gATG3, gATG9A, gATG12) in THP-1 and MV4-11 cells and analyzed cell growth for 7 consecutive days supported by Ibrahim Polat and Marlyn Thölken (AG Brandts) (**Figure 10**). In THP-1 cells all three gene knockouts impaired cell proliferation compared to cells transduced with a gRNA that does not target any human gene (gNHT), but ATG3 had the strongest effect. Interestingly, in MV4-11 cells only ATG3 showed significantly reduced proliferation among the three genes.

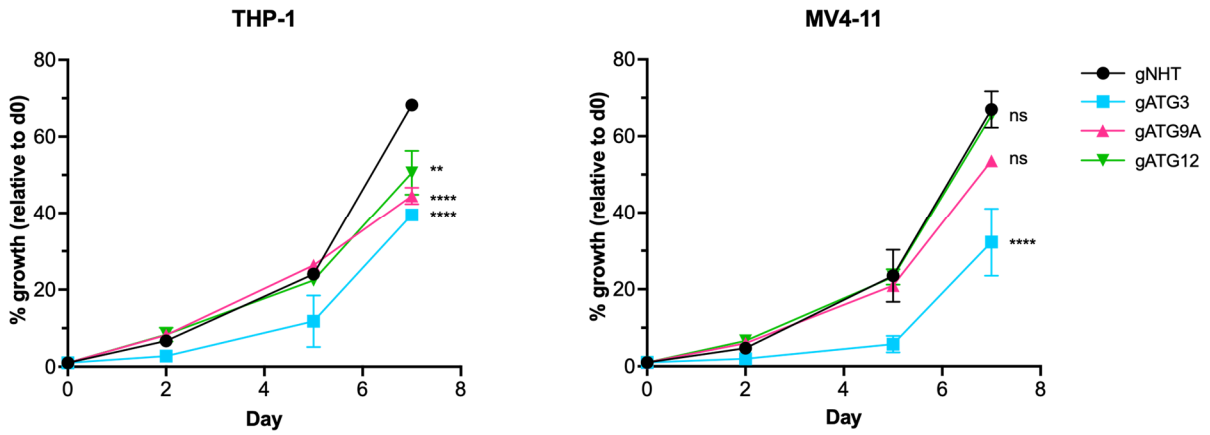

Figure 10. CRISPR/Cas9-mediated loss of the core autophagy genes ATG3, ATG9A, and ATG12 impairs AML cell growth. Growth analysis of CRISPR/Cas9-mediated deletion of ATG3, ATG9A, and ATG12 for 7 days in THP-1 and MV4-11 cells. 1x10^5 cells were seeded in a 96 well plate and cell number was determined microscopically using trypan blue exclusion on the indicated days. Medium was changed after every counting. Student's t-test was performed. ns, not significant, **p < 0.01, ****p < 0.0001.

To further validate the screen results, autophagy function was determined upon loss of ATG3, ATG9A, and ATG12 by using cell lines expressing the GFP-rLC3B-RFP fluorescent probe, which was firstly described by Kaizuka *et al*. (**Figure 11A**).[63] This autophagy reporter allows the quantitative measurement of autophagy flux. ATG4B cleaves the GFP-rLC3B-RFP construct, which results in equimolar levels of GFP-rLC3B and of RFP. As a control, RFP remains in the cytoplasma, and LC3B fused to GFP is inserted into the autophagosomal membrane and degraded after fusion with lysosomes resulting in quenching of the GFP signal. Thus, autophagic activity correlates with the inverse ratio of GFP/RFP signal.[63,138] In order to generate cells permanently expressing this autophagy reporter, I cloned the original GFP-rLC3B-RFP sequence into a pLenti-CRISPRv2-hygromycin plasmid to stably transduce cells by lentiviral infection. After transduction, cells were selected with puromycin for three days and autophagy flux was determined afterwards. Notably, in THP-1 cells ATG3 and ATG9A deletion showed a similar strong block in autophagy flux, whereas loss of ATG12 resulted in a moderate inhibition. In MV4-11 cells however, ATG3 showed the strongest autophagy block among the 3 analyzed genes (**Figure 11B**).[63] Therefore, I chose ATG3 depletion to study the impact of autophagy inhibition on AML. While the CRISPR/Cas9 system is often used to delete certain genes, off-target effects occur frequently,[139] and the generation of the corresponding cell lines is very time-consuming. Thus, this study used the acute depletion by short hairpin RNA (shRNA) targeting the 3'UTR of endogenous ATG3 as a tool for investigating the alterations that occur upon loss of ATG3.

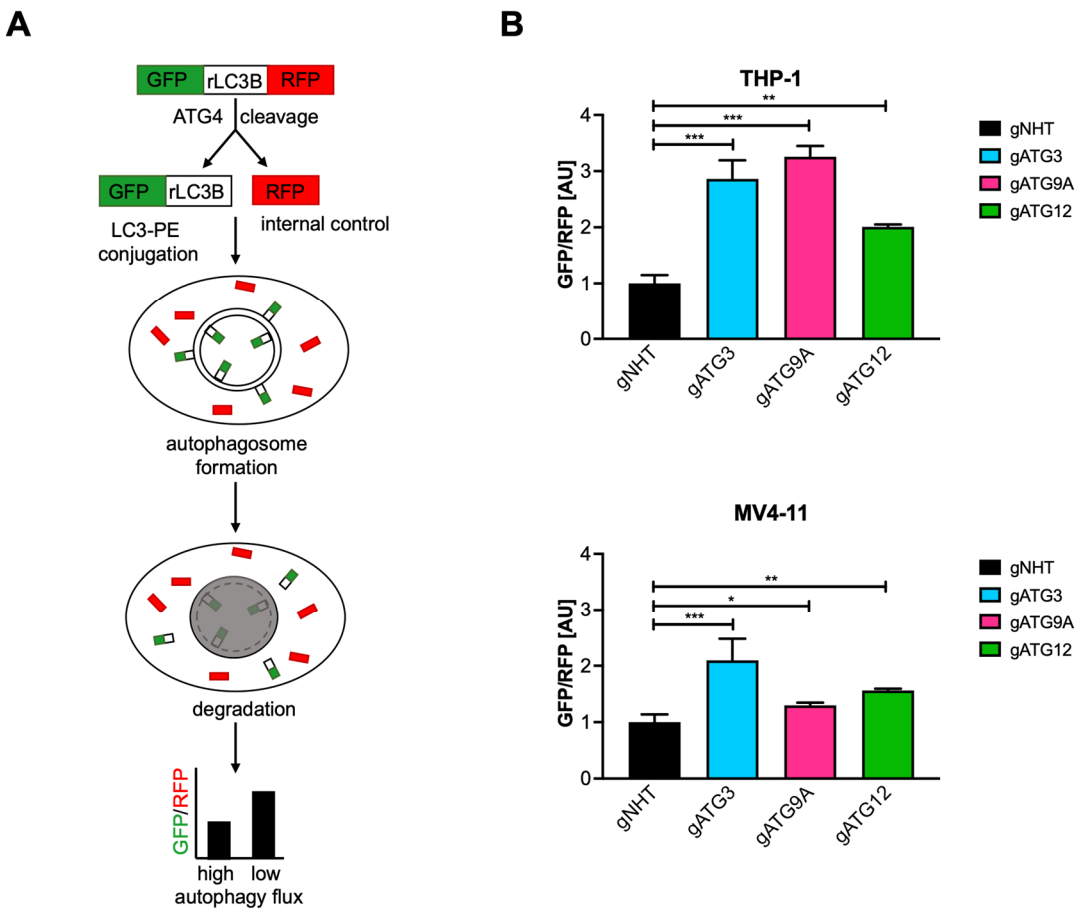

Figure 11. Loss of the core autophagy genes ATG3, ATG9A, and ATG12 impairs autophagy. (A) Scheme describing the principle of the autophagy flux reporter. (B) Autophagy flux was determined in THP-1 and MV4-11 cells expressing the GFP-rLC3B-RFP probe after knockout of ATG3, ATG9A, and ATG12 by CRISPR/Cas9 technology.[63] Figures were modified from Baker *et al.*, 2021. Student's t-test was performed in (B). *p < 0.05, **p < 0.01, ***p < 0.001.

4.2.2. ATG3 depletion by shRNA impairs proliferation and autophagy

Next, to confirm the functional role of ATG3 in proliferation and autophagy of AML cells using shRNA-mediated depletion of ATG3, I firstly transduced five different human AML cell lines, namely Molm13, HEL276, HL-60, THP-1, and MV4-11, with either shRNA targeting ATG3 (shATG3) or a control shRNA (shCtrl) which does not target any human gene. These cell lines were chosen to model the heterogeneity of AML in the best possible way as leukemic cells harbor several driver-mutations.[63] The cell lines MV4-11 and Molm13 harbor FLT3-ITD mutations, which are found in one quarter of AML cases and are linked to poor prognosis as well as frequent relapse,[63,140–142] whereas the other three cell lines are FLT3-wild type.[63,141–143] Additionally, THP-1, HL-60, and HEL cells harbor TP53 mutations, which were linked to poor chemotherapy response and a low overall patient survival.[63,144–146] With the generated sublines proliferation analyses were performed. Importantly, shRNA-mediated ATG3 depletion resulted in a significant growth disadvantage compared to control cells in THP-1 and MV4-11 cells.

In addition, the three other AML cell lines also showed significantly reduced cell proliferation (**Figure 12A**).[63] Western blot analysis confirmed the successful depletion of ATG3 expression in all cell lines (**Figure 12B**).

Additionally, to examine AML cell proliferation in a different way, I determined the colony formation capacity of AML cells upon ATG3 loss. To do so, AML cells transduced with shATG3 or shCtrl were cultured in methylcellulose medium for 7 days and the colonies were counted afterwards. I observed that the colony formation capacity was severely impaired in ATG3-deficient THP-1 and MV4-11 cells (**Figure 12C**). Together, these results indicate that loss of ATG3 impairs proliferation of leukemia cells.[63]

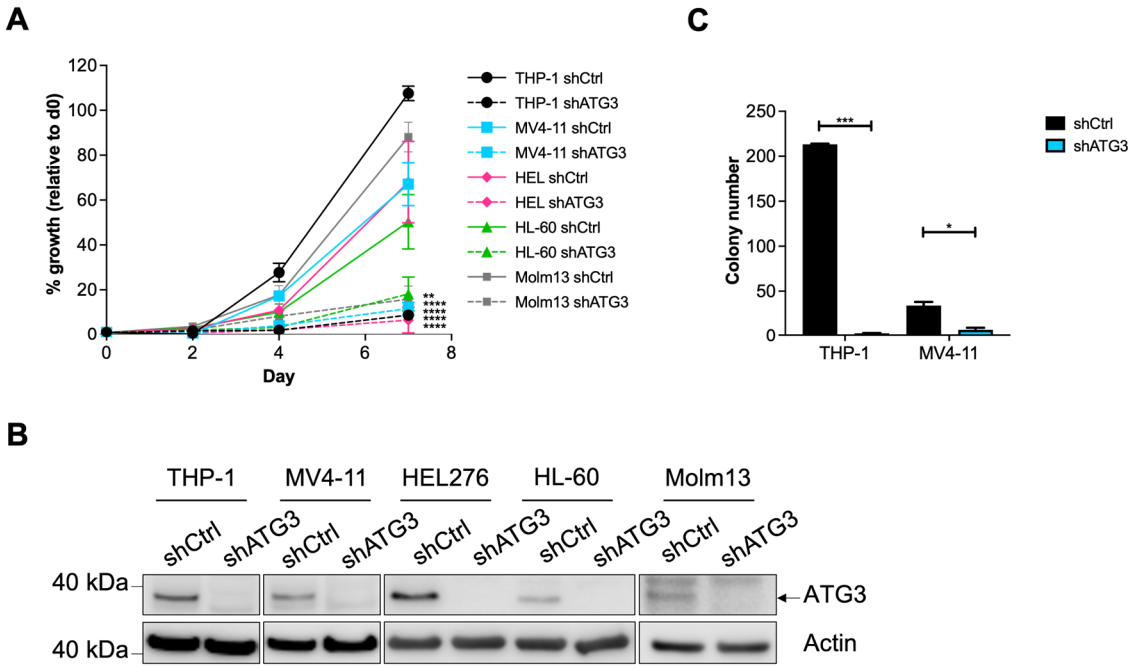

Figure 12. Loss of ATG3 impairs proliferation and colony formation capacity of AML cells. (A) Growth analysis of shRNA-mediated depletion of ATG3 (shATG3) or control (shCtrl) for 7 days. 10.000 cells were seeded in 150 µL medium in a 96 well plate at day 0 and cell number was determined microscopically using trypan blue exclusion on the indicated days. Medium was changed after every counting. Cell numbers are depicted as percentage of each time point normalized to day 0. (B) Western blot of cells harvested at day 7 with knockdown levels of ATG3 in the indicated cell lines. (C) Colony number of THP-1 and MV4-11 cells transduced with shCtrl or shATG3. Cells were seeded in methylcellulose and colonies were counted microscopically after 7 days.[63] Figures (A, C) were modified from Baker *et al.*, 2021. Student's t-test was performed in (A, C). *p < 0.05, **p < 0.01, ***p < 0.001, ****p < 0.0001.

As ATG3 is reported to be important for autophagy[113,114,147] and I found a block of autophagy flux upon ATG3 deletion (**Figure 11**), I further confirmed the impact of ATG3 depletion by shRNA on autophagy flux in THP-1 and MV4-11 cells expressing the autophagy flux probe. As expected, loss of ATG3 blocked autophagy flux under steady state conditions (**Figure 13A**)

in both cell lines. Similarly, inducing autophagy by starvation did not increase autophagic flux to normal levels in ATG3-depleted AML cells, indicating impaired autophagy flux upon loss of ATG3 (**Figure 13A**).[63] This was in line with impaired LC3 lipidation in ATG3-deficient THP-1 and MV4-11 cells, as immunoblotting showed significantly decreased LC3-II levels and consequently increased LC3-I levels. In addition, upon autophagy block by bafilomycin A1 treatment (Baf) higher LC3-I levels and lower LC3-II levels were visible (**Figure 13B**, **C**).[63]

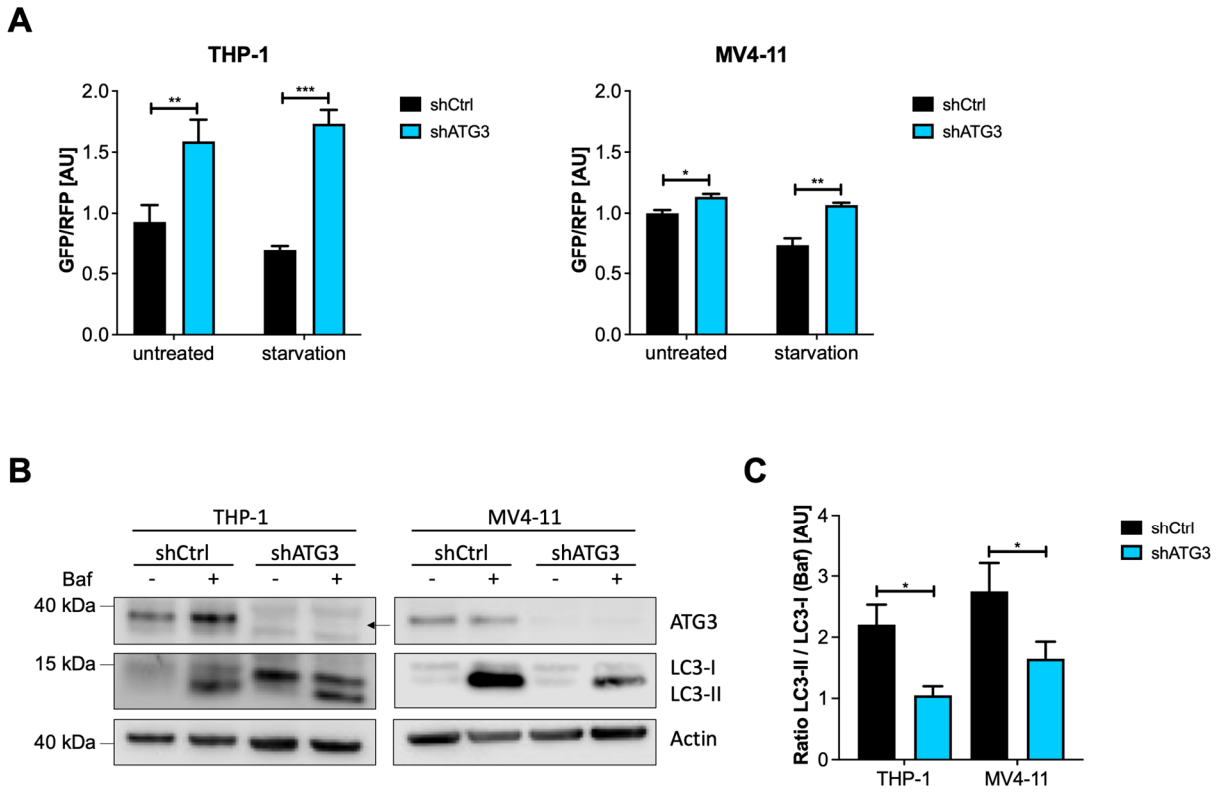

Figure 13. Loss of ATG3 impairs autophagy flux and LC3-lipidation. (A) Autophagy flux was determined using THP-1 and MV4-11 cells expressing GFP-rLC3B-RFP. Starvation was performed by incubation in PBS for 4 hours. (B) Representative western blot image showing LC3-I conjugation with PE to generate LC3-II. (C) Quantification of LC3 levels from (B) upon Baf treatment as LC3-II to LC3-I ratio.[63] Figures were modified from Baker *et al.*, 2021. Student's t-test was performed in (A, C). Error bars represent SEM. *p < 0.05, **p < 0.01, ***p < 0.001.

Furthermore, I assessed autophagosome formation by immunofluorescence staining of endogenous LC3 and quantified the accumulation of LC3-positive punctae after blocking autophagy (**Figure 14A**). In untreated conditions the number of LC3 punctae in ATG3-depleted AML cells was decreased and autophagy block by bafilomycin A1 (Baf) treatment did not increase the number of LC3 punctae in ATG3 deficiency to the level of control cells (**Figure 14B**).[63]

These results demonstrate the important function of ATG3 in LC3 lipidation and autophagosome formation in AML cells.[63]

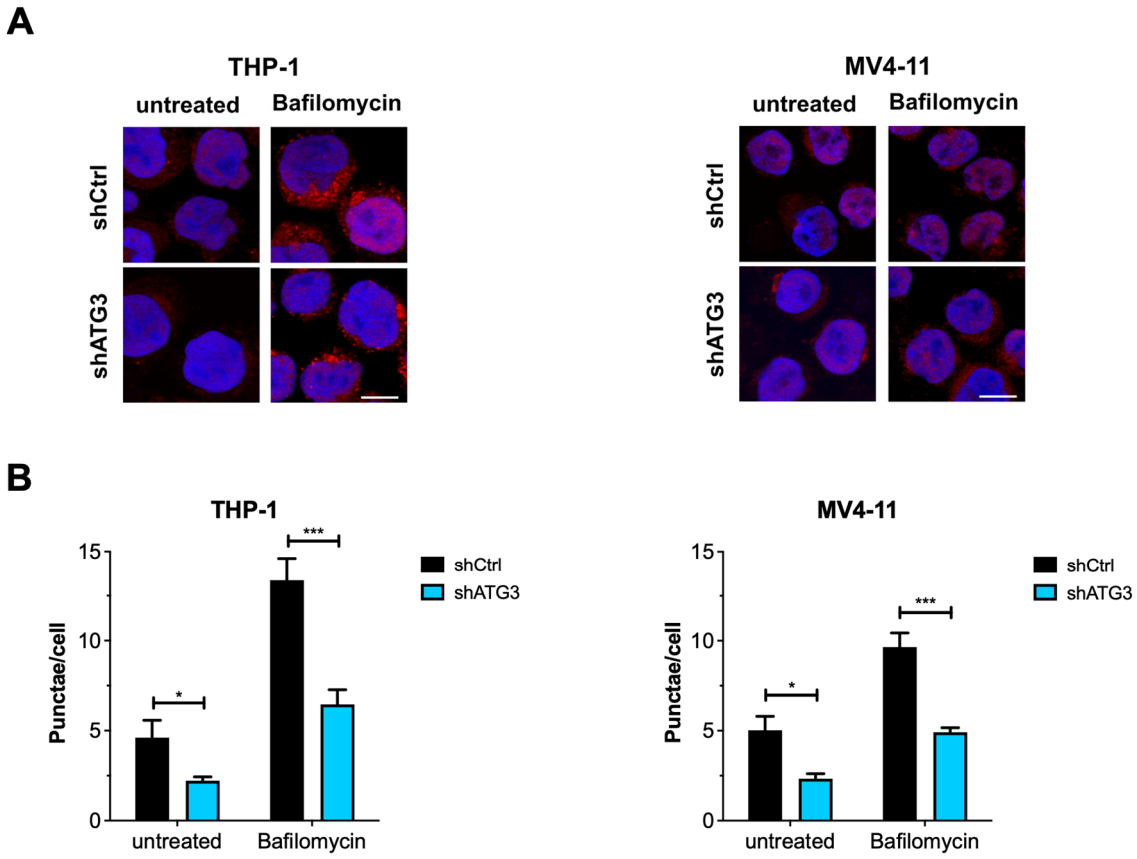

Figure 14. Autophagosome formation is impaired upon loss of ATG3. (A) Images of THP-1 and MV4-11 cells stained with an antibody against endogenous LC3B (red) and nuclear SytoxGreen staining (blue) analyzed by confocal microscopy. Inhibition of autophagic degradation was performed using 100 nM bafilomycin A1 (Baf) for 4 hours. Scale bar measures 10 µm. (B) To quantify the number of LC3 punctae per cell ImageJ was used.[63] Figures were modified from Baker *et al.*, 2021. Student's t-test was performed in (B). Error bars represent SEM. *p < 0.05, ***p < 0.001.

4.2.3. Loss of ATG3 increases apoptosis while retaining cell survival

Considering the role of ATG3 in leukemia cell proliferation, I further analyzed the effect of ATG3 depletion on cell cycle using BrdU and 7AAD staining followed by flow cytometry.[63] An incubation of cells with BrdU, an analog of thymidine, results in its incorporation into newly synthesized DNA during S-phase of the cell cycle.[148] BrdU levels within cells and 7AAD staining are then measured by flow cytometry. The cell cycle analysis showed a significantly reduced S-phase in both AML cell lines confirming impaired proliferation in ATG3-deficient cells. Interestingly, cell cycle was not arrested as G0/G1 and G2/M phase were unchanged upon loss of ATG3 (**Figure 15A**, **B**).[63]

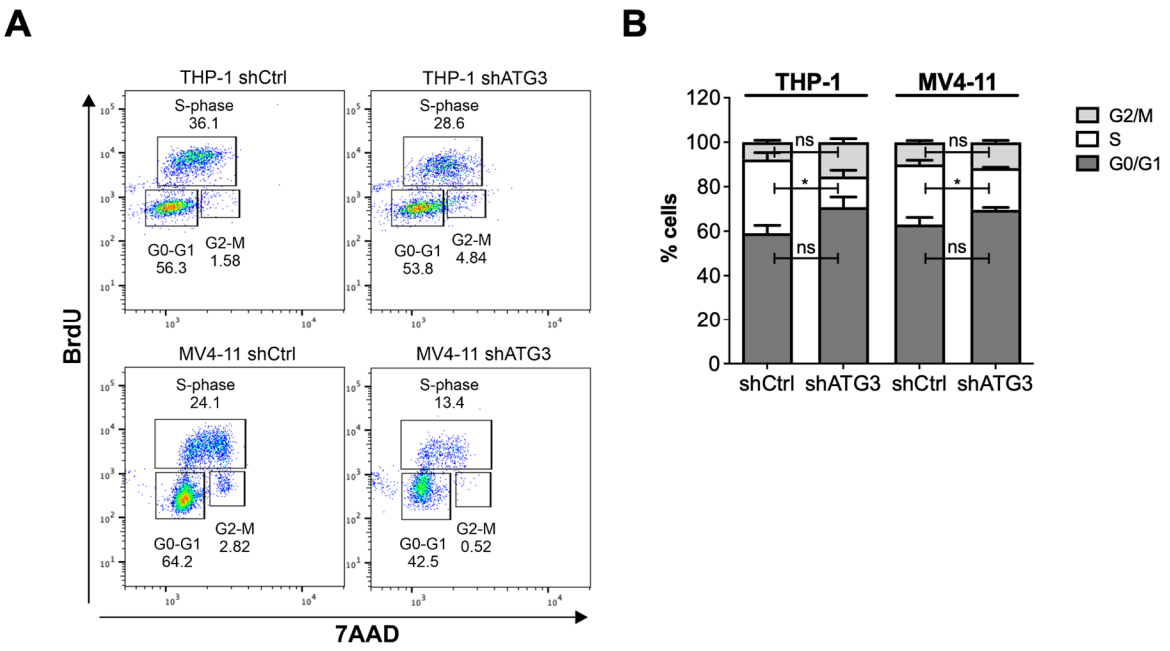

Figure 15. ATG3 depletion reduces S-phase in AML cells. (A) Analysis of the cell cycle of BrdU-7AAD stained control and ATG3 knockdown cells by using flow cytometry. (B) Quantification of BrdU+7AAD staining of THP-1 and MV4-11 cells. Cell-cycle phases were determined as follows: G0/G1 phase (BrdU negative; 2N DNA content), S-phase (BrdU positive), G2/M phase (BrdU negative; 4N DNA content).[63] Figures were modified from Baker *et al.*, 2021. Student's t-test was performed in (B). Error bars represent SEM. ns, not significant, *p < 0.05.

As proliferation and cell cycle are linked to apoptosis,[149] I analyzed whether reduced proliferation upon ATG3 loss was associated with increased apoptosis in both AML cell lines. Western blot analysis revealed elevated apoptosis induction shown by an increase of the apoptosis markers cleaved PARP and cleaved Caspase-3 after ATG3 knockdown (**Figure 16A**). I further quantified apoptosis levels by using annexinV-7AAD staining and flow cytometry analyses. AnnexinV binds to phosphatidylserine, which is located on the intracellular side of the plasma membrane in healthy cells. During early apoptosis, phosphatidylserine translocates to the external site and can be bound by fluorochrome-labeled annexinV. Additionally, 7AAD staining is performed to differentiate between early and late apoptosis.[150] AnnexinV-7AAD staining of THP-1 and MV4-11 cells confirmed that ATG3-depleted cells showed an increase in apoptosis in both cell lines compared to control cells (**Figure 16B**, **C**). Importantly, despite the induction of apoptosis in ATG3-depleted THP-1 and MV4-11 cells, still 45-50% of cells were alive after ATG3 loss, which is in line with the observation of reduced S-phase (**Figure 15**).[63]

Therefore, these results suggest that leukemia cells can still proliferate after the loss of ATG3.[63]

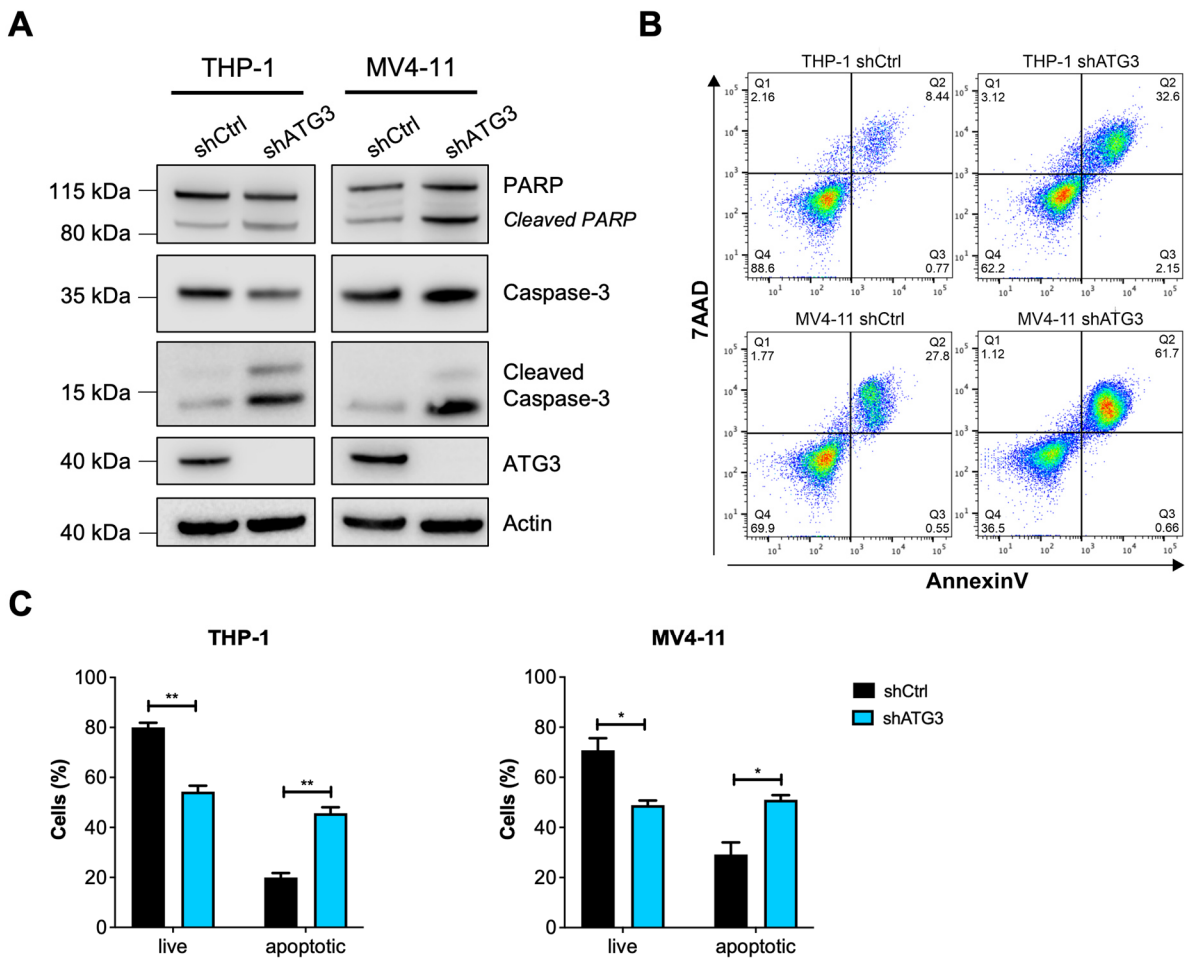

Figure 16. Loss of ATG3 induces apoptosis in leukemia cells. (A) Western blot showing different apoptosis marker in THP-1 and MV4-11 control and ATG3-depleted cells. (B) FACS plots of apoptosis staining with annexin V/7AAD. Q4 represents live cells, Q2 plus Q3 show apoptotic cells. (C) Quantification of live and apoptotic cells from annexin V/7AAD staining.[63] Figures (B–C) were modified from Baker *et al.*, 2021. Student's t-test was performed in (C). Error bars represent SEM. *p < 0.05, **p < 0.01.

4.3. Mitochondrial homeostasis is not altered by loss of ATG3

Since the proliferation data showed that AML cells can continue to proliferate after loss of ATG3 and that ATG3 depletion concomitantly impaired autophagy, I wanted to identify the mechanisms that compensate for autophagy loss.[63] A previous study from our lab and other studies have shown the necessity of maintaining mitochondrial homeostasis for leukemia cell survival, and that mitophagy, the degradation of damaged mitochondria, contributes to mitochondrial homeostasis.[63,151–153]

4.3.1. Mitochondrial degradation by mitophagy is not altered in ATG3-depleted cells

Knowing this, I analyzed the mitophagy flux by using THP-1 and MV4-11 cells expressing the mKEIMA reporter which is fused to a tandem repeat of the mitochondrial protein COXVIII pre-sequence, enabling the probe to localize to mitochondria. In dependence on neutral or acidic pH the fluorescent protein KEIMA reversibly changes its fluorescence. Therefore, it can be used as a reporter to monitor autophagosomes (neutral pH) or formed autolysosomes after fusion of autophagosomes with lysosomes (acidic pH) (**Figure 17A**).[63,154] To induce mitochondrial damage and activate mitophagy, I performed an oligomycin and antimycin A (O/A) treatment, inhibitors of ATPase and complex III of the ETC respectively, which induces mitochondrial depolarization. Mitophagy was also induced by deferiprone (DFP) treatment, an iron chelator, resulting in reduced intracellular iron levels and subsequently disturbance of mitochondrial iron homeostasis. Notably, flow cytometry analysis revealed that control and ATG3-depleted AML cells shifted into the pH4 high gate upon O/A and DFP treatment (**Figure 17B**). By quantifying mitophagy levels there was no significant difference in basal mitophagy as well as upon mitophagy induction (**Figure 17C**) suggesting that mitophagy is not altered in ATG3 deficiency.[63]

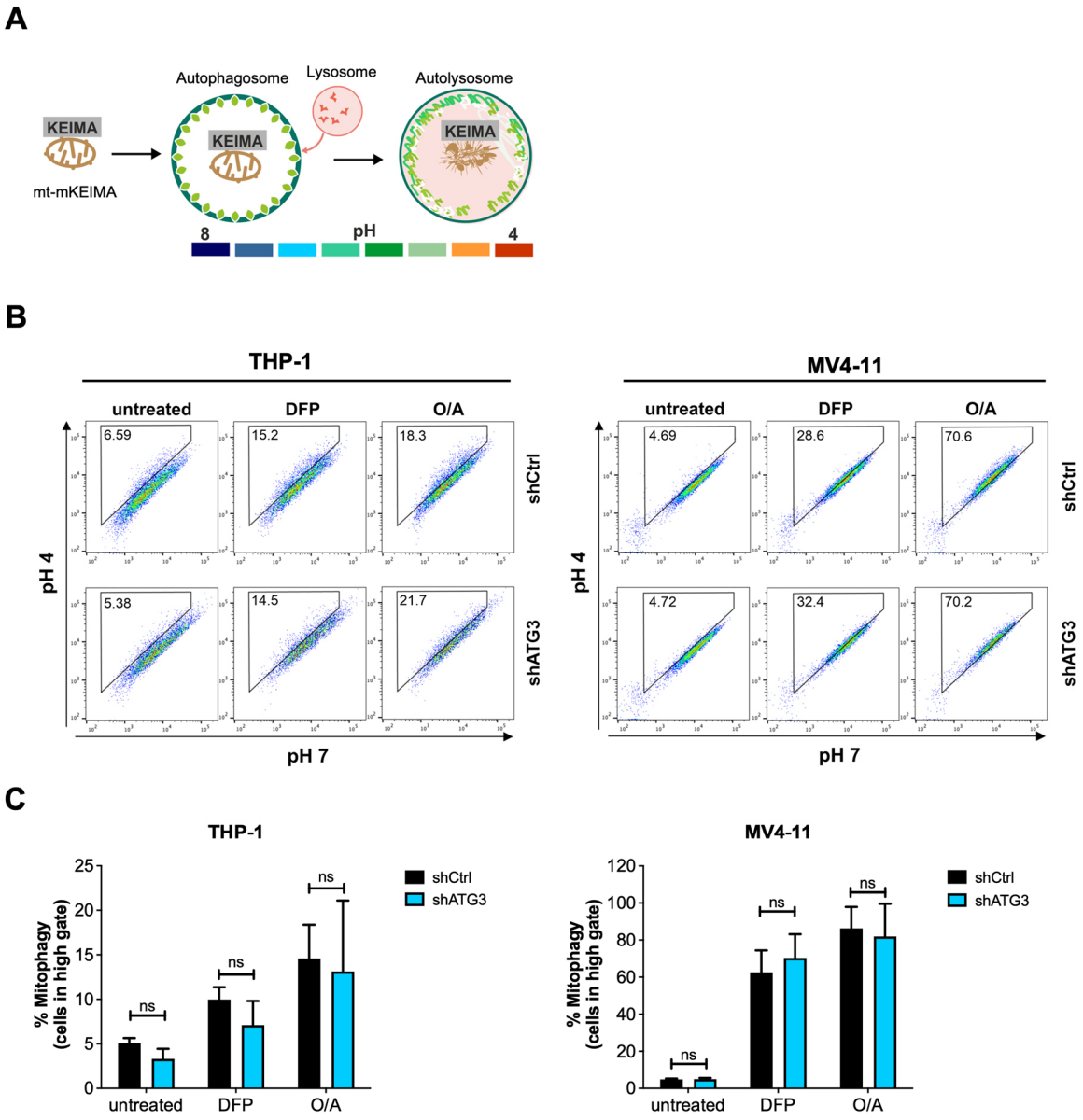

Figure 17. Mitophagy is not altered in ATG3-depleted AML cells. (A) Scheme of the mitochondrial mt-mKEIMA reporter. (B) Mitophagy was determined by flow cytometry in THP-1 and MV4-11 cells expressing the mt-mKEIMA reporter. Treatment with vehicle control, 400 µM DFP for 16 h, or 10 µM O/A (oligomycin/ antimycin A) for 8 h was performed. A shift of the cell population into the pH4 high gate represents mitophagy induction. (C) Quantification of cells in the pH4 high gate as percentage.[63] Figures were adapted from Baker *et al.*, 2021. Student's t-test was performed in (C). Error bars represent SEM. ns, not significant.

4.3.2. Mitochondrial membrane potential is not changed upon ATG3 loss

Subsequently, to further analyze mitochondrial homeostasis, I examined the mitochondrial membrane potential and performed a JC-1 staining.[63] JC-1 monomers accumulate as red fluorescent aggregates in healthy mitochondria, while a low membrane potential results in the presence of JC-1 monomers exhibiting a green fluorescence. Thus, mitochondrial depolarization is visualized by a decreasing red/green fluorescence ratio using flow

cytometry.[155] To induce mitochondrial depolarization as positive control, cells were treated for 15 min with 25 µM CCCP, an uncoupler of OXPHOS (**Figure 18A, B**). JC-1 staining of THP-1 and MV4-11 control and ATG3 knockdown cells resulted in a similar ratio of red/green fluorescence demonstrating that the mitochondrial membrane potential was not altered in ATG3 deficiency (**Figure 18B**). This result indicates similar levels of intact mitochondria in control and ATG3-depleted AML cells.[63]

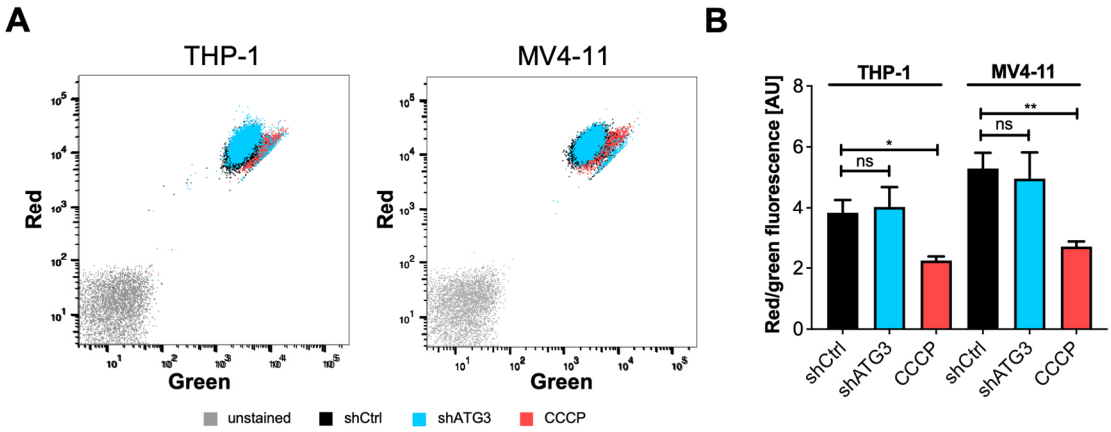

Figure 18. Mitochondrial membrane potential is not affected by loss of ATG3. (A) Flow cytometry blots showing JC-1 staining to assess mitochondrial membrane potential. 25 µM CCCP treatment was performed for 15 min as positive control to induce depolarization. (B) Quantification of red (intact) to green (depolarized) fluorescence in THP-1 and MV4-11 cells transduced with shCtrl or shATG3.[63] Figure was adapted from Baker *et al.*, 2021. Student's t-test was performed in (B). Error bars represent SEM. ns, not significant, *p < 0.05, **p < 0.01.

4.3.3. ATG3 depletion does not alter mitochondrial mass

As I found no change in mitophagy and mitochondrial polarization upon ATG3 depletion, I asked whether loss of ATG3 would change the mitochondrial mass of AML cells and performed MitoTracker™ Green staining by employing flow cytometry.[63] MitoTracker™ Green is a green fluorescent dye which localizes to mitochondria in living cells independently of the status of the mitochondrial membrane potential.[156] Interestingly, in both AML cell lines MitoTracker™ Green staining displayed no difference in overall mitochondrial mass in control and ATG3 knockdown cells (**Figure 19A** and **B**).[63] This was confirmed by western blot analysis of the expression levels of COXIV, a protein of the inner mitochondrial membrane[157]. Expression of COXIV was similar in control and ATG3 knockdown cells under steady state conditions (**Figure 19C**).[63]

Taken together, these results indicate that mitochondrial homeostasis and turnover were not altered upon loss of ATG3 shown by similar levels of mitophagy activity, membrane potential, and mitochondrial mass in ATG3-depleted AML cells compared to control cells.[63]

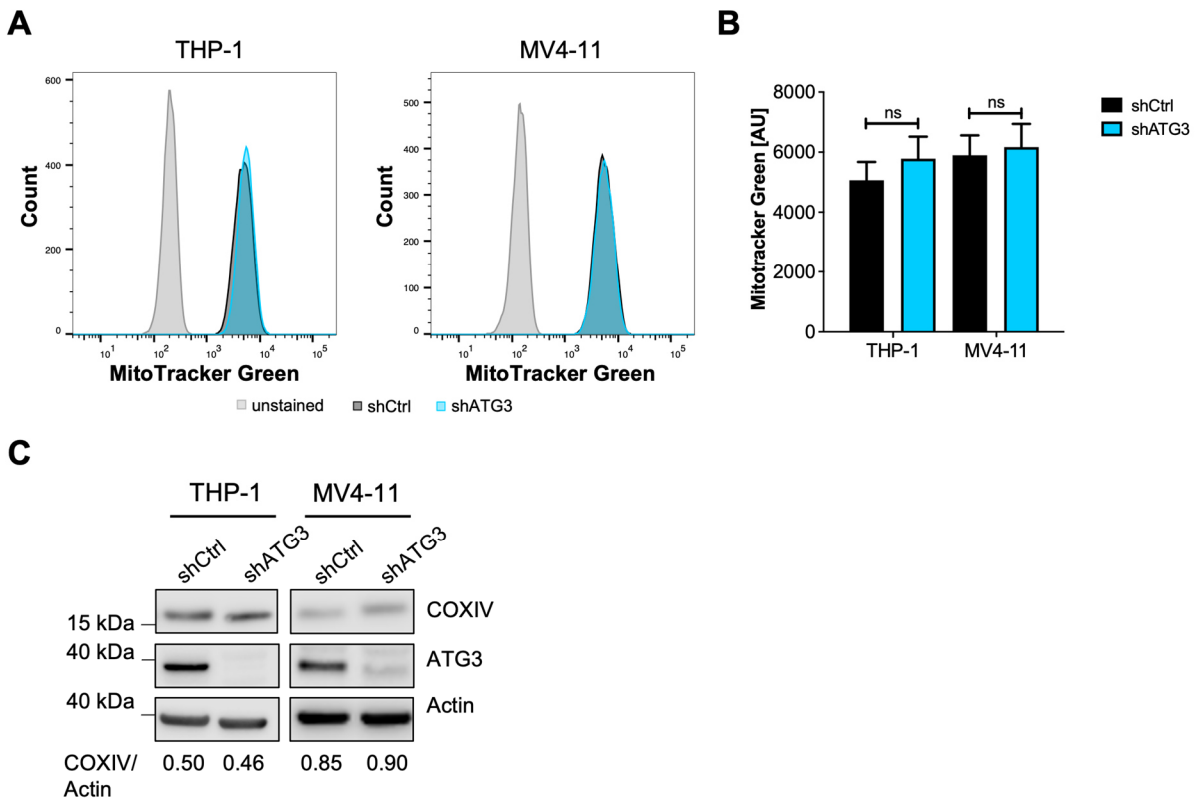

Figure 19. Mitochondrial mass is not altered upon ATG3 depletion. (A) Representative flow cytometry blots showing MitoTracker™ Green staining for analyzing overall mitochondrial mass. (B) Quantification of MitoTracker™ Green staining. (C) Representative western blot image of the endogenous expression of COXIV in control and ATG3 knockdown cells. For quantification the signal intensity of COXIV was normalized to ß-actin.[63] Figure was modified from Baker *et al*., 2021. Student's t-test was performed in (B). Error bars represent SEM. ns, not significant.

4.4. Mitochondrial activity is upregulated upon loss of ATG3

Since mitophagy and mitochondrial turnover were not increased in ATG3-depleted AML cells, I wondered whether mitochondrial function may be altered thereby contributing to the survival of ATG3-deficient cells. Therefore, I determined mitochondrial fitness by first analyzing the generation of mitochondrial reactive oxygen species.[63]

4.4.1. Loss of ATG3 increases reactive oxygen species

Reactive oxygen species (ROS) are mainly produced in mitochondria during ATP production. The generation of ATP via the electron transport chain during OXPHOS frequently results in the production of by-metabolites including superoxide radicals (O_2•−), hydrogen peroxide (H_2O_2), and hydroxyl radicals (OH•).[83,84,158,159] Therefore, ROS levels are a marker for mitochondrial fitness. Taking this into account, I on the one hand analyzed total ROS levels and on the other hand analyzed ROS specifically produced by mitochondria (mitochondrial superoxide).[63] The total intracellular ROS levels of THP-1 and MV4-11 cells transduced with

shCtrl or shATG3 were analyzed by dihydrorhodamine 123 (DHR) staining followed by flow cytometry measurement. DHR 123 is an uncharged, non-fluorescent and cell-permeable stain, which is oxidized intracellularly by ROS resulting in the generation of a green fluorescent product.[160] ATG3-depleted cells showed significantly enhanced levels of total intracellular ROS (**Figure 20A**, **B**).

Mitochondrial superoxide levels were determined by employing MitoSOX™ staining and measuring with flow cytometry. MitoSOX™ is a cell-permeable dye, which is oxidized exclusively by superoxide leading to a red fluorescent signal.[161] Similarly, to total ROS levels, I found that mitochondrial superoxide levels were significantly increased in both THP-1 and MV4-11 cells upon ATG3 depletion (**Figure 20C**, **D**).[63]

I further asked if this was an ATG3-specific finding, or this could also be observed for the loss of other core autophagy genes. Therefore, I performed an shRNA-mediated knockdown of ATG5 and ATG7 and analyzed total intracellular ROS levels and mitochondrial superoxide levels. Likewise, depletion of ATG5 and ATG7 showed an increase in total intracellular ROS and in mitochondrial superoxide levels in both cell lines (**Figure 20B**, **D**). Also, proliferation analysis of ATG5 and ATG7 depletion revealed reduced proliferation similar to ATG3 depletion (Appendix **Figure 32**).

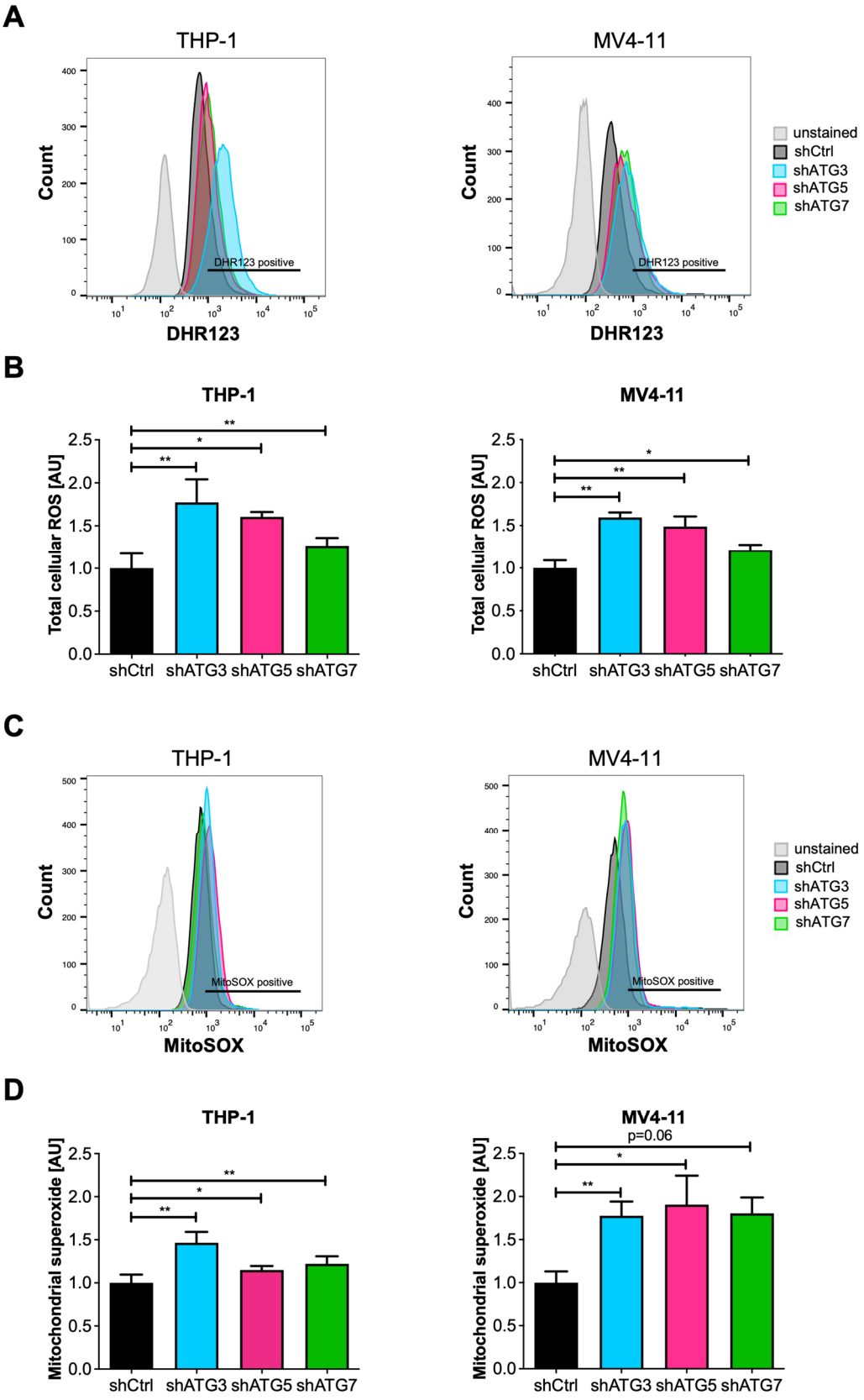

Figure 20. Loss of ATG3, ATG5, and ATG7 increases cellular ROS and mitochondrial superoxide levels. (A) Total intracellular ROS levels were analyzed by DHR 123 staining and flow cytometry. Histograms of unstained and DHR stained cell lines are shown. (B) Quantification of total intracellular ROS levels in ATG3, ATG5, and ATG7 knockdown cells. (C) Images of MitoSOX™ staining of THP-1 and MV4-11 cell lines to determine mitochondrial superoxide levels. (D) Quantification of MitoSOX™

staining in ATG3, ATG5, and ATG7 knockdown cells.[63] Figures (C–D) were modified from Baker *et al*., 2021. Student's t-test was performed in (B, D). Error bars represent SEM. *p < 0.05, **p < 0.01.

4.4.2. Loss of ATG3 increases ATP production by oxidative phosphorylation

As ATG3-depleted cells showed increased ROS levels, and mitochondrial ROS are mainly formed when ATP is generated,[158] I determined ATP levels produced per cell in THP-1 and MV4-11 cells using a luminescence viability assay.[63] To quantify ATP levels, Cell Titer Glo® reagent was used, which contains luciferin and luciferase. ATP is used to produce oxyluciferin from luciferin by luciferase resulting in a luminescence signal.[162] Notably, the comparison of the luminescence signal and normalization to cell number determined by trypan blue exclusion revealed that ATP levels per cell were significantly higher in ATG3-depleted cells compared to control cells (**Figure 21**).[63] A similar trend of increased ATP levels was observed for knockdown of ATG5 and ATG7 in both AML cell lines (**Figure 21**).

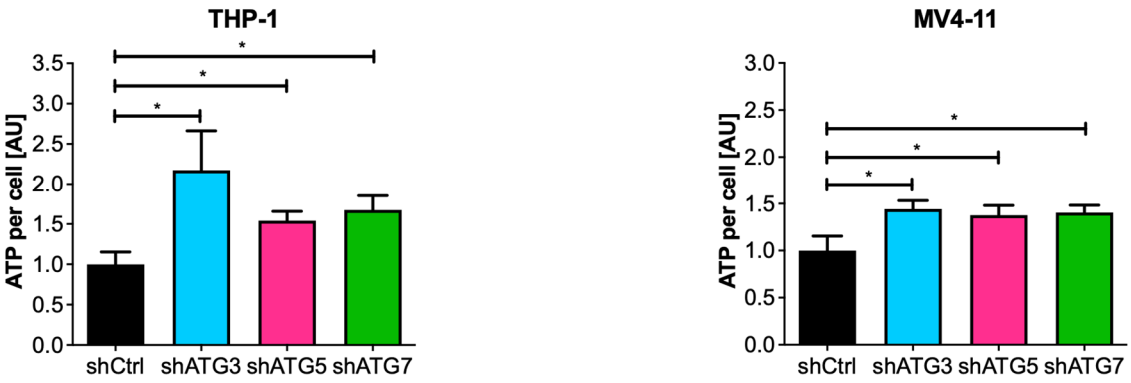

Figure 21. Loss of ATG3, ATG5, and ATG7 increases ATP levels per cell. Levels of ATP of control and knockdown cells were analyzed after incubation of cells for 72 h by using the Cell Titer Glo® luminescent cell viability assay. The luminescent signal was normalized to cell number counted after 3 days of incubation. Quantification of ATP levels is shown normalized to shCtrl cells.[63] Figure was modified from Baker *et al*., 2021. Student's t-test was performed. Error bars represent SEM. *p < 0.05.

Then, to quantify mitochondrial activity, OXPHOS was analyzed based on mitochondrial oxygen consumption in living AML cells (**Figure 22A**). The Seahorse XFe96 Flux analyzer was used to measure the oxygen consumption rate (OCR) in real-time.[63] By injecting oligomycin after basal measurement, the electron flow through the ETC is impaired causing a reduction of mitochondrial respiration. The 2nd injection of the uncoupler FCCP results in a collapse of the proton gradient and consequently the disruption of mitochondrial membrane potential, which results in maximal oxygen consumption. Finally, an injection of rotenone (complex I inhibitor) and antimycin A (complex III inhibitor) entirely stops mitochondrial respiration.[163]

Importantly, loss of ATG3 significantly increased the OCR of both THP-1 and MV4-11 cells (**Figure 22A**). Quantification of mitochondrial respiration revealed that basal respiration, the basal energy demand of cells, was upregulated as well as the highest attainable respiration of cells depicted as maximal respiration (**Figure 22B**). Furthermore, I quantified the production of mitochondrial ATP in the oxygen consumption rate measurements after injection of oligomycin. ATP production was increased upon loss of ATG3 (**Figure 22B**), which agrees with the data from **Figure 21**.[63]

In summary, these results demonstrate that ATG3 depletion increases mitochondrial activity and OXPHOS resulting in higher ATP levels in leukemia cells.[63]

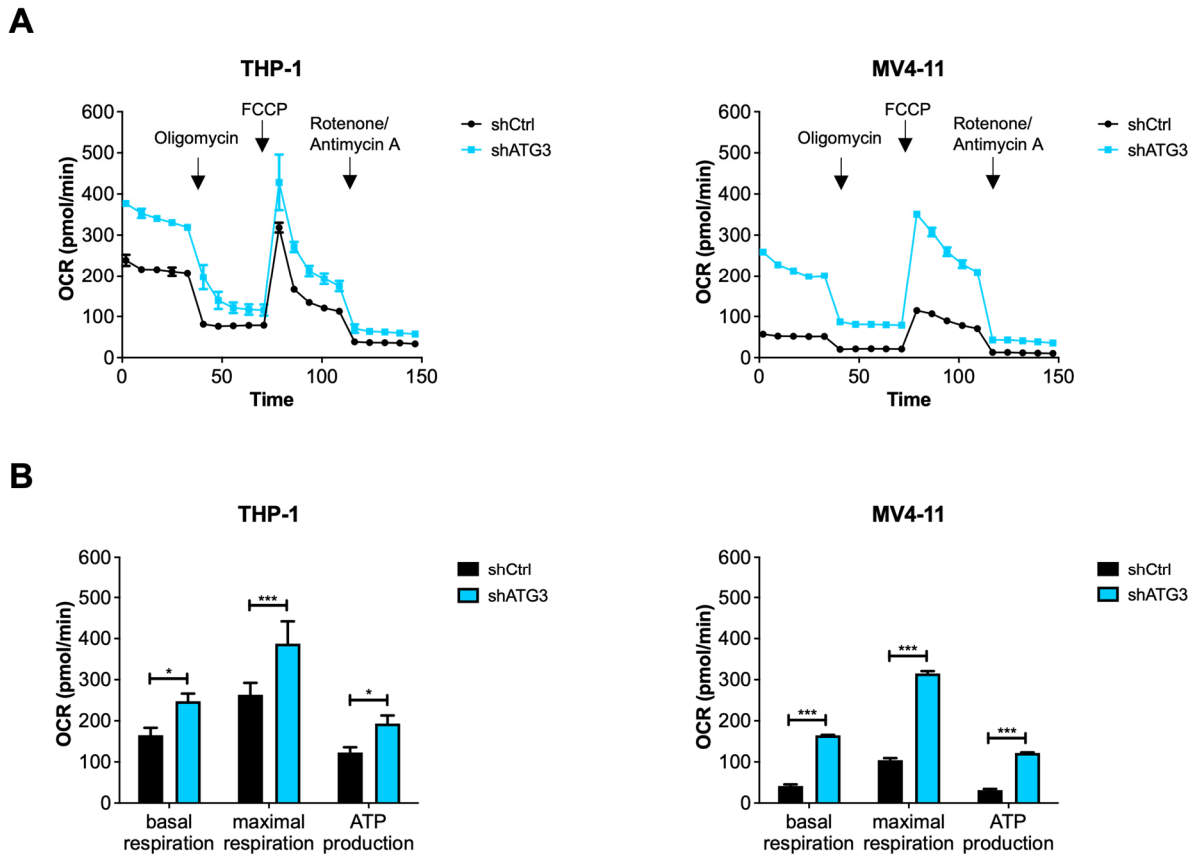

Figure 22. Oxidative phosphorylation is increased in ATG3-depleted AML cells. (A) Representative curves of the oxygen consumption rate (OCR) measurements performed by using the Agilent Seahorse XFe96 Flux Analyzer to analyze mitochondrial respiration in control and ATG3-depleted AML cells. (B) Quantification of OCR measurements to assess basal respiration, maximal respiration, and ATP production.[63] Figure was adapted from Baker *et al.*, 2021. Student's t-test was performed in (B). Error bars represent SEM. *p < 0.05, ***p < 0.001.

4.5. Rewiring of the central carbon metabolism in ATG3-deficient AML cells

As loss of ATG3 increased ROS production and the activity of oxidative phosphorylation, indicating an upregulated mitochondrial activity, and as mitochondria contribute to cellular metabolism in various ways,[164] I further investigated the underlying mechanisms by analyzing the metabolic alterations in THP-1 and MV4-11 cells.[63] Metabolic alterations can be analyzed by various methods including the quantitative uptake or release of metabolites, mass spectrometry, or nuclear magnetic resonance (NMR) spectroscopy.[132,165]

4.5.1. ATG3 depletion increases glucose and glutamine consumption

Glucose and glutamine are the two major carbon sources of cancer cells.[65] Therefore, I analyzed the consumption of glucose and glutamine in AML cells in the presence and absence of ATG3. To this end, cells were incubated in medium for 72 hours, which was harvested afterwards. The medium was used to measure the extracellular concentration of glucose and glutamine by spectrophotometry. Afterwards, the influx of both metabolites was calculated as glucose concentration per $1x10^6$ cells per hour. Loss of ATG3 increased the consumption of both glucose and glutamine in THP-1 and MV4-11 significantly (**Figure 23A**, **B**).[63]

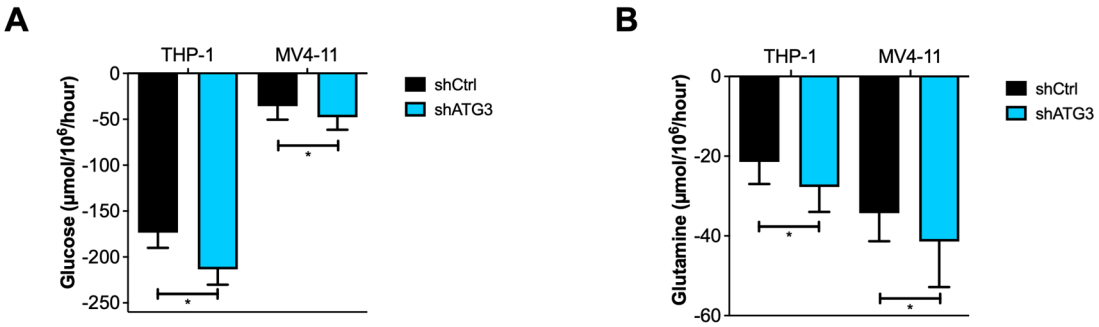

Figure 23. Loss of ATG3 increases consumption of glucose and glutamine. Consumption fluxes of (A) Glucose and (B) Glutamine are shown. Control and ATG3-depleted THP-1 and MV4-11 cells were cultivated for 72 hours, afterwards the medium was collected, and glucose and glutamine concentrations were measured by spectrophotometry. Fluxes were calculated by determining metabolite concentrations normalized to the cell number.[63] Figure was adapted from Baker *et al.*, 2021. Student's t-test was performed in (A, B). Error bars represent SEM. *p < 0.05.

4.5.2. ATG3 depletion alters central carbon metabolism in leukemia cells

For a more detailed analysis of the metabolic alterations in ATG3 deficiency, NMR spectroscopy analysis of my samples was performed in collaboration with Islam Alshamleh from the group of Harald Schwalbe at University Campus Riedberg. THP-1 and MV4-11 cells were cultivated for 24 hours in fresh medium and harvested afterwards. I performed the

extraction of metabolites with methanol and chloroform, and the polar fraction was then analyzed by Islam Alshamleh using NMR. The relative intracellular concentrations of key metabolites were determined in ATG3-depleted THP-1 and MV4-11 cells. By analyzing the NMR data, I found increased intracellular glutathione concentrations, an important ROS scavenger needed for redox balance, upon loss of ATG3 (**Figure 24**). Furthermore, molecules of the central carbon metabolism like glucose and lactate, as well as glutamine and glutamate displayed increased intracellular concentrations in ATG3-depleted cells (**Figure 24**). Also, succinate, and fumarate, which are both TCA cycle intermediates, showed increased levels upon ATG3 loss (**Figure 24**).[63]

Taken together, these results indicate that the central carbon metabolism is upregulated in AML cells in the absence of ATG3.[63]

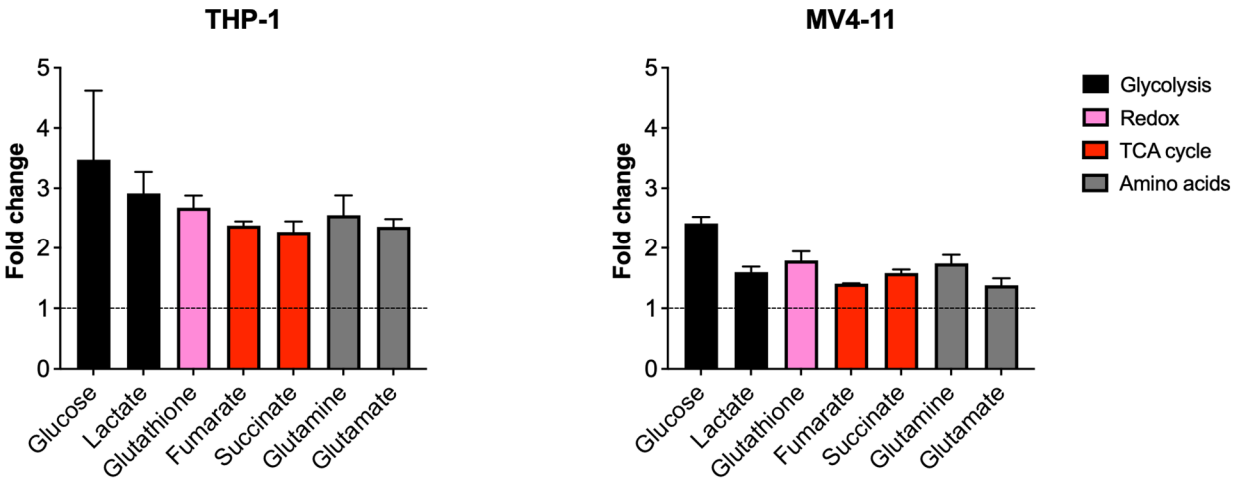

Figure 24. ATG3-depleted THP-1 and MV4-11 cells rewire their central carbon metabolism. Bar graph shows the intracellular concentrations of central metabolites depicted as fold change (normalized to control) in THP-1 and MV4-11 cells upon loss of ATG3 and measured by NMR. The dotted line depicts the normalized control.[63] Figure was adapted from Baker *et al.*, 2021.

4.6. ATG3 depletion upregulates the glycolytic pathway in leukemia cells

As loss of ATG3 resulted in rewiring of the central carbon metabolism, as well as in an increased uptake and elevated intracellular levels of glucose, I focused on glucose metabolism.[63] Autophagy was previously shown to be regulated by glycolysis.[69] Taking this into account, I analyzed the induction of autophagy flux upon glycolysis inhibition by treating control and ATG3-depleted AML cells with 2-deoxy glucose (2-DG), an glucose analog, for 24 hours.[63] As reported by Chu *et al.*, I also observed that the inhibition of glycolysis resulted in an induction of autophagy in control cells.[63,69] Upon loss of ATG3 autophagy was blocked and 2-DG treatment did not induce autophagy flux (**Figure 25**).[63]

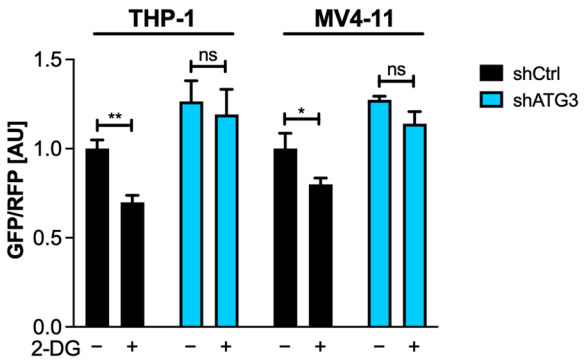

Figure 25. Autophagy is regulated by glycolysis. Autophagy flux was determined by using the GFP-LC3B-RFP reporter. GFP/RFP ratio was normalized to untreated control cells (– 2-DG). Cells were treated with 1 mM 2-DG for 24 hours.[63] Figure was adapted from Baker *et al*., 2021. Student's t-test was performed. Error bars represent SEM. ns, not significant, *p < 0.05, **p < 0.01.

4.6.1. Loss of ATG3 increases glucose uptake and utilization

As a next step, I determined the fate of carbon that is derived from glucose to analyze the consequences of increased glucose consumption upon ATG3 loss.[63] The investigation of the ^{13}C incorporation, which occurs through the artificial enrichment of molecules containing ^{13}C such as glucose into the metabolites of central carbon metabolism, is a widely applied method that provides access to the regulation of metabolism in living cells.[166,167] For ^{13}C incorporation, isotope-labeled glucose (U-$^{13}C_6$-glucose) was added to glucose-free medium, and cells were cultured in isotope-labeled medium for 24 hours. Labeled carbon derived from glucose was incorporated according to **Figure 26A** and polar metabolites were extracted from THP-1 and MV4-11 cells. Afterwards tracer-based NMR measurements of my samples were performed by Islam Alshamleh and Daniel Hymon from the group of Harald Schwalbe at University Campus Riedberg.[63]

By analyzing the NMR results, I found significant labeling in several secondary metabolites and glycolytic end-products (Appendix **Figure 33**). Moreover, a significant intracellular increase of ^{13}C labeled glucose was found in THP-1 and MV4-11 cells upon loss of ATG3 indicating an increased uptake of glucose in autophagy deficiency. I also observed a significant incorporation of ^{13}C into lactate in both ATG3-depleted AML cell lines demonstrating an increased utilization of glucose and enhanced production of lactate in the absence of ATG3 (**Figure 26B**).[63]

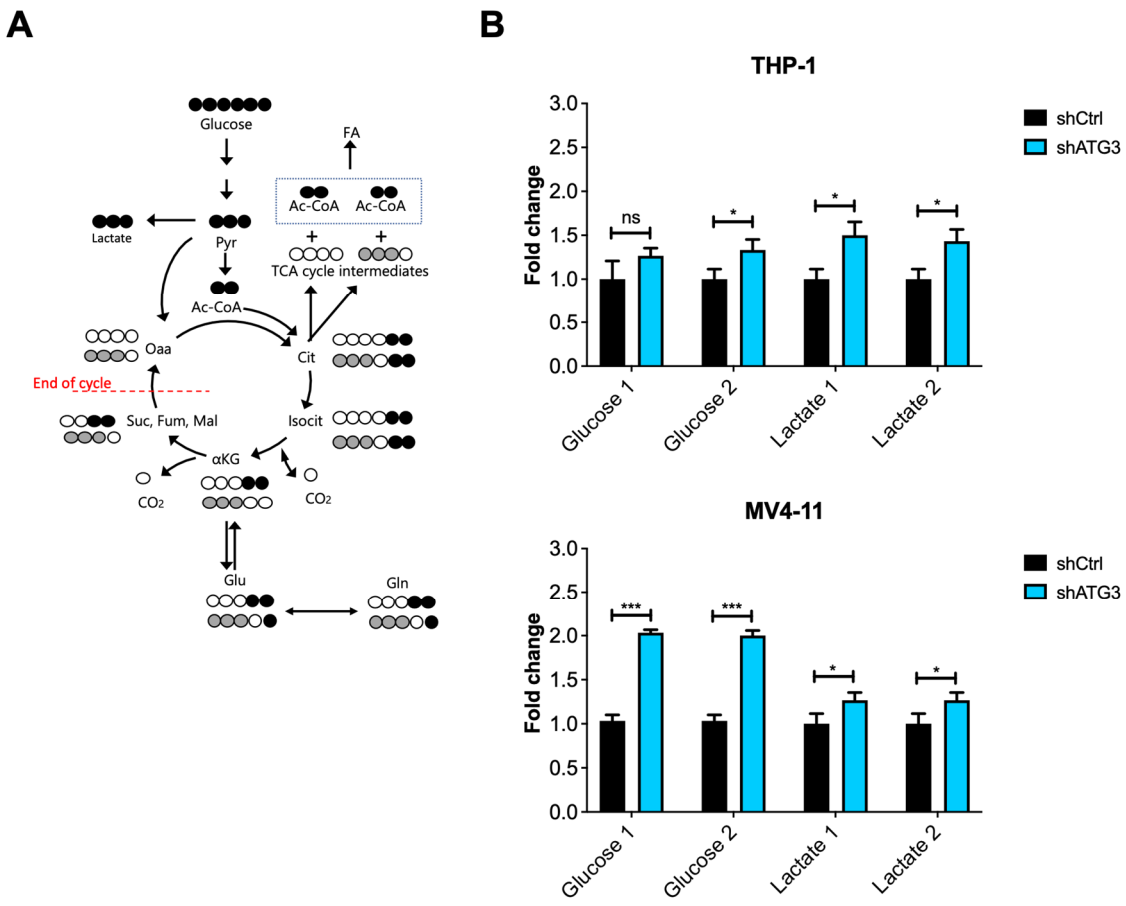

Figure 26. Loss of ATG3 activates glycolysis. (A) Carbon atom transition map using [U-$^{13}C_6$]-glucose as a tracer. Pyruvate can enter mitochondria either via acetyl-CoA (Ac-CoA) or oxaloacetate (Oaa). Black molecules show the ^{13}C labeling pattern of Ac-CoA fueling the TCA cycle during the first cycle of oxidation. Gray molecules demonstrate the entry of pyruvate into the TCA cycle. The first turn of the TCA cycle is shown here. α-KG, α-Ketoglutarate; Cit, citrate; FA, fatty acids; Fum, fumarate; Gln, glutamine; Glu, glutamate; Isocit, isocitrate; Mal, malate; Suc, succinate. (B) Fold change of glucose and lactate analyzed by [U-$^{13}C_6$]-glucose tracer-based NMR and normalized to control cells.[63] Figure was modified from Baker *et al.,* 2021. Student's t-test was performed in (B). Error bars represent SEM. ns, not significant, *p < 0.05, ***p < 0.001.

4.6.2. Lactate is retained intracellularly in ATG3-depleted AML cells

As NMR analysis revealed that glycolysis was increased, which was accompanied by a high production of lactate, I was further interested whether the increased lactate production resulted in a higher export or an intracellular accumulation of lactate.[63] During glycolysis, the conversion of glucose to pyruvate takes place, and pyruvate is subsequently converted into lactate by the enzyme lactate dehydrogenase (LDH). To maintain a stable intracellular pH, glycolytic cancer cells transport lactate and protons into the extracellular medium.[168] I therefore measured the concentration of extracellular lactate using a colorimetric analysis of medium that was harvested after 72 hours (**Figure 27A**). Interestingly, the extracellular lactate concentration was not increased in ATG3 knockdown cells. In THP-1 cells extracellular lactate levels were similar to control cells, and in MV4-11 cells loss of ATG3 even reduced extracellular lactate

levels.[63] I also analyzed the ^{13}C incorporation into lactate present in the medium that was harvested simultaneously to the cells of the tracer-based NMR experiment. These lactate levels therefore refer to the concentration of extracellular lactate of the isotope-labeled glucose analysis (**Figure 27B**). ^{13}C labeled carbon was found in similar levels in control and ATG3-depleted cells, indicating that the export of lactate was not altered upon loss of ATG3.

I further measured the extracellular acidification rate (ECAR) in real-time in living cells by using the Seahorse XFe96 Flux analyzer. ECAR measures the acidification that occurs upon release of lactate and protons into the extracellular medium, which are produced during the conversion of pyruvate to lactate. Before ECAR measurement the cells were incubated for one hour in glucose-free medium. After basal measurement in glucose-free medium, 10 mM glucose was injected thereby inducing glycolysis. During glycolysis, an increase in ECAR follows as protons and lactate are released extracellularly. With the second injection of oligomycin, OXPHOS is inhibited resulting in a shift of energy production to glycolysis, which further increases ECAR. As a last step, the injection of 2-DG results in an inhibition of glycolysis and ECAR decreases.[63,169] In THP-1 and MV4-11 cells knockdown of ATG3 resulted in a decreased ECAR after glucose injection (**Figure 27C**). Furthermore, oligomycin did not significantly increase ECAR upon loss of ATG3. 2-DG injection decreased ECAR independently of ATG3 indicating that the extracellular acidification occurs due to glycolysis. The quantification of ECAR showed significant reduction of basal acidification in ATG3-depleted AML cells, which was calculated by the difference of ECAR before and after glucose injection. Also, the maximal acidification, the difference in ECAR of oligomycin and glucose injection, was significantly decreased upon loss of ATG3 (**Figure 27D**).[63]

Taken together, these results demonstrate that loss of ATG3 strongly activates glycolysis in AML cells, resulting in an increased production of lactate, which is retained intracellularly.[63]

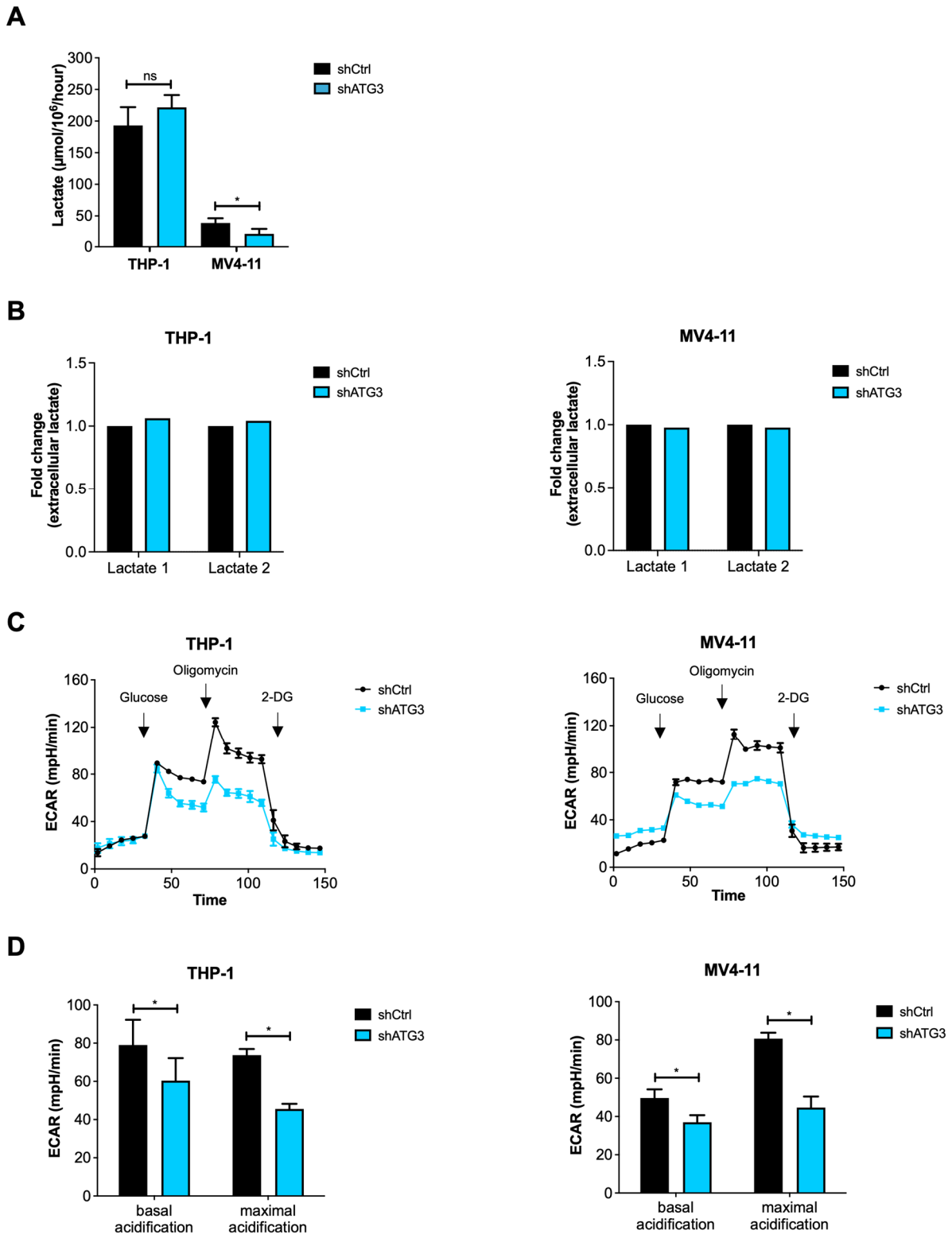

Figure 27. Lactate is retained intracellularly in AML cells upon loss of ATG3. (A) Extracellular lactate concentration of THP-1 and MV4-11 cells was analyzed by spectrophotometry 72 hours after incubation of cells in normal medium. (B) Fold change of lactate in the [U-$^{13}C_6$]-glucose containing medium after 24 hours analyzed by tracer-based NMR and normalized to control cells. (C) Extracellular acidification rate (ECAR) measurements to determine lactate excretion using the Seahorse XFe96 Analyzer. Representative curves are depicted. (D) Bar graph depicts the quantification of ECAR. Basal acidification was calculated as the difference of ECAR before and after glucose injection. Maximal acidification was calculated as the difference of oligomycin and glucose injection.[63] Figures (A,

C, D) were adapted from Baker *et al*., 2021. Student's t-test was performed in (A, D). Error bars represent SEM. ns, not significant, *p < 0.05.

4.7. ATG3-depleted AML cells depend on OXPHOS for cell survival

The observed activation of glycolysis and upregulation of mitochondrial respiration upon loss of ATG3 suggest that metabolic alterations are important for the survival of ATG3-depleted AML cells. Therefore, I wondered whether ATG3-depleted AML cells are dependent on both pathways for maintaining cell survival when autophagy is impaired.[63]

4.7.1. Loss of ATG3 activates TCA cycle and increases glutathione production

As I found increased OXPHOS (**Figure 22**), ATP levels (**Figure 21**), and higher intracellular concentrations of fumarate and succinate (**Figure 24**), I analyzed the mitochondrial metabolism in more detail by analyzing the ^{13}C incorporation derived from glucose in the tracer-based NMR experiment (**Figure 28**). I found an increased incorporation of ^{13}C in the amino acids glutamine and arginine upon loss of ATG3 in THP-1 and MV4-11 cells.[63] Glutamine and arginine can be generated from glutamate, which can be produced from α-Ketoglutarate.[170] The ^{13}C incorporation indicates that glutamine and arginine are possibly produced from α-Ketoglutarate from the TCA cycle.[63,171,172] Furthermore, a significant enrichment of ^{13}C incorporation was found in succinate upon loss of ATG3, showing the activation of TCA cycle and mitochondrial metabolism in ATG3-depleted AML cells.[63]

Additionally, I observed a significant incorporation of carbon derived from glucose in glutathione upon loss of ATG3 in both AML cell lines (**Figure 28**), which is in line with the previous results (**Figure 24**). This result suggests that ATG3 deficiency leads to an upregulation of glutathione production thereby maintaining redox balance in AML cells.[63]

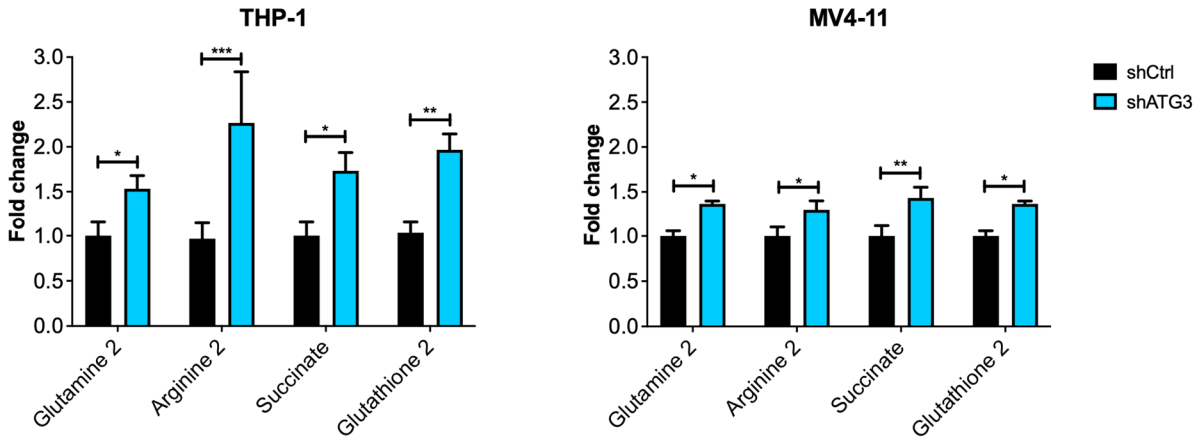

Figure 28. Activation of TCA cycle and glutathione production in ATG3-depleted AML cells. Fold change of metabolites analyzed by [U-$^{13}C_6$]-glucose tracer-based NMR normalized to control cells.[63] Figure was adapted from Baker *et al*., 2021. Student's t-test was performed. Error bars represent SEM. *p < 0.05, **p < 0.01, ***p < 0.001.

However, several metabolites also showed a different accumulation of carbon derived from glucose in THP-1 and MV4-11 cells upon loss of ATG3 (**Figure 29,** Appendix **Figure 33**). For instance, the ^{13}C incorporation into the TCA cycle intermediate malate, which is generated from fumarate, was not significantly upregulated in both cell lines in the absence of ATG3, but a trend was visible for THP-1 cells. For aspartate, no difference was observed in THP-1 cells. But in MV4-11 cells, loss of ATG3 significantly upregulated aspartate levels. Furthermore, the amino acid glutamate showed significantly higher ^{13}C labeled carbon levels in ATG3-depleted THP-1 cells compared to control cells. In MV4-11 cells however, glutamate levels did not differ between control and knockdown cells. Also, ^{13}C labelled alanine accumulated in THP-1 cells upon loss of ATG3, whereas in MV4-11 cells no significant difference could be observed. Moreover, the amino acid proline showed significant lower levels in ATG3-depleted MV4-11 cells, but not in THP-1 cells. Thus, the tracer-based NMR results indicate that the intracellular levels of several metabolites were similarly altered by the compensatory mechanism in ATG3 deficiency (**Figure 26, 28**), but as THP-1 and MV4-11 cells are different AML cell lines with different driver mutations, the enrichment of ^{13}C labeling in other metabolites was variable (**Figure 29**).

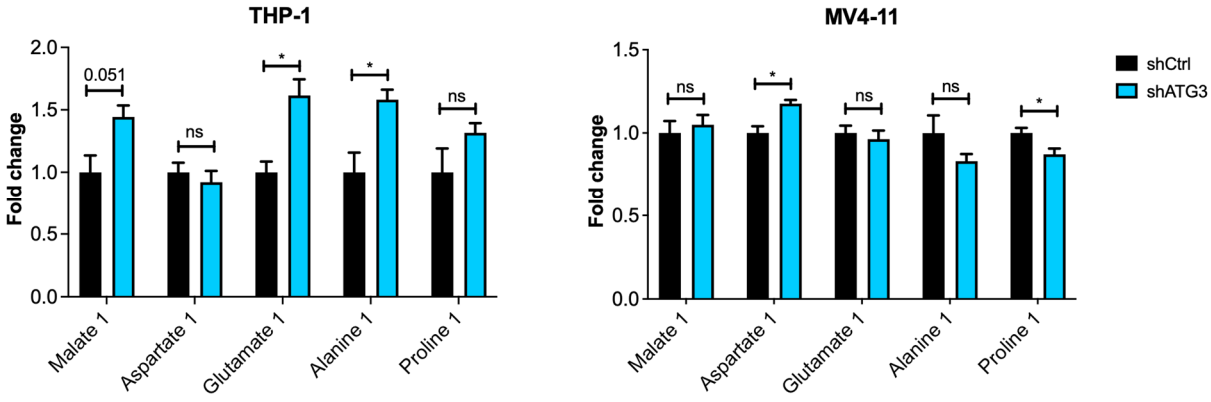

Figure 29. ^{13}C incorporation into different metabolites varies between AML cell lines upon loss of ATG3. Bar graph depicts the fold change of metabolites of the tracer-based NMR experiment using [U-$^{13}C_6$]-glucose. Values are normalized to control cells. Student's t-test was performed. Error bars represent SEM. ns, not significant, *p < 0.05.

4.7.2. ATG3 depletion sensitizes leukemia cells to inhibition of mitochondrial metabolism

The increase in mitochondrial OXPHOS and TCA cycle upon loss of ATG3 suggest that AML cells highly rely on mitochondrial metabolism. To analyze the dependence of AML cells on mitochondrial metabolism, I firstly deprived AML cells from glutamine.[63] Glutamine is a carbon source entering the TCA cycle after conversion to glutamate and subsequently to α-Ketoglutarate, a process termed glutaminolysis. Many cancer cells rely on glutaminolysis for sufficient generation of energy and cell proliferation.[66] Control and ATG3-depleted AML cells were cultivated with or without glutamine for 7 days and counted at the indicated time points. Interestingly, THP-1 and MV4-11 cells showed a reduction in cell growth that was independent of ATG3 when glutamine was deprived (**Figure 30A**).[63]

To directly compare the dependence of ATG3-depleted AML cells on glucose or mitochondrial metabolism, glycolysis or OXPHOX were shut down by using 2-DG or O/A treatment, respectively. THP-1 and MV4-11 cells were treated with the inhibitors for 24 hours and cells were counted by trypan blue exclusion (**Figure 30B**, **C**). Control cells showed reduced proliferation with both glycolysis inhibition and OXPHOS inhibition. Notably, 2-DG treatment did not impair proliferation but rather had no effect in ATG3-depleted AML cells indicating that the cells were resistant to the inhibition of glycolysis. Importantly, OXPHOS inhibition by O/A treatment significantly impaired cell proliferation upon loss of ATG3. This reduction in proliferation upon O/A treatment was more severe in ATG3 knockdown cells compared to control cells (**Figure 30C**).[63] In summary, this data suggests that the survival of AML cells highly relies on mitochondrial metabolism, particularly OXPHOS, upon loss of ATG3.[63]

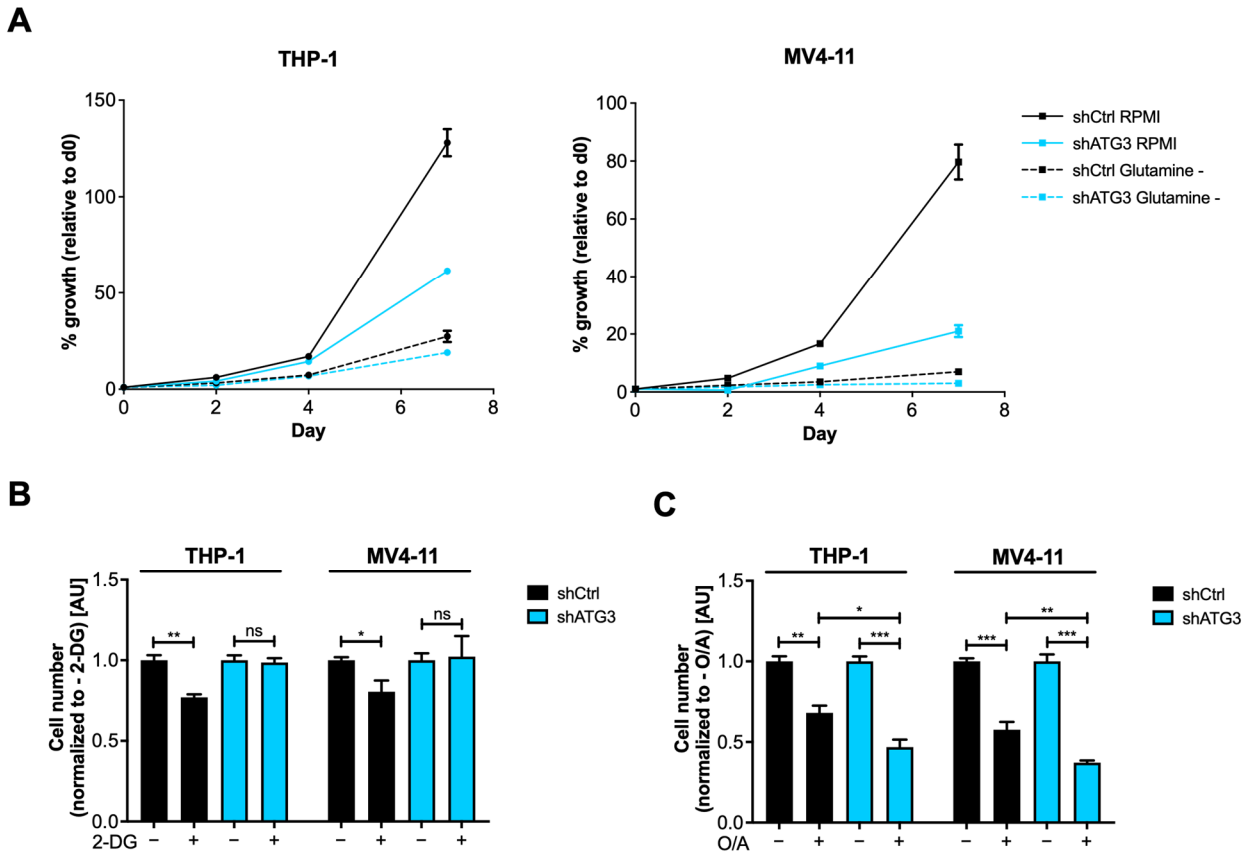

Figure 30. ATG3 depletion sensitizes leukemia cells to OXPHOS inhibition. (A) Proliferation curves of THP-1 and MV4-11 cells upon loss of ATG3. Control and ATG3-depleted AML cells were incubated in normal or glutamine-deprived medium. Cells were seeded on day 0 and cultivated for 7 consecutive days. Cells were counted on indicated days using trypan blue exclusion. (B) Bar graph depicts the relative cell number of control and ATG3 knockdown AML cells treated with 1 mM 2-DG for 24 hours normalized to untreated conditions. (C) THP-1 cells were treated with 2 µM and MV4-11 cells with 1 µM of each oligomycin and antimycin A (O/A). Treatment was performed for 24 hours, and cell number was normalized to untreated conditions.[63] Figures were adapted from Baker *et al.*, 2021. Student's t-test was performed in (B, C). Error bars represent SEM. ns, not significant, *p < 0.05, **p < 0.01, ***p < 0.001.

5. Discussion

In this study, ATG3 was identified as an important core autophagy gene for the survival of AML cells in a CRISPR/Cas9 proliferation screen using a library targeting 192 autophagy-related genes. Autophagy deficiency by shRNA-mediated depletion of ATG3 revealed that human AML cells rewire their energy metabolism as a compensatory mechanism to maintain cell survival upon ATG3 loss. In detail, NMR analysis showed an increased activation of glycolysis and OXPHOS when ATG3 was depleted accompanied by elevated ROS levels and increased ATP production. Importantly, ATG3-deficient AML cells were resistant to the inhibition of glycolysis by 2-DG treatment, but OXPHOS inhibition by oligomycin/ antimycin A treatment severely impaired AML cell survival. These results indicate the dependence on mitochondrial metabolism as an arising metabolic vulnerability when autophagy is impaired by loss of ATG3.[63]

5.1. The role of autophagy in acute myeloid leukemia

Several studies have demonstrated that autophagy is important for AML cell survival. Yet, there are different conclusions about the role of autophagy in AML. On the one hand, there is evidence of a tumor-suppressive role for autophagy in AML.[63] Watson *et al*. found that deletion of the core autophagy genes ATG5 and ATG7 contributes to AML cell proliferation *in vivo* and *in vitro*.[52,63] On the other hand, Sumitomo *et al*. showed that apoptosis was induced and progression of murine leukemia cells was impaired upon loss of ATG5 and ATG7,[57] indicating the tumor-promoting function of autophagy.[63] Therefore, the role of autophagy in AML cell survival or cell death is still controversial and may be affected by the stage of tumorigenesis.[47,63,173]

CRISPR/Cas9 screening is emerging as a tool to identify genes that are important for the survival of various cancers, including AML.[174–176] In several CRISPR/Cas9 screens, knockout of different core autophagy genes strongly inhibited autophagy and inhibition of autophagy adversely correlated with cell proliferation.[63,133,177] In this study, 23 autophagy-related genes were identified as dropout hits (**Figure 7**, **8**) and among those were three core autophagy genes, which reduced AML cell proliferation upon deletion (**Figure 9**, **10**).[63] Particularly ATG3 deletion impaired leukemogenesis of BCR-Abl positive cells by promoting p53-mediated apoptosis.[119] This is in agreement with the impaired proliferation of AML cells I observed upon loss of ATG3 in proliferation analyses of different AML cell lines as well as in the reduced S-phase of the cell cycle analysis by BrdU staining (**Figure 12**, **15**). Furthermore, flow cytometry and western blot revealed an induction of apoptosis similar to the observations by Altman *et al*. (**Figure 16**). Taken together, these results indicate the importance of ATG3 for

the survival of AML cells.[63] However, proliferation, cell cycle, and apoptosis analyses showed that even though autophagy inhibition by ATG3 depletion impaired AML cell growth, reduced S-phase, and resulted in around 50% cell death, ATG3-depleted cells could still proliferate slowly (**Figure 12, 15, 16**). These observations suggest that compensatory mechanisms occur in these AML cells to overcome ATG3 loss.[63]

ATG3 is a crucial factor involved in autophagosome formation and contributes as an E2-like enzyme to the lipidation of LC3.[113] Deletion of ATG3 resulted in impaired autophagosome and autolysosome formation in mouse embryonic fibroblasts.[118] In CML, loss of ATG3 disrupted autophagy, shown by reduced accumulation of the ATG8 proteins LC3-II, Gate-16, and GABARAP and a smaller number of GFP-LC3 punctae per cell.[119] Similarly, I observed impaired autophagy flux upon CRISPR/Cas9-mediated loss or shRNA-mediated depletion of ATG3 measured by the autophagy flux reporter in two AML cell lines (**Figure 11, 13**). Furthermore, ATG3 depletion led to reduced LC3-II levels, and less LC3-positive punctae in THP-1 and MV4-11 cells (**Figure 13**, **14**). In summary, these results show the essential role of ATG3 in autophagosome formation.[63]

However, a few studies have pointed out a non-canonical way of autophagy, which happens independently of ATG5, ATG7, ATG3 and LC3-lipidation. In Drosophila, the E1-like and E2-like enzymes Atg7 and Atg3 and the lipidation of Atg8a were shown to be indispensable for autophagy under nutrient conditions.[178] Furthermore, under cytotoxic stress induced by the cytostatic agent etoposide double membrane structures like autophagosomes and autolysosomes were observed in ATG5$^{-/-}$ MEFs indicating an alternative macroautophagy pathway. Alternative macroautophagy was further observed under nutrient stress and only the ULK1 complex and the PI3K complex were shown to be important for the formation of autophagosomal structures whereas ATG7, ATG9, ATG12, ATG16 and LC3-lipidation were not.[179] Nevertheless, these two studies were not performed in the context of cancer and may not represent the mechanism of autophagy as it takes place in leukemia. I observed a clear block of autophagy in ATG3-depleted THP-1 cells, which could not partially be rescued by starvation-induced autophagy. Therefore, ATG3-independent autophagy was not examined in this study. In MV4-11 cells however, a complete block of autophagy by loss of ATG3 was not achieved, shown by the slight induction of autophagy upon starvation (**Figure 13**). Also, autophagy was analyzed using LC3-based assays in this study and therefore no conclusion can be drawn regarding the occurrence of alternative autophagy in AML cells upon loss of ATG3.

5.2. The role of autophagy and ATG3 in mitochondrial homeostasis

The regulation and maintenance of mitochondrial homeostasis by autophagy was demonstrated in several studies. Disruption of a complex consisting of ATG12 and ATG3 did not impair starvation-induced autophagy but resulted in an accumulation of fragmented mitochondria.[180] In contrast, ATG3-dependent autophagy was shown to be important for the regulation of mitochondrial homeostasis.[181,182] In cancer, mitochondrial homeostasis was significantly disturbed by the loss of core autophagy genes. Deletion of ATG7 caused an accumulation of swollen and deformed mitochondria in lung cancer cells.[183] Furthermore, disorganized mitochondrial cristae, impaired OXPHOS, and impaired mitophagy were observed upon loss of ATG7.[59] In contrast, Hirota *et al*. showed that selective degradation of mitochondria by mitophagy does not occur via the canonical autophagy pathway, but is mediated by an alternative autophagy pathway in which autophagy-related genes are not required.[184] Similarly, I did not observe differences in mitophagy flux between control and ATG3-depleted AML cells measured by the mt-mKEIMA reporter (**Figure 17**). Furthermore, the mitochondrial membrane potential was not disturbed, and the mitochondrial mass was not altered in ATG3-depleted AML cells compared to control cells (**Figure 18**, **19**), suggesting that mitochondrial function and turnover were unaffected by loss of ATG3. This data suggests that ATG3 is not needed for the maintenance of mitochondrial homeostasis by mitophagy, which is a novel finding, also in the context of AML. However, little is still known about the role of ATG3 in mitochondrial homeostasis and to understand the different functions of autophagy-related genes in bulk autophagy and mitophagy, further studies are needed.[63]

Another aspect of mitochondrial homeostasis is mitochondrial function, which plays a key role in tumorigenesis and is important for cancer stem cell survival and drug resistance.[185] In leukemia, loss of ATG7 resulted in increased ROS levels accompanied by an upregulated mitochondrial activity.[57,63,186] This is in line with the results in this study showing that upon loss of ATG3, as well as ATG5 and ATG7, AML cells displayed enhanced cellular ROS and mitochondrial superoxide levels (**Figure 20**).[63] As a staining of total ROS by DHR123 also depicts superoxide levels, it is expected that total ROS and mitochondrial superoxide are both increased in AML knockdown cells (**Figure 20**). The increased mitochondrial ROS levels could not be explained by a disruption of mitochondrial membrane potential[187] as I did not observe higher levels of mitochondrial depolarization upon loss of ATG3 (**Figure 18**).[63] Knowing this and given the fact, that mitochondrial ROS are a by-product of OXPHOS,[83] it is likely that the higher levels of mitochondrial superoxide are a result of increased mitochondrial respiration occurring to overcome ATG3 loss.[63] Furthermore, increased oxidative stress also induces apoptosis,[149] which might be one explanation for the increased apoptosis levels in both AML cell lines after ATG3 loss (**Figure 16**).

In accordance with the elevated mitochondrial superoxide levels, higher glutamine and glutathione concentrations were observed in ATG3-deficient AML cells (**Figure 24**). Glutamine is one major precursor of glutathione, which is a tripeptide consisting of cysteine, glycine, and glutamate.[188] Glutathione was linked to cancer progression and chemotherapy resistance and was particularly shown to be crucial for neutralizing peroxides from mitochondria.[63,82,189] Leukemia cells showed an aberrant glutathione metabolism indicated by elevated glutathione levels and a higher vulnerability towards an inhibition of the glutathione pathway.[63,190] In this study, I observed high levels of ROS and elevated glutathione production originating from glucose-derived carbon upon ATG3-deficiency in AML cells (**Figure 20**, **28**), indicating that the redox homeostasis is altered, and that this changes in redox state might compensate for ATG3 deficiency and contribute to cell survival.[63] However, glutathione is not the only ROS scavenger. NADPH, needed for ROS neutralization, is primarily generated at the oxidative branch of the pentose phosphate pathway, as well as during the generation of pyruvate from malate by malic enzyme and the production of α-KG from isocitrate by isocitrate dehydrogenase.[63,191] Hence, elevated ROS levels could require increased NADPH production, which is achieved by upregulated TCA cycle activity that occurs upon loss of ATG3 (**Figure 28**).[63]

In breast cancer cells, loss of ATG5 and ATG7 resulted in increased basal and maximal respiration.[63,192] Also AML cells displayed higher basal oxygen consumption compared to healthy HSCs.[193] In line with this, I found elevated oxygen consumption shown by increased basal and maximal respiration, as well as ATP production in ATG3-depleted THP-1 and MV4-11 cells (**Figure 22**).[63] The upregulation of OXPHOS was further reflected by the increased concentrations of succinate and fumarate observed upon loss of ATG3 (**Figure 24**),[63] as the TCA cycle and OXPHOS are closely linked.[91] Moreover, increased ATP levels (**Figure 21**), upregulated OXPHOS (**Figure 22**), and elevated mitochondrial ROS levels (**Figure 20**) were not accompanied by enhanced mitochondrial damage (**Figure 18**), indicating increased mitochondrial activity to compensate autophagy deficiency by loss of ATG3.[63] However, the question arises how the upregulation of mitochondrial respiration is achieved without hyperpolarization of the membrane potential, since ATP production and mitochondrial membrane potential are usually balanced.[194] As JC-1 analysis revealed no alterations in the membrane potential of mitochondria (**Figure 18**), further analyses are needed to answer this question.[63] Nevertheless, other studies also showed that increased ATP production is possible without a significant hyperpolarization of mitochondria as hyperpolarization depends on several factors including ATP synthase activity.[195,196] In addition, it was observed that a mild depolarization and an increased expression of hexokinase result in a higher mitochondrial respiration accompanied by increased ATP production when glucose is available.[197]

It is also noted that both AML cell lines showed a substantial higher OCR upon ATG3 loss compared to control cells (**Figure 22**). One cause for the observed increase in basal respiration might be a higher availability of ADP or of substrates, such as succinate, for mitochondrial respiration.[63,198] Indeed, NMR analysis revealed that the succinate concentration was elevated upon loss of ATG3 (**Figure 24, 28**). To completely understand the underlying mechanism of upregulated OXPHOS to overcome ATG3 deficiency, a more detailed analysis of mitochondrial respiration and membrane potential would be necessary with other assays, as inhibitor treatments affect the physiological processes in mitochondria during Seahorse analysis.[63,199]

5.3. Metabolic rewiring in leukemia

5.3.1. Alterations of the glycolytic pathway

By metabolic rewiring proliferating cancer cells can adjust to altered conditions by shifting from glycolysis to OXPHOS or vice versa.[63,200] Cancer cells are known to consume larger amounts of glucose and produce more lactate by glycolysis compared to their healthy counterparts.[201] Also AML cells were shown to upregulate glycolysis and strongly depend on glucose metabolism.[68,77,78] Notably, the consumption of glucose analyzed by spectrophotometry was significantly increased in ATG3-depleted AML cells (**Figure 23**) and tracer-based NMR analysis revealed an upregulation of glucose uptake and utilization to lactate in ATG3-deficient AML cells (**Figure 24**, **26**).[63]

Many cancer cells, which rely on glycolysis for energy production thereby producing excessive amounts of lactate, export the generated lactate via MCT transporters to prevent intracellular acidification. Intracellular acidification subsequently results in cell death.[63,72] Saulle *et al*. found that MCT-4 was overexpressed in AML cells, which negatively correlated with patient survival, and proposed the inhibition of MCT-4 in combination with conventional chemotherapy as a novel therapeutic option for AML.[202] Furthermore, AML cells were shown to require an alkalic intracellular pH for proliferation as knockout of MCT-4, which mediates the export of protons and lactate, impaired leukemia cell growth.[203] Surprisingly, in ATG3 deficiency, lactate production was not accompanied by increased lactate excretion as expected but lactate excretion was decreased shown by the extracellular lactate concentration measurements and ECAR analysis (**Figure 27**). These results suggest that ATG3 might be involved in the regulation of intracellular pH by lactate export. Loss of ATG3 may impair the capacity of lactate excretion in AML cells resulting in an accumulation of lactate inside the cell.[63] As lactate is also converted to pyruvate and subsequently fuels the TCA cycle, it can further serve as a source for energy generation, and for biosynthesis of lipids and amino acids.[63,168,204] Consequently, instead of exporting the produced lactate, the ATG3-depleted AML cells might

further metabolize it. Thus, further investigation of lactate metabolism in AML cells upon impaired autophagy deficiency would contribute to the understanding of the arising compensatory mechanism.[63]

5.3.2. Alterations of mitochondrial metabolism

Cancer cells that rely on oxidative phosphorylation need glutamine as an energy source for mitochondria. Glutamine is considered essential for cancer cells as the synthesis of glutamine is insufficient to meet the needs of glutamine by glutamine-utilizing enzymes.[205,206] Guo *et al*. found that in starvation glutamine supplementation could rescue impaired mitochondrial function, reduced ATP levels, and decreased nucleotide pools upon ATG7 deficiency in Ras-driven lung cancer cells thereby promoting cell survival.[59,63] In this study, ATG3 depletion resulted in an increased glutamine uptake (**Figure 23**). Also, the necessity of glutamine for AML cell proliferation was observed, which was not dependent on ATG3 (**Figure 30**).[63] Furthermore, the increase of ^{13}C labelled carbon levels in glutamine and arginine upon loss of ATG3, as well as in glutathione, which was derived from glutamine, indicate an upregulated mitochondrial metabolism in ATG3-depleted AML cells (**Figure 24**, **28**).[63]

Increased mitochondrial respiration measured by oxygen consumption and the quantification of ATP levels revealed enhanced OXPHOS and ATP production in ATG3-deficient AML cells (**Figure 21**, **22**), which is in line with the observation that blocking autophagy by ATG7 depletion increased mitochondrial respiration, and TCA cycle activity in CML cells, suggesting a role of autophagy in regulating cellular metabolism.[186] In this work, also loss of ATG5 or ATG7 resulted in increased mitochondrial superoxide levels and ATP production, indicating a more general autophagy phenotype than an ATG3-specific phenotype (**Figure 20**, **21**). MitoTracker™ Green and western blot analysis showed that control and ATG3-depleted AML cells did not differ in their mitochondrial mass (**Figure 19**).[63] Therefore, the increased OXPHOS can probably not be explained by a higher number of mitochondria in ATG3-depleted THP-1 and MV4-11 cells. NMR analysis further revealed increased concentrations of the TCA cycle intermediates fumarate and succinate (**Figure 24**) as well as glucose-derived succinate by tracer-based NMR (**Figure 28**) in ATG3-depleted AML cells. This data suggests that the TCA cycle activity was upregulated upon autophagy deficiency.[63] This increased TCA cycle activity could further explain enhanced ATP production since NADH and $FADH_2$ generated in the TCA cycle are used for electron transfer in the ETC to produce ATP.[91] Taken together, loss of ATG3 increased both glycolysis and OXPHOS in AML cells (**Figure 22**, **24**, **26**), which is in contrast to a study showing that leukemia cells switched their metabolism from glycolysis to oxidative phosphorylation upon loss of ATG7.[63,186] One reason for this particular switch observed by Karvela *et al.* could be a compensation to increase ATP production, since

glycolysis yields very little ATP, or a negative feedback from the high ATP levels that resulted from an upregulated OXPHOS, which consequently impaired glycolysis.[63,74,186]

5.3.3. The diversity of metabolic reprogramming in leukemia cells

Tracer-based NMR analysis also showed that THP-1 and MV4-11 cells differ in their production and accumulation of some glucose-derived metabolites (**Figure 29**). This is expected based on the fact that the two AML cell lines differed in their proliferation rates (**Figure 12**) and harbor various driver mutations,[141,142,145] implying a profoundly different metabolism. In contrast to the TCA cycle intermediate succinate, malate concentration was not increased in ATG3 deficiency (**Figure 29**), but there was a trend towards an increase in THP-1 cells. Since the fold change of the amino acid aspartate was not altered in THP-1 cells but increased significantly in MV4-11 cells upon loss of ATG3 (**Figure 29**), one possible reason for the differences in fold change of both metabolites could be a different utilization of the malate aspartate shuttle. This shuttle transfers electrons across the mitochondrial membrane, which are required for mitochondrial respiration,[207] and was identified to contribute to the NAD^+/NADH homeostasis in leukemia cells.[208] A recent study investigated the role of the malate aspartate shuttle in colon cancer and found that the cancer cells, which showed increased glycolysis and OXPHOS, rely on this shuttle for NAD+/NADH homeostasis to support the oxidation of glucose-derived lactate in mitochondria.[209]

In general, amino acids are needed for protein synthesis, nucleotide synthesis, fatty acid synthesis, redox homeostasis, and to feed the TCA cycle.[170] Several amino acids were analyzed by using tracer-based NMR in this work. Among those, also alanine and proline were differently labelled in THP-1 and MV4-11 cells in ATG3 deficiency (**Figure 28**). However, further analyses, including the activity and expression of certain enzymes, are necessary to make valid assumptions about the meaning of changes in the various metabolic pathways. Interestingly, in contrast to glutamine levels (**Figure 28**), ^{13}C labelled glutamate was increased in THP-1 cells upon loss of ATG3 but not in MV4-11 cells (**Figure 29**). Glutamate is important for the synthesis of glutamine, alanine, aspartate, and proline amongst others. AML cells were shown to depend on glutamate, as well as its precursors glutamine and proline, and on enzymes involved in glutamate synthesis.[170] As the glutamate metabolism is very complex, a more detailed analysis would be necessary to elucidate the metabolic mechanisms behind the different levels of glutamate in THP-1 and MV4-11 cells upon loss of ATG3. However, only certain metabolites could be detected and analyzed by NMR spectroscopy, and therefore the described assumptions and conjectures need to be investigated and verified by other methods to understand the relevance of the different ^{13}C accumulation in each metabolite for overall metabolism.

Interestingly, I observed that both AML cell lines vary in their dependency on glucose and glutamine. THP-1 cells showed a higher glucose dependency and higher lactate production levels compared to MV4-11 cells, while MV4-11 cells displayed a higher glutamine consumption (**Figure 23**, **27**). The varying utilization of glucose and glutamine in both AML cell lines could be explained by their p53 status. MV4-11 cells express a p53 wild-type protein, while THP-1 cells display a partial deletion in p53.[145] p53 regulates the expression of autophagy genes and ATG7 was found to negatively regulate its activation connecting both homeostasis maintaining pathways.[210,211] Moreover in healthy cells, p53 is known to regulate cellular metabolism by reducing glycolysis and promoting OXPHOS.[212] However, despite differences in some metabolites both THP-1 and MV4-11 cells increased their glucose uptake, glycolysis, and mitochondrial metabolism upon loss of ATG3 (**Figure 22, 23, 26, 28**).

5.4. Mitochondrial dependence of AML cells

Several studies pointed out that metabolism regulates autophagy,[104] which was shown by inhibition of glycolysis and consequent induction of autophagy.[69,90] Likewise, autophagy flux of THP-1 and MV4-11 cells was increased when cells were treated with 2-DG to inhibit glycolysis (**Figure 25**). The inhibition of glycolysis further resulted in impaired AML cell proliferation of control cells (**Figure 30**). Interestingly, ATG3-depleted AML cells were resistant to impaired glycolysis as these cells could still proliferate when treated with 2-DG (**Figure 30**). However, inhibition of OXPHOS by oligomycin and antimycin A dramatically decreased cell proliferation of ATG3-deficient AML cells (**Figure 30**).[63] This is in accordance with a study showing that OXPHOS was upregulated in AML cells compared to normal HSCs. They further found that inhibition of mitochondrial translation impaired AML cell survival.[213] Also, Škrtić *et al*. observed the sensitivity of leukemia cells to pharmacological inhibition of mitochondrial translation.[193] Furthermore, inhibition of mitochondrial metabolism by mitotoxic drugs, which severely inhibited AML cell survival, was possible at low doses that did not affect healthy blood cells pointing to mitochondria as a potential therapeutic target.[214] In summary, the dependence of leukemia cells on mitochondria and mitochondrial metabolism further increased in the absence of ATG3.[63]

A study by Suganuma *et al*. analyzed several AML cell lines and found different dependencies on energy metabolism pathways. THP-1 cells were described as OXPHOS-dependent due to the decreased cell proliferation after OXPHOS inhibition by oligomycin compared to inhibition of glycolysis by 2-DG.[63,215] In contrast, I found that cell growth of THP-1 control cells was impaired to a similar extent by treatment with glycolysis and OXPHOS inhibitors (**Figure 30**). Importantly, sensitivity to OXPHOS inhibition significantly increased upon ATG3 knockdown (**Figure 30**). This result suggests that AML cells are more dependent on OXPHOS in ATG3

deficiency.[63] Furthermore, targeting mitochondria is used as a therapeutic strategy against different cancers.[63,83,216,217] Different approaches were investigated with drugs against the TCA cycle, OXPHOS, the ETC, ROS homeostasis, glycolysis, and mitochondrial DNA, amongst others.[216] Combining the lysosomal inhibitor HCQ and the mitochondrial DNA inhibitors mitoxantrone and etoposide is already tested in first clinical studies.[63,218] Moreover, novel autophagy inhibitors like SBI-0206965 combined with the BCL-2 inhibitor venetoclax (involved in apoptosis) showed promising first results for the treatment of AML.[63,219] The data obtained in this work demonstrate the arising vulnerability of ATG3-deficient AML cells towards mitochondrial inhibition, suggesting that a combination of mitochondrial and autophagy inhibition may be a promising therapeutical strategy for AML. Additionally, considering that ATG3 is an E2-like conjugating enzyme, the combination of an ATG3 specific inhibitor with mitochondrial inhibitors in AML may be an interesting therapeutic option.[63]

5.5. Conclusion

In conclusion, this work identified ATG3 as an important autophagy-related gene for the proliferation, autophagy function, and metabolic regulation in AML cells. Upon disruption of autophagy by ATG3 depletion, proliferation was impaired and AML cells rewired their metabolism by upregulating glycolysis accompanied by an increased production of lactate that remained inside the cell. AML cells further increased their glutamine consumption, and hyperactivated their TCA cycle and their mitochondrial oxidative phosphorylation, resulting in increased ATP levels. Moreover, ROS levels were increased likely because of increased OXPHOS, as well as levels of the ROS scavenger glutathione. Inhibition of OXPHOS strongly impaired cell survival of ATG3-depleted AML cells indicating a metabolic vulnerability that arose from autophagy impairment by ATG3 depletion (summarized in **Figure 31**).[63]

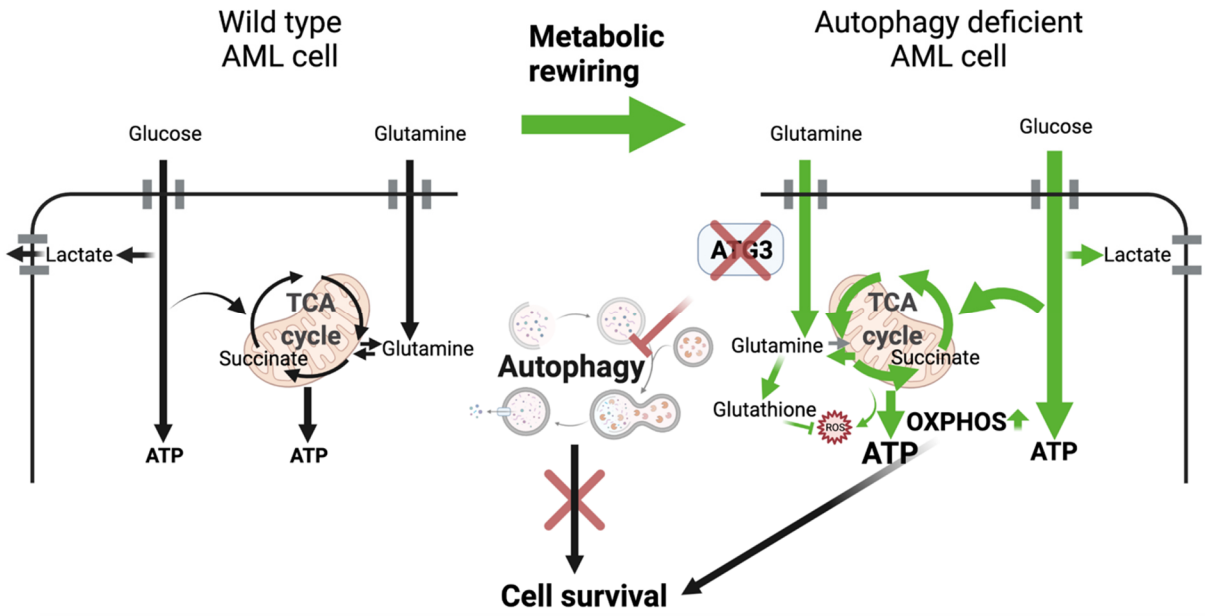

Figure 31. Metabolic rewiring in ATG3-deficient AML cells. Glucose uptake and glycolysis were upregulated upon ATG3 depletion accompanied by increased production of lactate, which remained inside the cells as lactate export was not upregulated. Loss of ATG3 increased glutamine consumption and TCA cycle and OXPHOS activity leading to increased ATP levels and enhanced ROS levels. These alterations, referred to collectively as metabolic rewiring, promote cell survival of AML cells and lead to increased dependence on OXPHOS upon loss of ATG3.[63] This figure was adapted from *Baker et al.*, 2021.

6. Outlook

In this study the role of ATG3 in cell proliferation and in cellular and mitochondrial metabolism of AML cells has been intensively studied. However, some unanswered questions remain.

6.1. Molecular mechanisms of the metabolic alterations upon loss of ATG3

One open question addresses the molecular mechanisms that are causing the observed metabolic alterations. The detailed mechanism of how AML cells are able to upregulate glucose uptake, glycolysis, TCA cycle and OXPHOS upon loss of ATG3 needs to be further investigated.

Different studies have pointed out the increase of glucose transporter expression and the altered activation of enzymes involved in different metabolic pathways in AML.[68] To analyze the molecular mechanisms by which autophagy-deficient AML cells upregulate their glucose uptake, changes in the expression of different proteins like glucose transporters, the initial glycolysis enzyme hexokinase, or other glycolytic enzymes by western blot analyses could be of interest. For a more detailed analysis and to link the metabolic alterations to changes in protein expression mass spectrometry could be the method of choice to study the proteome of AML cells in the presence and absence of ATG3. Furthermore, upregulation of macropinocytosis by the transcription factor NRF2 was identified as a compensatory mechanism to allow nutrient uptake from extracellular sources for energy production upon autophagy inhibition in cancer cells.[220] Macropinocytosis is a form of bulk endocytosis in cells and is used to take up extracellular fluids containing macromolecules from the medium. [220,221] It can be analyzed by using fluorescence-labeled dextran and monitoring the uptake of dextran, which due to its size can only be taken up via macropinocytosis. Therefore, it would be interesting to study whether an upregulation of macropinocytosis could explain the increase in glucose uptake in ATG3-deficient AML cells.

It would further be interesting to investigate why both glycolysis and OXPHOS were upregulated in ATG3-deficient AML cells.[63] Usually, glycolysis and OXPHOS cooperate but also compete for maintaining cellular energy homeostasis.[71] In hypoxia upregulation of glycolysis compensates for weakened ATP production by OXPHOS for energy balance. On the other hand, normal function of OXPHOS regulates glycolytic activity.[71] Increased sensitivity towards mitochondria inhibiting agents in leukemic cells has been described,[94,213] and AML cells are known to depend on OXPHOS,[214,218] but the question remains why autophagy deficiency results in the dramatic increase in OXPHOS dependency.[63]

6.2. Relation of ATG3's enzymatic activity to the proliferation and metabolic phenotypes in ATG3-depleted AML cells

As loss of ATG3 impaired leukemia cell proliferation and resulted in an altered energy metabolism, the question arises whether impaired autophagy caused the observed phenotypic changes. The direct relationship between the E2-like enzymatic activity of ATG3 and the observed proliferation impairment and altered metabolic phenotype needs further investigation to elucidate whether an autophagy-independent function of ATG3 is important in this scenario.[63] Radoshevich *et al*. found an autophagy-independent role of the ATG3-ATG12 complex in maintaining mitochondrial homeostasis.[180] However, this was challenged by other studies.[181,182] To address this issue, ATG3 mutants with a point mutation inhibiting its E2-like enzymatic activity could be analyzed for their growth and metabolic phenotype and compared to ATG3 wild-type expressing AML cells. This kind of experiment is challenging to perform though, as I observed in preliminary experiments that the expression of ATG3 is tightly regulated, and minor expression changes unexceptionally result in an immediate autophagy block. Therefore, an inducible expression of mutant ATG3 in ATG3-deficient AML cells might be a useful tool to answer this question. Furthermore, inhibition of the enzymatic activity by an ATG3 inhibitor could be used to evaluate the potential of ATG3 inhibition for the treatment of AML in *in vivo* AML xenograft models.[63]

6.3. Causes for apoptosis induction upon loss of ATG3

In addition, this study analyzed the alterations that occur upon loss of ATG3 to promote cell survival. However, around 50% of cells die (**Figure 16**) and the reasons remain elusive. Thus, analyzing the mechanisms inducing apoptosis in autophagy-deficient AML cells could help to understand the alterations occurring upon ATG3 deletion. Other studies have shown that AML cells are susceptible to oxidative stress, which induced apoptosis.[213] In preliminary experiments with NAC, an antioxidant reducing ROS levels within cells, treatment slightly reduced mitochondrial superoxide levels (Appendix **Figure 34A**), which was accompanied by slightly increased cell survival in ATG3-deficient AML cells compared to untreated cells (Appendix **Figure 34B**). Nevertheless, the concentration that was needed to promote cell survival was very high, resulting in cytotoxic effects in AML cells expressing ATG3 (Appendix **Figure 34B**). Therefore, further studies are needed to elucidate whether the high ROS levels that occur upon ATG3 loss contribute to the induction of apoptosis in AML cells. Also, the increased production and reduced export rate of lactate leading to high intracellular lactate levels and potentially to an intracellular pH acidification in ATG3-depleted AML cells might contribute to apoptosis induction. AML cells are known to prefer an alkaline intracellular pH and knockout of the monocarboxylate transporter 4, resulted in lactate accumulation and

impaired cell survival.[222] Experiments analyzing intracellular pH and the effect of acidic pH in AML cells might contribute to understanding the cause of increased apoptosis upon ATG3 loss.

7. Zusammenfassung

Die akute myeloische Leukämie (AML) ist eine aggressive Erkrankung des Knochenmarks, welche als Folge genetischer und epigenetischer Veränderungen entsteht. Durch die klonale Expansion von undifferenzierten myeloischen Vorläuferzellen reichern sich primitive Blasten im Knochenmark an, welche nicht funktional sind. Dadurch wird die normale Hämatopoese beeinträchtigt und es kommt zum Knochenmarksversagen. Die AML hat im Vergleich zu anderen Leukämien die höchste Inzidenz weltweit. Sie entwickelt sich aufgrund einer vorangegangenen Krebstherapie, primärer hämatologischer Erkrankungen oder überwiegend *de novo* bei vorher gesunden Patienten. Der Krankheitsverlauf ist akut, sehr progressiv und führt unbehandelt zum Tod des Patienten. Trotz des Fortschritts in der AML-Therapie haben die meisten Patienten eine schlechte Prognose, weshalb dringend neue Therapieansätze für die Behandlung benötigt werden. Verschiedene Studien konnten zeigen, dass die Autophagie bei der Entstehung und Aufrechterhaltung von AML eine Rolle spielt.

Autophagie ist ein evolutionär konservierter Abbauprozess, bei dem zelluläre Komponenten in sogenannten Autophagosomen eingeschlossen werden. Diese Autophagosomen fusionieren mit Lysosomen und die zellulären Komponenten werden nachfolgend durch lysosomale Enzyme abgebaut. ATG3, das als E2-ähnliches Konjugationsenzym die Lipidierung von LC3 herbeiführt, ist bekanntermaßen wichtig für die Autophagosomenbildung. Als zentraler Regulator von Zellüberleben, Homöostase und Stoffwechsel dient die Autophagie unter Stressbedingungen wie Nährstoffentzug als Nährstoffquelle durch die Wiederverwertung von Makromolekülen. AML-Zellen benötigen ein konstantes Nährstoff- und Energieniveau, um ihre Vermehrung und ihr Überleben aufrechtzuerhalten. Dieses wird durch eine Umstellung von Stoffwechselwegen, insbesondere des mitochondrialen Stoffwechsels einschließlich der oxidativen Phosphorylierung (OXPHOS) und des Tricarbonsäurezyklus (TCA Zyklus), erreicht.

Mehrere Studien haben die Hemmung der Autophagie für die Behandlung von Krebs untersucht und als vielversprechenden Ansatz vorgestellt. Doch eine Monotherapie mit Autophagie-Inhibitoren erzielte nur eine geringfügige Wirksamkeit. Eine mögliche Erklärung hierfür ist die Entstehung von Kompensationsmechanismen, die zum Ausgleich der Autophagie-Hemmung in Krebszellen entstehen. Bis heute sind diese Kompensations-mechanismen kaum untersucht. Ziel dieser Arbeit ist es, ein geeignetes Autophagie-Gen zu identifizieren, mit dem sich die Rolle der Autophagie für das Überleben von AML-Zellen untersuchen lässt. Die kompensatorischen Mechanismen, die durch eine Hemmung der Autophagie in AML-Zellen entstehen können, um das Zellüberleben zu sichern, sollen untersucht werden, um neue metabolische Angriffspunkte zu identifizieren, die für potentielle Kombinationstherapien genutzt werden könnten.

Um wichtige Autophagie-Gene zu identifizieren, deren Verlust eine Proliferationsstörung in AML-Zellen verursacht, welche durch Kompensationsmechanismen überwunden werden kann, wurde zu Beginn der Arbeit ein fokussierter CRISPR/Cas9 Screen durchgeführt. Dieser Screen nutzte eine Library mit Sequenzen von 192 Autophagie-relevanten Genen. Dafür wurden zwei humane AML-Zelllinien mit Library-enthaltendem Virus transduziert, selektiert und für 34 Tage kultiviert. Die Analyse der Screen-Ergebnisse zeigte, dass 23 Autophagie-relevante Gene in beiden Zelllinien wichtig für die Proliferation von AML-Zellen waren. Unter diesen 23 Genen waren drei sogenannte „core autophagy genes“, nämlich ATG3, ATG9A und ATG12, welche eine wichtige Funktion in der Autophagosomenbildung erfüllen. Es ist bekannt, dass diese „core autophagy genes“ bei verschiedenen Krebsarten, einschließlich der AML, eine sehr geringe Häufigkeit von Punktmutationen aufweisen. Darüber hinaus ergaben Transkriptom-Analysen eine weitgehend unveränderte Genexpression der „core autophagy genes“, was auf ihre Notwendigkeit für das Zellüberleben bei den meisten Krebsarten hindeutet. Daher wurde der Fokus für die Validierung der Screen-Ergebnisse auf diese drei identifizierten Gene gelegt. Die Validierungsexperimente zeigten, dass der Verlust von ATG3 eine signifikante Proliferationsstörung in den beiden AML-Zelllinien THP-1 und MV4-11 verursachte, während der Verlust von ATG9A und ATG12 nur für THP-1 Zellen zu vermindertem Zellwachstum führte. Außerdem zeigte die Messung des Autophagie-Fluxes, welcher mithilfe des GFP-LC3B-RFP Fluoreszenzreporters bestimmt wurde, dass der Verlust von ATG3 die Autophagie in beiden Ziellinien stark beeinträchtigte. Deshalb wurde die Depletion von ATG3 in AML-Zellen für alle weiteren Experimente zur Untersuchung der Mechanismen, die zum Ausgleichen der Autophagie-Hemmung entstehen, benutzt.

In fünf verschiedenen AML-Zelllinien wurde die Expression von ATG3 mit small hairpin RNA (shRNA) reduziert. In allen Zelllinien führte der Verlust von ATG3 zu verminderter Zellproliferation. Darüber hinaus wurde eine funktionelle Analyse zur Koloniebildung durchgeführt. In THP-1 und MV4-11 Zellen führte der Knockdown von ATG3 nach sieben Tagen zur signifikanten Reduktion der Kolonienbildung. Diese Ergebnisse zeigen, dass der Verlust von ATG3 die Proliferation von AML-Zellen beeinträchtigt.

Als Nächstes wurde die zentrale Rolle von ATG3 in der Autophagosomenbildung bestätigt. Eine Western-Blot-Analyse zeigte eine beeinträchtigte LC3-Lipidierung, und eine Immunfluoreszenzanalyse der Autophagosomenbildung mittels konfokaler Mikroskopie ergab eine geringere Anzahl von Autophagosomen in ATG3-defizienten Zellen. Dies zeigt, dass ATG3 für die Autophagiefunktion von großer Bedeutung ist.

Da der Verlust von ATG3 die Proliferation von AML-Zellen beeinträchtigt, wurden weitere funktionale Analysen durchgeführt. Die Zellzyklusanalyse ergab, dass der Verlust von ATG3 in einer reduzierten S-Phase resultierte, was die verminderte Proliferation in ATG3-depletierten AML-Zellen bestätigt. Doch der Zellzyklus wurde durch den ATG3 Verlust grundsätzlich nicht gestoppt. Darüber hinaus ergab die Analyse der Apoptose, dass diese unter dem Verlust von ATG3 erhöht war. Doch es lebten etwa 50% der Zellen weiter. Diese Beobachtungen deuten darauf hin, dass AML-Zellen trotz des Verlusts der ATG3-abhängigen Autophagie weiter proliferieren können.

Um die Mechanismen zu identifizieren, die die Proliferation der ATG3-depletierten Zellen ermöglicht, wurden zunächst die Auswirkungen des ATG3-Verlusts auf die mitochondriale Homöostase untersucht, da wir und andere zeigen konnten, dass die mitochondriale Homöostase und Mitophagie wichtig für das Überleben von AML Zellen ist. Die Mitophagie, der spezifische Abbau geschädigter Mitochondrien, wurde mithilfe eines mt-mKEIMA Reporters in An- und Abwesenheit von Mitochondrien-schädigender Stoffe, die die Mitophagie aktivieren, gemessen. Der Mitophagie-Flux unterschied sich zwischen Kontroll- und ATG3-depletierten Zellen unter basalen und Mitophagie-induzierenden Stressbedingungen nicht. Auch das mitochondriale Membranpotenzial war unverändert und die mitochondriale Masse war bei Kontroll- und ATG3-depletierten AML-Zellen gleich. Dies deutet darauf hin, dass die mitochondriale Homöostase und der mitochondriale Umsatz durch den Verlust von ATG3 nicht beeinträchtigt sind.

Darauffolgend wurde untersucht, ob die mitochondriale Funktion durch den Verlust von ATG3 verändert ist. Reaktive Sauerstoffspezies (ROS) entstehen hauptsächlich während der OXPHOS in Mitochondrien und sind deshalb ein Marker für mitochondriale Fitness. Deshalb wurden zuerst die ROS-Level in AML-Zellen und auch speziell die ROS-Level in den Mitochondrien analysiert. Sowohl zelluläres ROS als auch mitochondriale ROS-Level waren nach dem Verlust von ATG3 signifikant erhöht. Weiterhin wurde untersucht, ob dies ATG3-spezifische Beobachtungen sind oder ob der Verlust von anderen wichtigen Autophagie-Genen wie ATG5 und ATG7 zu ähnlichen Ergebnissen führt. In der Tat führte die Depletion von ATG5 und ATG7 zu einem ähnlichen Anstieg an zellulärem und mitochondrialem ROS. Da die ROS-Level durch den ATG3 Verlust erhöht waren, jedoch keine Schädigung der Mitochondrien beobachtet wurde, wurde nachfolgend der ATP-Gehalt pro Zelle in ATG3-depletierten Zellen bestimmt. Die Messung des ATP-Spiegels in THP-1 und MV4-11 Zellen ergab, dass mehr ATP in ATG3-depletierten AML-Zellen vorhanden ist. Auch ein Verlust von ATG5 und ATG7 erhöhte die ATP-Level in AML-Zellen. Um die mitochondriale Aktivität genauer zu quantifizieren, wurde die oxidative Phosphorylierung basierend auf der Rate des Sauerstoffverbrauchs (OCR, „oxygen consumption rate“) mithilfe

von Seahorse-Messungen bestimmt. Bemerkenswert ist, dass die Rate des Sauerstoffverbrauchs nach dem Verlust von ATG3 in AML-Zellen erhöht war. Die Quantifizierung der mitochondrialen Atmung ergab, dass die basale Respiration, der Energiebedarf der Zellen unter Ausgangsbedingungen, erhöht war. Auch die maximale Respiration, die von den Zellen erreicht werden kann, war signifikant gesteigert. Die Quantifizierung der ATP Produktion aus den OCR Daten ergab, dass nach ATG3 Verlust mehr ATP produziert wurde. Diese Ergebnisse demonstrieren eine gesteigerte mitochondriale Aktivität durch OXPHOS bei Autophagie-Defizienz.

Da Mitochondrien eine wichtige Rolle im zellulären Metabolismus spielen, wurden die metabolischen Veränderungen in ATG3-defizienten AML Zellen untersucht, um die Mechanismen zu verstehen, durch die der Verlust von ATG3 zu einer erhöhten OXPHOS und einer erhöhten mitochondrialen ROS Produktion führt. Zunächst wurde der Glukose- und Glutaminverbrauch von THP-1- und MV4 11-Zellen nach Verlust von ATG3 untersucht. Die Bestimmung der extrazellulären Konzentration dieser beiden Metabolite und die Berechnung des Verbrauchs ergaben, dass der Verlust von ATG3 den Glukose- und Glutaminverbrauch erhöhte. Um die metabolischen Veränderungen nach der Autophagie-Hemmung genauer zu identifizieren, wurde eine kernmagnetische Resonanzspektroskopie (NMR)-Analyse durchgeführt und die intrazellulären Konzentrationen der wichtigsten Stoffwechselprodukte in THP-1- und MV4-11-Zellen in Abwesenheit von ATG3 bestimmt. Es wurden erhöhte intrazelluläre Konzentrationen von Glutathion, einem Antioxidans, das für das Redox-Gleichgewicht verantwortlich ist, festgestellt. Darüber hinaus wurden erhöhte Konzentrationen wichtiger Metabolite des zentralen Kohlenstoffstoffwechsels wie Glukose, Glutamin, Glutamat und Laktat sowie der TCA-Zyklus-Zwischenprodukte Fumarat und Succinat festgestellt. Zusammenfassend deuten diese Daten stark darauf hin, dass AML-Zellen nach dem Verlust von ATG3 ihren Energiestoffwechsel hochregulieren.

Auf der Basis der beobachteten Zunahme der intrazellulären Glukosekonzentration, die mit einer verstärkten Glukoseeinnahme in ATG3-depletierten AML-Zellen einherging, wurde zunächst die Glykolyse genauer betrachtet. Es ist bekannt, dass die Autophagie durch die Glykolyse reguliert wird. Dies wurde durch eine Hemmung der Glykolyse mittels 2-Desoxyglukose (2-DG) bestätigt. Hier führte 2-DG zur Autophagie-Induktion in Kontrollzellen, während der Verlust von ATG3 die Autophagie-Induktion durch 2-DG blockierte.

Um die Folgen des erhöhten Glukoseverbrauchs in AML-Zellen mit Autophagie-Defizienz zu verstehen, wurde der Verbleib des aus Glukose gewonnenen Kohlenstoffs in An- und Abwesenheit von ATG3 untersucht. Dazu wurden THP-1 und MV4-11 Zellen 24 Stunden lang

in Medium mit isotopenmarkierter Glukose (^{13}C) kultiviert und anschließend Tracer-basierte NMR-Messungen durchgeführt. ATG3-defiziente Zellen zeigten eine intrazelluläre Zunahme der ^{13}C-Markierung in Glukose sowie einen deutlich erhöhten Einbau von ^{13}C in Laktat. Interessanterweise wurde durch spektrophotometrische Messungen kein Anstieg der extrazellulären Laktatkonzentration in ATG3-depletierten Zellen festgestellt, obwohl eine gleichzeitige Anreicherung von intrazellulärem Laktat beobachtet wurde. Um diese Beobachtung zu bestätigen und die Exportrate des Laktats zu bestimmen, wurde die extrazelluläre Ansäuerungsrate (ECAR) gemessen. Diese extrazelluläre Ansäuerungsrate war in beiden Zelllinien in Abwesenheit von ATG3 reduziert. Insgesamt zeigen diese Daten, dass die Glykolyse in AML-Zellen nach dem Verlust von ATG3 sehr aktiv ist, was zu einer erhöhten Produktion von intrazellulärem Laktat führt, welches nicht in die extrazelluläre Umgebung exportiert wird.

Die Beobachtung, dass die Glykolyse in Abwesenheit von ATG3 stark aktiviert und die ATP-Konzentration erhöht ist, lässt vermuten, dass eine metabolische Umstellung eine wichtige Rolle für das Überleben dieser AML-Zellen spielt. Da der Verlust von ATG3 eine erhöhte OXPHOS und eine Zunahme intrazellulärer Konzentrationen von TCA-Zyklus-Zwischenprodukten verursacht, wurde nachfolgend der mitochondriale Stoffwechsel mithilfe der ^{13}C-Inkorporation aus dem Tracer-basierten NMR-Experiment analysiert. Eine signifikante Anreicherung von markiertem Kohlenstoff wurde in Succinat gefunden, was die Aktivierung des mitochondrialen Stoffwechsels bei ATG3 Verlust beweist. Darüber hinaus wiesen Glutamin und Arginin eine erhöhte ^{13}C-Markierung auf, was auf ihre Produktion aus α-Ketoglutarat, einem Zwischenprodukt des TCA-Zyklus, hinweist und die Hochregulierung des mitochondrialen Stoffwechsels unter ATG3 Verlust zeigt. In Übereinstimmung mit den früheren Ergebnissen wurde auch ein signifikanter ^{13}C-Einbau in Glutathion nach dem Verlust von ATG3 in beiden Zelllinien beobachtet. Dies deutet darauf hin, dass der Verlust von ATG3 zu einer Hochregulierung der Glutathion-Produktion zur Aufrechterhaltung der Redox-Homöostase von AML-Zellen führt.

Da die Glykolyse und OXPHOS unter ATG3 Verlust hochreguliert wurden, wurde die Abhängigkeit der Leukämiezellen von beiden Stoffwechselwegen untersucht. Dazu wurden THP-1- und MV4-11-Zellen 24 Stunden lang entweder mit dem Glykolyse-Inhibitor 2-DG oder dem OXPHOS-Inhibitor Oligomycin/Antimycin A (O/A) behandelt. Der Proliferationstest zeigte, dass die Behandlung mit 2-DG und O/A in beiden AML-Zelllinien in Anwesenheit von ATG3 das Zellwachstum einschränkte. Insbesondere die ATG3-depletierten AML-Zellen waren resistent gegen die Glykolyse-Hemmung, da sie nach der 2-DG-Behandlung keinen Proliferationsdefekt zeigten. Auffallend ist, dass die OXPHOS-Inhibitoren Oligomycin und Antimycin A das Zellwachstum im Vergleich zu den Kontrollzellen deutlich reduzierten.

Diese Ergebnisse legen nahe, dass ATG3-defiziente AML-Zellen auf die mitochondriale oxidative Phosphorylierung für ihr Überleben angewiesen sind.

Zusammenfassend wurde in dieser Arbeit ATG3 als wichtiges Autophagie-Gen identifiziert, welches eine prominente Rolle in der AML-Proliferation und der Regulierung des Stoffwechsels spielt. Darüber hinaus zeigte die Untersuchung von Kompensations-mechanismen, die bei einer Hemmung der Autophagie durch ATG3 Verlust in AML-Zellen entstehen, die Abhängigkeit vom mitochondrialen Stoffwechsel als metabolischen Angriffspunkt auf.

8. References

1. Guo Y, Niu C, Breslin P, et al. c-Myc-mediated control of cell fate in megakaryocyte-erythrocyte progenitors. *Blood*. 2009;114(10):2097–2106.
2. Weissman IL. Stem cells: Units of development, units of regeneration, and units in evolution. *Cell*. 2000;100(1):157–168.
3. Koschade SE, Brandts CH. Selective Autophagy in Normal and Malignant Hematopoiesis. *J. Mol. Biol.* 2020;432(1):261–282.
4. Chopra M, Bohlander SK. The cell of origin and the leukemia stem cell in acute myeloid leukemia. *Genes Chromosom. Cancer*. 2019;58(12):850–858.
5. Dong Y, Shi O, Zeng Q, et al. Leukemia incidence trends at the global, regional, and national level between 1990 and 2017. *Exp. Hematol. Oncol.* 2020;9(14):1–11.
6. Appelbaum FR, Rowe JM, Radich J, Dick JE. Acute myeloid leukemia. *Hematol. Am. Soc. Hematol. Educ. Progr.* 2001;62–86.
7. De Kouchkovsky I, Abdul-Hay M. 'Acute myeloid leukemia: A comprehensive review and 2016 update.' *Blood Cancer J.* 2016;6(7):.
8. Vakiti A, Mewawalla P. Acute Myeloid Leukemia. Treasure Island (FL): StatPearls Publishing; 2021.
9. Tomaszewski EL, Fickley CE, Maddux L, et al. The Patient Perspective on Living with Acute Myeloid Leukemia. *Oncol. Ther.* 2016;4(2):225–238.
10. Arber DA, Orazi A, Hasserjian R, et al. The 2016 revision to the World Health Organization classification of myeloid neoplasms and acute leukemia. *Blood*. 2016;127(20):2391–2405.
11. Grimwade D, Walker H, Oliver F, et al. The importance of diagnostic cytogenetics on outcome in AML: Analysis of 1,612 patients entered into the MRC AML 10 trial. *Blood*. 1998;92(7):2322–2333.
12. Ou Z, Yu D, Liang Y, et al. Analysis of the Global Burden of Disease study highlights the trends in death and disability-adjusted life years of leukemia from 1990 to 2017. *Cancer Commun.* 2020;40(11):598–610.
13. Wang HI, Aas E, Howell D, et al. Long-term medical costs and life expectancy of acute myeloid leukemia: A probabilistic decision model. *Value Heal.* 2014;17(2):205–214.
14. Döhner H, Weisdorf DJ, Bloomfield CD. Acute Myeloid Leukemia. *N. Engl. J. Med.* 2015;373(12):1136–1152.
15. Faruqi A, Tadi P. Cytarabine. Treasure Island: StatPearls Publishing; 2021.
16. Venkatesh P, Kasi A. Anthracyclines. Treasure Island: StatPearls Publishing; 2021.
17. Pelcovits A, Niroula R. Acute Myeloid Leukemia: A Review. *R. I. Med. J. (2013)*. 2020;103(3):38–40.
18. Cassileth PA, Harrington DP, Hines JD, et al. Maintenance chemotherapy prolongs remission duration in adult acute nonlymphocytic leukemia. *J. Clin. Oncol.* 1988;6(4):583–587.
19. Thol F, Heuser M. Treatment for Relapsed / Refractory Acute Myeloid Leukemia. *HemaSphere*. 2021;5(6):e572.
20. Winer ES, Stone RM. Novel therapy in Acute myeloid leukemia (AML): moving toward targeted approaches. *Ther. Adv. Hematol.* 2019;10:1–18.
21. Rothe K, Porter V, Jiang X. Current outlook on autophagy in human leukemia: Foe in cancer stem cells and drug resistance, friend in new therapeutic interventions. *Int. J.*

Mol. Sci. 2019;20(3):.

22. Du W, Xu A, Huang Y, et al. The role of autophagy in targeted therapy for acute myeloid leukemia. *Autophagy*. 2020;22:1–15.
23. Wolpin BM, Rubinson DA, Wang X, et al. Phase II and Pharmacodynamic Study of Autophagy Inhibition Using Hydroxychloroquine in Patients With Metastatic Pancreatic Adenocarcinoma. *Oncologist*. 2014;19(6):637–638.
24. Rangwala R, Leone R, Chang YC, et al. Phase I trial of hydroxychloroquine with dose-intense temozolomide in patients with advanced solid tumors and melanoma. *Autophagy*. 2014;10(8):1369–1379.
25. Towers CG, Wodetzki D, Thorburn A. Autophagy and cancer: Modulation of cell death pathways and cancer cell adaptations. *J. Cell Biol.* 2020;219(1):1–15.
26. Briceño E, Reyes S, Sotelo J. Therapy of glioblastoma multiforme improved by the antimutagenic chloroquine. *Neurosurg. Focus*. 2003;14(2):3.
27. Levy JMM, Thompson JC, Griesinger AM, et al. Autophagy inhibition improves chemosensitivity in BRAFV600E brain tumors. *Cancer Discov.* 2014;4(7):773–780.
28. Towers CG, Fitzwalter BE, Regan D, et al. Cancer Cells Upregulate NRF2 Signaling to Adapt to Autophagy Inhibition. *Dev. Cell*. 2019;50(6):690-703.e6.
29. Dikic I, Elazar Z. Mechanism and medical implications of mammalian autophagy. *Nat. Rev. Mol. Cell Biol.* 2018;19(6):349–364.
30. Mizushima N. Autophagy in protein and organelle turnover. *Cold Spring Harb. Symp. Quant. Biol.* 2011;76:397–402.
31. Lahiri V, Hawkins WD, Klionsky DJ. Watch What You (Self-) Eat: Autophagic Mechanisms that Modulate Metabolism. *Cell Metab.* 2019;29(4):803–826.
32. Mizushima N, Yoshimori T, Ohsumi Y. The Role of Atg Proteins in Autophagosome Formation. *Annu. Rev. Cell Dev. Biol.* 2011;27(1):107–132.
33. Shaid S, Brandts CH, Serve H, Dikic I. Ubiquitination and selective autophagy. *Cell Death Differ.* 2013;20(1):21–30.
34. Li X, He S, Ma B. Autophagy and autophagy-related proteins in cancer. *Mol. Cancer*. 2020;19(1):1–16.
35. Kroemer G, Mariño G, Levine B. Autophagy and the Integrated Stress Response. *Mol. Cell*. 2010;40(2):280–293.
36. Dossou AS, Basu A. The emerging roles of mTORC1 in macromanaging autophagy. *Cancers (Basel)*. 2019;11(1422):.
37. Egan D, Kim J, Shaw RJ, Guan K-L. The autophagy initiating kinase ULK1 is regulated via opposing phosphorylation by AMPK and mTOR. *Autophagy*. 2011;7(6):643–646.
38. Kim J, Kim YC, Fang C, et al. Differential regulation of distinct Vps34 complexes by AMPK in nutrient stress and autophagy. *Cell*. 2013;17(152(1–2)):290–303.
39. Yamamoto H, Fujioka Y, Suzuki SW, et al. The Intrinsically Disordered Protein Atg13 Mediates Supramolecular Assembly of Autophagy Initiation Complexes. *Dev. Cell*. 2016;38(1):86–99.
40. Funderburk SF, Wang QJ, Yue Z. The Beclin 1-VPS34 complex - at the crossroads of autophagy and beyond. *Trends Cell Biol.* 2010;20(6):355–362.
41. Russell RC, Tian Y, Yuan H, et al. ULK1 induces autophagy by phosphorylating Beclin-1 and activating VPS34 lipid kinase. *Nat. Cell Biol.* 2013;15(7):741–750.
42. Papinski D, Schuschnig M, Reiter W, et al. Early Steps in Autophagy Depend on

Direct Phosphorylation of Atg9 by the Atg1 Kinase. *Mol. Cell*. 2014;53(3):471–483.

43. Mizushima N, Kuma A, Kobayashi Y, et al. Mouse Apg16L, a novel WD-repeat protein, targets to the autophagic isolation membrane with the Apg12-Apg5 conjugate. *J. Cell Sci.* 2003;116(9):1679–1688.
44. Kabeya Y, Mizushima N, Ueno T, et al. LC3, a mammalian homolog of yeast Apg8p, is localized in autophagosome membranes after processing. *EMBO J.* 2003;19(21):5720–5728.
45. Geng J, Klionsky DJ. The Atg8 and Atg12 ubiquitin-like conjugation systems in macroautophagy. *EMBO Rep.* 2008;9(9):859–864.
46. Chun Y, Kim J. Autophagy: An Essential Degradation Program for Cellular Homeostasis and Life. *Cells*. 2018;7(12):278.
47. Galluzzi L, Pietrocola F, Bravo-San Pedro JM, et al. Autophagy in malignant transformation and cancer progression. *EMBO J.* 2015;34(7):856–880.
48. Rao S, Tortola L, Perlot T, et al. A dual role for autophagy in a murine model of lung cancer. *Nat. Commun.* 2014;5(3056):.
49. Liang XH, Jackson S, Seaman M, et al. Induction of autophagy and inhibition of tumorigenesis by beclin 1. *Nature*. 1999;402(6762):672–676.
50. Yue Z, Jin S, Yang C, Levine AJ, Heintz N. Beclin 1, an autophagy gene essential for early embryonic development, is a haploinsufficient tumor suppressor. *Proc. Natl. Acad. Sci. U. S. A.* 2003;100(25):15077–15082.
51. Takamura A, Komatsu M, Hara T, et al. Autophagy-deficient mice develop multiple liver tumors. *Genes Dev.* 2011;25(8):795–800.
52. Watson A, Riffelmacher T, Stranks A, et al. Autophagy limits proliferation and glycolytic metabolism in acute myeloid leukemia. *Cell Death Discov.* 2015;1:15008.
53. Jin J, Britschgi A, Schläfli AM, et al. Low Autophagy (ATG) Gene Expression Is Associated with an Immature AML Blast Cell Phenotype and Can Be Restored during AML Differentiation Therapy. *Oxid. Med. Cell. Longev.* 2018;2018:1–16.
54. Yang S, Wang X, Contino G, et al. Pancreatic cancers require autophagy for tumor growth. *Genes Dev.* 2011;25(7):717–729.
55. Wei H, Wei S, Gan B, et al. Suppression of autophagy by FIP200 deletion inhibits mammary tumorigenesis. *Genes Dev.* 2011;25(14):1510–1527.
56. Poillet-Perez L, Xie X, Zhan L, et al. Autophagy maintains tumour growth through circulating arginine. *Nature*. 2018;563(7732):569–573.
57. Sumitomo Y, Koya J, Nakazaki K, et al. Cytoprotective autophagy maintains leukemia-initiating cells in murine myeloid leukemia. *Blood*. 2016;128(12):1614–1624.
58. Guo JY, Chen HY, Mathew R, et al. Activated Ras requires autophagy to maintain oxidative metabolism and tumorigenesis. *Genes Dev.* 2011;25(5):460–470.
59. Guo JY, Teng X, Laddha S V., et al. Autophagy provides metabolic substrates to maintain energy charge and nucleotide pools in Ras-driven lung cancer cells. *Genes Dev.* 2016;30(15):1704–1717.
60. Piya S, Kornblau SM, Ruvolo VR, et al. Atg7 suppression enhances chemotherapeutic agent sensitivity and overcomes stroma-mediated chemoresistance in acute myeloid leukemia. *Blood*. 2016;128(9):1260–1269.
61. Lebovitz CB, Robertson AG, Goya R, et al. Cross-cancer profiling of molecular alterations within the human autophagy interaction network. *Autophagy*. 2015;11(9):1668–1687.

62. Amaravadi R, Kimmelman AC, White E. Recent insights into the function of autophagy in cancer. *Genes Dev.* 2016;30(17):1913–1930.

63. Baker F, Polat IH, Abou-El-Ardat K, et al. Metabolic Rewiring Is Essential for AML Cell Survival to Overcome Autophagy Inhibition by Loss of ATG3. *Cancers (Basel).* 2021;13(23):6142.

64. Hanahan D, Weinberg RA. Hallmarks of cancer: The next generation. *Cell*. 2011;144(5):646–674.

65. Vazquez A, Kamphorst JJ, Markert EK, et al. Cancer metabolism at a glance. *J. Cell Sci.* 2016;129(18):3367–3373.

66. Wang Z, Liu F, Fan N, et al. Targeting Glutaminolysis: New Perspectives to Understand Cancer Development and Novel Strategies for Potential Target Therapies. *Front. Oncol.* 2020;10(589508):589508.

67. Phan LM, Yeung SCJ, Lee MH. Cancer metabolic reprogramming: importance, main features, and potentials for precise targeted anti-cancer therapies. *Cancer Biol. Med.* 2014;11(1):1–19.

68. Kreitz J, Schönfeld C, Seibert M, et al. Metabolic Plasticity of Acute Myeloid Leukemia. *Cells*. 2019;8(8):805.

69. Chu Y, Chang Y, Lu W, et al. Regulation of autophagy by glycolysis in cancer. *Cancer Manag. Res.* 2020;12:13259–13271.

70. Wang L, Pavlou S, Du X, et al. Glucose transporter 1 critically controls microglial activation through facilitating glycolysis. *Mol. Neurodegener.* 2019;14(2):1–15.

71. Zheng J. Energy metabolism of cancer: Glycolysis versus oxidative phosphorylation (review). *Oncol. Lett.* 2012;4(6):1151–1157.

72. Xie J, Wu H, Dai C, et al. Beyond Warburg effect - Dual metabolic nature of cancer cells. *Sci. Rep.* 2014;4:4927.

73. Altenberg B, Greulich KO. Genes of glycolysis are ubiquitously overexpressed in 24 cancer classes. *Genomics*. 2004;84(6):1014–1020.

74. Lunt SY, Vander Heiden MG. Aerobic glycolysis: Meeting the metabolic requirements of cell proliferation. *Annu. Rev. Cell Dev. Biol.* 2011;27:441–464.

75. Xiao H, Wang J, Yan W, et al. GLUT1 regulates cell glycolysis and proliferation in prostate cancer. *Prostate*. 2018;78(2):86–94.

76. Jiao L, Wang S, Zheng Y, et al. Betulinic acid suppresses breast cancer aerobic glycolysis via caveolin-1/NF-κB/c-Myc pathway. *Biochem. Pharmacol.* 2019;161:149–162.

77. Chen WL, Wang JH, Zhao AH, et al. A distinct glucose metabolism signature of acute myeloid leukemia with prognostic value. *Blood*. 2014;124(10):1645–1654.

78. Lapa B, Gonçalves AC, Jorge J, et al. Acute myeloid leukemia sensitivity to metabolic inhibitors: glycolysis showed to be a better therapeutic target. *Med. Oncol.* 2020;37(8):1–13.

79. Dai S, Peng Y, Zhu Y, et al. Glycolysis promotes the progression of pancreatic cancer and reduces cancer cell sensitivity to gemcitabine. *Biomed. Pharmacother.* 2020;121:109521.

80. Abdel-Wahab AF, Mahmoud W, Al-Harizy RM. Targeting glucose metabolism to suppress cancer progression: prospective of anti-glycolytic cancer therapy. *Pharmacol. Res.* 2019;150:104511.

81. Lu SC. Glutathione synthesis. *Biochim. Biophys. Acta - Gen. Subj.* 2013;1830(5):3143–3153.

82. Marí M, Morales A, Colell A, García-Ruiz C, Fernández-Checa JC. Mitochondrial glutathione, a key survival antioxidant. *Antioxidants Redox Signal.* 2009;11(11):2685–2700.

83. Forrester SJ, Kikuchi DS, Hernandes MS, Xu Q, Griendling KK. Reactive Oxygen Species in Metabolic and Inflammatory Signaling. *Circ. Res.* 2018;122(6):877–902.

84. Venditti P, Di Stefano L, Di Meo S. Mitochondrial metabolism of reactive oxygen species. *Mitochondrion*. 2013;13(2):71–82.

85. Gregory MA, Nemkov T, Park HJ, et al. Targeting glutamine metabolism and redox state for leukemia therapy. *Clin. Cancer Res.* 2019;25(13):4079–4090.

86. Jacque N, Ronchetti AM, Larrue C, et al. Targeting glutaminolysis has antileukemic activity in acute myeloid leukemia and synergizes with BCL-2 inhibition. *Blood*. 2015;126(11):1346–1356.

87. Hassanein M, Hoeksema MD, Shiota M, et al. SLC1A5 mediates glutamine transport required for lung cancer cell growth and survival. *Clin. Cancer Res.* 2013;19(3):560–570.

88. Hassanein M, Qian J, Hoeksema MD, et al. Targeting SLC1a5-mediated glutamine dependence in non-small cell lung cancer. *Int. J. Cancer*. 2015;137(7):1587–1597.

89. Wang Q, Beaumont KA, Otte NJ, et al. Targeting glutamine transport to suppress melanoma cell growth. *Int. J. Cancer*. 2014;135(5):1060–1071.

90. Shiratori R, Furuichi K, Yamaguchi M, et al. Glycolytic suppression dramatically changes the intracellular metabolic profile of multiple cancer cell lines in a mitochondrial metabolism-dependent manner. *Sci. Rep.* 2019;9(1):18699.

91. Martínez-Reyes I, Chandel NS. Mitochondrial TCA cycle metabolites control physiology and disease. *Nat. Commun.* 2020;11(102):.

92. Acin-Perez R, Enriquez JA. The function of the respiratory supercomplexes: The plasticity model. *Biochim. Biophys. Acta - Bioenerg.* 2014;1837(4):444–450.

93. Gonzalez Herrera KN, Lee J, Haigis MC. Intersections between mitochondrial sirtuin signaling and tumor cell metabolism. *Crit. Rev. Biochem. Mol. Biol.* 2015;50(3):242–255.

94. Kuntz EM, Baquero P, Michie AM, et al. Targeting mitochondrial oxidative phosphorylation eradicates therapy-resistant chronic myeloid leukemia stem cells. *Nat. Med.* 2017;23(10):1234–1240.

95. Lee K min, Giltnane JM, Balko JM, et al. MYC and MCL1 Cooperatively Promote Chemotherapy-Resistant Breast Cancer Stem Cells via Regulation of Mitochondrial Oxidative Phosphorylation. *Cell Metab.* 2017;26(4):633-647.e7.

96. Farge T, Saland E, de Toni F, et al. Chemotherapy resistant human acute myeloid leukemia cells are not enriched for leukemic stem cells but require oxidative metabolism. *Cancer Discov.* 2017;7(7):716–735.

97. Vazquez F, Lim JH, Chim H, et al. PGC1α Expression Defines a Subset of Human Melanoma Tumors with Increased Mitochondrial Capacity and Resistance to Oxidative Stress. *Cancer Cell*. 2013;23(3):287–301.

98. Sajnani K, Islam F, Smith RA, Gopalan V, Lam AKY. Genetic alterations in Krebs cycle and its impact on cancer pathogenesis. *Biochimie*. 2017;135:164–172.

99. Chen L, Liu T, Zhou J, et al. Citrate synthase expression affects tumor phenotype and drug resistance in human ovarian carcinoma. *PLoS One*. 2014;9(12):1–19.

100. Figueroa ME, Abdel-Wahab O, Lu C, et al. Leukemic IDH1 and IDH2 Mutations Result in a Hypermethylation Phenotype, Disrupt TET2 Function, and Impair Hematopoietic

Differentiation. *Cancer Cell*. 2010;18(6):553–567.

101. Dalla Pozza E, Dando I, Pacchiana R, et al. Regulation of succinate dehydrogenase and role of succinate in cancer. *Semin. Cell Dev. Biol.* 2020;98(March):4–14.

102. Lehtonen HJ, Kiuru M, Ylisaukko-oja SK, et al. Increased risk of cancer in patients with fumarate hydratase germline mutation. *J. Med. Genet.* 2006;43(6):523 LP – 526.

103. Hardie DG, Ross FA, Hawley SA. AMPK: A nutrient and energy sensor that maintains energy homeostasis. *Nat. Rev. Mol. Cell Biol.* 2012;13(4):251–262.

104. Galluzzi L, Pietrocola F, Levine B, Kroemer G. Metabolic control of Autophagy. *Cell*. 2014;159(6):1263–1276.

105. Guo JY, Karsli-Uzunbas G, Mathew R, et al. Autophagy suppresses progression of K-ras-induced lung tumors to oncocytomas and maintains lipid homeostasis. *Genes Dev.* 2013;27(13):1447–1461.

106. Guo JY, White E. Autophagy is required for mitochondrial function, lipid metabolism, growth, and fate of KRASG12D-driven lung tumors. *Autophagy*. 2013;9(10):1636–1638.

107. Bhatt V, Khayati K, Hu ZS, et al. Autophagy modulates lipid metabolism to maintain metabolic flexibility for Lkb1-deficient kras-driven lung tumorigenesis. *Genes Dev.* 2019;33(3–4):150–165.

108. Kawaguchi M, Aoki S, Hirao T, Morita M, Ito K. Autophagy is an important metabolic pathway to determine leukemia cell survival following suppression of the glycolytic pathway. *Biochem. Biophys. Res. Commun.* 2016;474(1):188–192.

109. Ye M, Wang S, Wan T, et al. Combined inhibitions of glycolysis and AKT/autophagy can overcome resistance to EGFR-targeted therapy of lung cancer. *J. Cancer*. 2017;8(18):3774–3784.

110. Zhao YG, Zhang H. Core autophagy genes and human diseases. *Curr. Opin. Cell Biol.* 2019;61:117–125.

111. Fang D, Xie H, Hu T, Shan H, Li M. Binding Features and Functions of ATG3. *Front. Cell Dev. Biol.* 2021;9(June):1–12.

112. Tanida I, Tanida-Miyake E, Komatsu M, Ueno T, Kominami E. Human Apg3p/Aut1p homologue is an authentic E2 enzyme for multiple substrates, GATE-16, GABARAP, and MAP-LC3, and facilitates the conjugation of hApg12p to hApg5p. *J. Biol. Chem.* 2002;277(16):13739–13744.

113. Wang S, Li Y, Ma C. Atg3 promotes Atg8 lipidation via altering lipid diffusion and rearrangement. *Protein Sci.* 2020;29(6):1511–1523.

114. Zheng Y, Qiu Y, Grace CRR, et al. A switch element in the autophagy E2 Atg3 mediates allosteric regulation across the lipidation cascade. *Nat. Commun.* 2019;10(1):3600.

115. Yamada Y, Suzuki NN, Hanada T, et al. The crystal structure of Atg3, an autophagy-related ubiquitin carrier protein (E2) enzyme that mediates Atg8 lipidation. *J. Biol. Chem.* 2007;282(11):8036–8043.

116. Ohashi K, Otomo T. Identification and characterization of the linear region of ATG3 that interacts with ATG7 in higher eukaryotes. *Biochem. Biophys. Res. Commun.* 2015;463(3):447–452.

117. Metlagel Z, Otomo C, Takaesu G, Otomo T. Structural basis of ATG3 recognition by the autophagic ubiquitin-like protein ATG12. *Proc. Natl. Acad. Sci. U. S. A.* 2013;110(47):18844–18849.

118. Sou Y, Satoshi W, Jun-ichi I, et al. The Atg8 Conjugation System Is Indispensable for

Proper Development of Autophagic Isolation Membranes in Mice. *Mol. Biol. Cell*. 2008;19(4762–4775):4762–4775.

119. Altman BJ, Jacobs SR, Mason EF, et al. Autophagy is essential to suppress cell stress and to allow BCR-Abl-mediated leukemogenesis. *Oncogene*. 2011;30(16):1855–1867.
120. Wang T, Yu N, Qian M, et al. ERK-mediated autophagy promotes inactivated Sendai virus (HVJ-E)-induced apoptosis in HeLa cells in an Atg3-dependent manner. *Cancer Cell Int.* 2018;18(1):1–13.
121. Hua L, Zhu G, Wei J. MicroRNA-1 overexpression increases chemosensitivity of non-small cell lung cancer cells by inhibiting autophagy related 3-mediated autophagy. *Cell Biol. Int.* 2018;42(9):1240–1249.
122. Huang W, Zeng C, Hu S, Wang L, Liu J. ATG3, a target of miR-431-5p, promotes proliferation and invasion of colon cancer via promoting autophagy. *Cancer Manag. Res.* 2019;11:10275–10285.
123. Li X, Zhou Y, Yang L, et al. LncRNA NEAT1 promotes autophagy via regulating miR-204/ATG3 and enhanced cell resistance to sorafenib in hepatocellular carcinoma. *J. Cell. Physiol.* 2020;235(4):3402–3413.
124. Cao Q, Liu F, Yang Z, et al. Prognostic value of autophagy related proteins ULK1, Beclin 1, ATG3, ATG5, ATG7, ATG9, ATG10, ATG12, LC3B and p62/SQSTM1 in gastric cancer. *Am. J. Transl. Res.* 2016;8(9):3831–3847.
125. Wang L, Song J, Zhang J, et al. Lentiviral vector-mediate ATG3 overexpression inhibits growth and promotes apoptosis of human SKM-1 cells. *Mol. Biol. Rep.* 2014;41(4):2093–2099.
126. Galluzzi L, Green DR. Autophagy-Independent Functions of the Autophagy Machinery. *Cell*. 2019;177(7):1682–1699.
127. Ma K, Fu W, Tang M, et al. PTK2-mediated degradation of ATG3 impedes cancer cells susceptible to DNA damage treatment. *Autophagy*. 2017;13(3):579–591.
128. O'Sullivan TE, Geary CD, Weizman O El, et al. Atg5 Is Essential for the Development and Survival of Innate Lymphocytes. *Cell Rep.* 2016;15(9):1910–1919.
129. Martinez J, Malireddi RKS, Lu Q, et al. Molecular characterization of LC3-associated phagocytosis reveals distinct roles for Rubicon, NOX2 and autophagy proteins. *Nat. Cell Biol.* 2015;17(7):893–906.
130. Murrow L, Malhotra R, Debnath J. ATG12-ATG3 interacts with Alix to promote basal autophagic flux and late endosome function. *Nat. Cell Biol.* 2015;17(3):300–310.
131. Ludwig C, Günther UL. MetaboLab - advanced NMR data processing and analysis for metabolomics. *BMC Bioinformatics*. 2011;12:.
132. Alshamleh I, Krause N, Richter C, et al. Real-Time NMR Spectroscopy for Studying Metabolism. *Angew. Chemie - Int. Ed.* 2020;59(6):2304–2308.
133. Diehl V, Wegner M, Grumati P, et al. Minimized combinatorial CRISPR screens identify genetic interactions in autophagy. *Nucleic Acids Res.* 2021;49(10):5684–5704.
134. Choi A, Jang I, Han H, et al. iCSDB: An integrated database of CRISPR screens. *Nucleic Acids Res.* 2021;49(D1):D956–D961.
135. Li Q V., Dixon G, Verma N, et al. Genome-scale screens identify JNK–JUN signaling as a barrier for pluripotency exit and endoderm differentiation. *Nat. Genet.* 2019;51(6):999–1010.
136. Ishibashi K, Fujita N, Kanno E, et al. Atg16L2, a novel isoform of mammalian Atg16L that is not essential for canonical autophagy despite forming an Atg12-5-16L2 complex. *Autophagy*. 2011;7(12):1500–1513.

137. Khor B, Conway KL, Omar AS, et al. Distinct Tissue-Specific Roles for the Disease-Associated Autophagy Genes ATG16L2 and ATG16L1. *J. Immunol.* 2019;203(7):1820–1829.

138. Kaizuka T, Morishita H, Hama Y, et al. An Autophagic Flux Probe that Releases an Internal Control. *Mol. Cell*. 2016;64(4):835–849.

139. Zhang XH, Tee LY, Wang XG, Huang QS, Yang SH. Off-target effects in CRISPR/Cas9-mediated genome engineering. *Mol. Ther. - Nucleic Acids*. 2015;4(11):e264.

140. Moreno I, Martín G, Bolufer P, et al. Incidence and prognostic value of FLT3 internal tandem duplication and D835 mutations in acute myeloid leukemia. *Haematologica*. 2003;88(1):19–24.

141. Cao T, Jiang N, Liao H, et al. The FLT3-ITD mutation and the expression of its downstream signaling intermediates STAT5 and Pim-1 are positively correlated with CXCR4 expression in patients with acute myeloid leukemia. *Sci. Rep.* 2019;9(1):1–10.

142. Reiter K, Polzer H, Krupka C, et al. Tyrosine kinase inhibition increases the cell surface localization of FLT3-ITD and enhances FLT3-directed immunotherapy of acute myeloid leukemia. *Leukemia*. 2018;32(2):313–322.

143. Elmeliegy M, Haese J Den, Talati C, Wetzler M, Jusko WJ. Towards better combination regimens of cytarabine and FLT3 inhibitors in acute myeloid leukemia. *Cancer Chemother. Phramacology*. 2020;86(3):325–337.

144. Dutta S, Pregartner G, Rücker FG, et al. Functional classification of tp53 mutations in acute myeloid leukemia. *Cancers (Basel).* 2020;12(3):1–16.

145. Sugimoto K, Toyoshima H, Sakai R, et al. Frequent mutations in the p53 gene in human myeloid leukemia cell lines. *Blood*. 1992;79(9):2378–2383.

146. Weisberg E, Halilovic E, Cooke VG, et al. Inhibition of wild-type p53-expressing AML by the novel small molecule HDM2 inhibitor CGM097. *Mol. Cancer Ther.* 2015;14(10):2249–2259.

147. Martens S, Fracchiolla D. Activation and targeting of ATG8 protein lipidation. *Cell Discov.* 2020;6(23):.

148. Crane AM, Bhattacharya SK. The Use of Bromodeoxyuridine Incorporation Assays to Assess Corneal Stem Cell Proliferation. *Corneal Regen. Med. Methods Protoc.* 2013;65–70.

149. Vermeulen K, Berneman ZN, Van Bockstaele DR. Cell cycle and apoptosis. *Cell Prolif.* 2003;36(3):165–175.

150. Lakshmanan I, Batra SK. Protocol for Apoptosis Assay by Flow Cytometry Using Annexin V Staining Method. *Bio-protocol*. 2013;3(6):e374.

151. Nguyen TD, Shaid S, Vakhrusheva O, et al. Loss of the selective autophagy receptor p62 impairs murine myeloid leukemia progression and mitophagy. *Blood*. 2019;133(2):168–179.

152. Dykstra KM, Fay HRS, Massey AC, et al. Inhibiting autophagy targets human leukemic stem cells and hypoxic AML blasts by disrupting mitochondrial homeostasis. *Blood Adv.* 2021;5(8):2087–2100.

153. Pei S, Minhajuddin M, Adane B, et al. AMPK/FIS1-Mediated Mitophagy Is Required for Self-Renewal of Human AML Stem Cells. *Cell Stem Cell*. 2018;23(1):86–100.

154. Katayama H, Kogure T, Mizushima N, Yoshimori T, Miyawaki A. A sensitive and quantitative technique for detecting autophagic events based on lysosomal delivery. *Chem. Biol.* 2011;18(8):1042–1052.

155. Sivandzade F, Bhalerao A, Cucullo L. Analysis of the Mitochondrial Membrane Potential Using the Cationic JC-1 Dye as a Sensitive Fluorescent Probe. *Bio-protocol*. 2019;9(1):e3128.

156. Puleston D. Detection of Mitochondrial Mass, Damage, and Reactive Oxygen Species by Flow Cytometry. *Cold Spring Harb. Protoc.* 2015;9:pdb.prot086298.

157. Zong S, Wu M, Gu J, et al. Structure of the intact 14-subunit human cytochrome c oxidase. *Cell Res.* 2018;28(10):1026–1034.

158. Zhao RZ, Jiang S, Zhang L, Yu Z Bin. Mitochondrial electron transport chain, ROS generation and uncoupling (Review). *Int. J. Mol. Med.* 2019;44(1):3–15.

159. Clemente M, Polat IH, Albert J, et al. Platinacycles Containing a Primary Amine Platinum(II) Compounds for Treating Cisplatin-Resistant Cancers by Oxidant Therapy. *Organometallics*. 2018;37(20):3502–3514.

160. Balaiya S, Chalam K V. An In vitro Assay to Quantify Nitrosative Component of Oxidative Stress. *J. Mol. Genet. Med.* 2014;8(3):120.

161. Kauffman ME, Kauffman MK, Traore K, et al. MitoSOX-Based Flow Cytometry for Detecting Mitochondrial ROS. *React. Oxyg. species (Apex, N.C.)*. 2016;2(5):361–370.

162. Riss T, Moravec R, Niles A, et al. Cell Viability Assays. Bethesda (MD): Eli Lilly & Company and the National Center for Advancing Translational Sciences; 2016.

163. Plitzko B, Loesgen S. Measurement of Oxygen Consumption Rate (OCR) and Extracellular Acidification Rate (ECAR) in Culture Cells for Assessment of the Energy Metabolism. *Bio-protocol*. 2018;8(10):e2850.

164. Spinelli JB, Haigis MC. The multifaceted contributions of mitochondria to cellular metabolism. *Nat. Cell Biol.* 2018;20(7):745–754.

165. Dasgupta A, Shukla SK, Gunda V, King RJ, Singh PK. Evaluating the metabolic alterations in pancreatic cancer. *Pancreat. Cancer. Methods Mol. Biol.* 2019;1882:221–228.

166. Selivanov VA, Benito A, Miranda A, et al. MIDcor, an R-program for deciphering mass interferences in mass spectra of metabolites enriched in stable isotopes. *BMC Bioinformatics*. 2017;18(1):88.

167. Katzir R, Polat IH, Harel M, et al. The landscape of tiered regulation of breast cancer cell metabolism. *Sci. Rep.* 2019;9(1):17760.

168. de la Cruz-López KG, Castro-Muñoz LJ, Reyes-Hernández DO, García-Carrancá A, Manzo-Merino J. Lactate in the Regulation of Tumor Microenvironment and Therapeutic Approaches. *Front. Oncol.* 2019;9:1143.

169. Zhang J, Zhang Q. Using Seahorse Machine to Measure OCR and ECAR in Cancer Cells. *Cancer Metab. Methods Mol. Biol.* 2019;353–363.

170. Bhingarkar A, Vangapandu H V., Rathod S, Hoshitsuki K, Fernandez CA. Amino Acid Metabolic Vulnerabilities in Acute and Chronic Myeloid Leukemias. *Front. Oncol.* 2021;11:694526.

171. Xiao D, Zeng L, Yao K, et al. The glutamine-alpha-ketoglutarate (AKG) metabolism and its nutritional implications. *Amino Acids*. 2016;48(9):2067–2080.

172. Dioguardi FS. To give or not to give? Lessons from the arginine paradox. *J. Nutrigenet. Nutrigenomics*. 2011;4:90–98.

173. Evangelisti C, Evangelisti C, Chiarini F, et al. Autophagy in acute leukemias: A double-edged sword with important therapeutic implications. *Biochim. Biophys. Acta - Mol. Cell Res.* 2015;1853(1):14–26.

174. Tzelepis K, Koike-Yusa H, De Braekeleer E, et al. A CRISPR Dropout Screen

Identifies Genetic Vulnerabilities and Therapeutic Targets in Acute Myeloid Leukemia. *Cell Rep.* 2016;17(4):1193–1205.

175. Dai M, Yan G, Wang N, et al. In vivo genome-wide CRISPR screen reveals breast cancer vulnerabilities and synergistic mTOR/Hippo targeted combination therapy. *Nat. Commun.* 2021;12(1):.
176. Jung HR, Oh Y, Na D, et al. CRISPR screens identify a novel combination treatment targeting BCL-XL and WNT signaling for KRAS/BRAF-mutated colorectal cancers. *Oncogene*. 2021;40(18):3287–3302.
177. Morita K, Hama Y, Izume T, et al. Genome-wide CRISPR screen identifies TMEM41B as a gene required for autophagosome formation. *J. Cell Biol.* 2018;217(11):3817–3828.
178. Chang TK, Shravage B V., Hayes SD, et al. Uba1 functions in Atg7- and Atg3-independent autophagy. *Nat. Cell Biol.* 2013;15(9):1067–1078.
179. Nishida Y, Arakawa S, Fujitani K, et al. Discovery of Atg5/Atg7-independent alternative macroautophagy. *Nature*. 2009;461(7264):654–658.
180. Radoshevich L, Murrow L, Chen N, et al. ATG12 conjugation to ATG3 regulates mitochondrial homeostasis and cell death. *Cell*. 2010;142(4):590–600.
181. Liu K, Zhao Q, Liu P, et al. ATG3-dependent autophagy mediates mitochondrial homeostasis in pluripotency acquirement and maintenance. *Autophagy*. 2016;12(11):2000–2008.
182. Besteiro S, Brooks CF, Striepen B, Dubremetz JF. Autophagy protein Atg3 is essential for maintaining mitochondrial integrity and for normal intracellular development of toxoplasma gondii tachyzoites. *PLoS Pathog.* 2011;7(12):e1002416.
183. Strohecker AM, Guo JY, Karsli-Uzunbas G, et al. Autophagy Sustains Mitochondrial Glutamine Metabolism and Growth of BRAFV600E–Driven Lung Tumors. *Cancer Discov.* 2013;3(11):1272–1285.
184. Hirota Y, Yamashita S ichi, Kurihara Y, et al. Mitophagy is primarily due to alternative autophagy and requires the MAPK1 and MAPK14 signaling pathways. *Autophagy*. 2015;11(2):332–343.
185. García-Heredia JM, Carnero A. Role of Mitochondria in Cancer Stem Cell Resistance. *Cells*. 2020;9(7):1693.
186. Karvela M, Baquero P, Kuntz EM, et al. ATG7 regulates energy metabolism, differentiation and survival of Philadelphia-chromosome-positive cells. *Autophagy*. 2016;12(6):936–948.
187. Sundqvist M, Christenson K, Björnsdottir H, et al. Elevated mitochondrial reactive oxygen species and cellular redox imbalance in human NADPH-oxidase-deficient phagocytes. *Front. Immunol.* 2017;8(DEC):1–11.
188. Pizzorno J. Glutatione! *Integr. Med.* 2014;13(1):8–12.
189. Kennedy L, Sandhu JK, Harper ME, Cuperlovic-culf M. Role of glutathione in cancer: From mechanisms to therapies. *Biomolecules*. 2020;10(10):1429.
190. Pei S, Minhajuddin M, Callahan KP, et al. Targeting aberrant glutathione metabolism to eradicate human acute myelogenous leukemia cells. *J. Biol. Chem.* 2013;288(47):33542–33558.
191. Chen L, Zhang Z, Hoshino A, et al. NADPH production by the oxidative pentose-phosphate pathway supports folate metabolism. *Nat. Metab.* 2019;1(3):404–415.
192. Vanzo R, Bartkova J, Merchut-Maya JM, et al. Autophagy role(s) in response to oncogenes and DNA replication stress. *Cell Death Differ.* 2019;27(3):1134–1153.

193. Škrtić M, Sriskanthadevan S, Jhas B, et al. Inhibition of Mitochondrial Translation as a Therapeutic Strategy for Human Acute Myeloid Leukemia. *Cancer Cell*. 2011;20(5):674–688.

194. Zorova LD, Popkov VA, Plotnikov EY, et al. Mitochondrial membrane potential. *Anal. Biochem.* 2018;552:50–59.

195. Rieger B, Arroum T, Borowski M, Villalta J, Busch KB. Mitochondrial F1 FO ATP synthase determines the local proton motive force at cristae rims. *EMBO Rep.* 2021;e52727:.

196. Kahancová A, Sklenář F, Ježek P, Dlasková A. Overexpression of native IF1 downregulates glucose-stimulated insulin secretion by pancreatic INS-1E cells. *Sci. Rep.* 2020;10(1):1551.

197. Vyssokikh MY, Holtze S, Averina OA, et al. Mild depolarization of the inner mitochondrial membrane is a crucial component of an anti-aging program. *Proc. Natl. Acad. Sci. U. S. A.* 2020;117(12):6491–6501.

198. Maruyama D, Hirata N, Miyashita R, Kawaguchi R, Yamakage M. Substrate-dependent modulation of oxidative phosphorylation in isolated mitochondria following in vitro hypoxia and reoxygenation injury. *Exp. Clin. Cardiol.* 2013;18(2):158–160.

199. Leverve XM, Fontaine E. Role of substrates in the regulation of mitochondrial function in situ. *IUBMB Life*. 2001;52(3–5):221–229.

200. Jia D, Lu M, Jung KH, et al. Elucidating cancer metabolic plasticity by coupling gene regulation with metabolic pathways. *Proc. Natl. Acad. Sci. U. S. A.* 2019;116(9):3909–3918.

201. Liberti M V, Locasale JW. The Warburg Effect: How Does it Benefit Cancer Cells? *Trends Biochem. Sci.* 2016;41(3):211–218.

202. Saulle E, Spinello I, Quaranta MT, et al. Targeting Lactate Metabolism by Inhibiting MCT1 or MCT4 Impairs Leukemic Cell Proliferation, Induces Two Different Related Death-Pathways and Increases Chemotherapeutic Sensitivity of Acute Myeloid Leukemia Cells. *Front. Oncol.* 2021;10(February):1–16.

203. Man C-H, Scadden DT, Mercier F, et al. Epigenetic Activation of the pH Regulator MCT4 in Acute Myeloid Leukemia Exploits a Fundamental Metabolic Process of Enhancing Cell Growth through Proton Shifting. *Blood*. 2019;134(Supplement_1):3765.

204. Chen YJ, Mahieu NG, Huang X, et al. Lactate metabolism is associated with mammalian mitochondria. *Nat. Chem. Biol.* 2016;12(11):937–943.

205. Yoo HC, Yu YC, Sung Y, Han JM. Glutamine reliance in cell metabolism. *Exp. Mol. Med.* 2020;52(9):1496–1516.

206. Zhang J, Pavlova NN, Thompson CB. Cancer cell metabolism: the essential role of the nonessential amino acid, glutamine. *EMBO J.* 2017;36(10):1302–1315.

207. Broeks MH, van Karnebeek CDM, Wanders RJA, Jans JJM, Verhoeven-Duif NM. Inborn disorders of the malate aspartate shuttle. *J. Inherit. Metab. Dis.* 2021;44(4):792–808.

208. Lopez-Alarcon L, Eboli ML. Oxidation of Reduced Cytosolic Nicotinamide Adenine Dinucleotide by The Malate-Aspartate shuttle in the K-562 Human Leukemia Cell Line. *Cancer Res.* 1986;46:5589–5591.

209. Altinok O, Poggio JL, Stein DE, et al. Malate–aspartate shuttle promotes L-lactate oxidation in mitochondria. *J. Cell. Physiol.* 2019;1–13.

210. Kenzelmann Broz D, Mello SS, Bieging KT, et al. Global genomic profiling reveals an extensive p53-regulated autophagy program contributing to key p53 responses.

Genes Dev. 2013;27(9):1016–1031.

211. Yang Y, Karsli-Uzunbas G, Poillet-Perez L, et al. Autophagy promotes mammalian survival by suppressing oxidative stress and p53. *Genes Dev.* 2020;34(9–10):688–700.
212. Gomes AS, Ramos H, Soares J, Saraiva L. P53 and Glucose Metabolism: an Orchestra To Be Directed in Cancer Therapy. *Pharmacol. Res.* 2018;131:75–86.
213. Sriskanthadevan S, Jeyaraju D V., Chung TE, et al. AML cells have low spare reserve capacity in their respiratory chain that renders them susceptible to oxidative metabolic stress. *Blood*. 2015;125(13):2120–2130.
214. Panina SB, Baran N, Brasil da Costa FH, Konopleva M, Kirienko N V. A mechanism for increased sensitivity of acute myeloid leukemia to mitotoxic drugs. *Cell Death Dis.* 2019;10(8):617.
215. Suganuma K, Miwa H, Imai N, et al. Energy metabolism of leukemia cells: Glycolysis versus oxidative phosphorylation. *Leuk. Lymphoma*. 2010;51(11):2112–2119.
216. Dong L, Neuzil J. Targeting mitochondria as an anticancer strategy. *Cancer Commun.* 2019;39(1):63.
217. Molina JR, Sun Y, Protopopova M, et al. An inhibitor of oxidative phosphorylation exploits cancer vulnerability. *Nat. Med.* 2018;24(7):1036–1046.
218. Panina SB, Pei J, Kirienko N V. Mitochondrial metabolism as a target for acute myeloid leukemia treatment. *Cancer Metab.* 2021;9(17):.
219. Bhattacharya S, Piya S, McQueen T, et al. Inhibition of Unc-51 like Autophagy Activating Kinase 1 (ULK1) Is Highly Synergistic with Chemotherapy and Bcl2 Inhibition in Acute Myeloid Leukemia (AML). *Blood*. 2017;130(Supplement 1):1248.
220. Su H, Yang F, Fu R, et al. Cancer cells escape autophagy inhibition via NRF2-induced macropinocytosis. *Cancer Cell*. 2021;39:1–16.
221. Recouvreux MV, Commisso C. Macropinocytosis: A metabolic adaptation to nutrient stress in cancer. *Front. Endocrinol. (Lausanne).* 2017;8:261.
222. Man C-H, Scadden DT, Mercier F, et al. Epigenetic Activation of the pH Regulator MCT4 in Acute Myeloid Leukemia Exploits a Fundamental Metabolic Process of Enhancing Cell Growth through Proton Shifting. *Blood*. 2019;134(Supplement_1):3765–3765.

9. Appendix

9.1. Figures

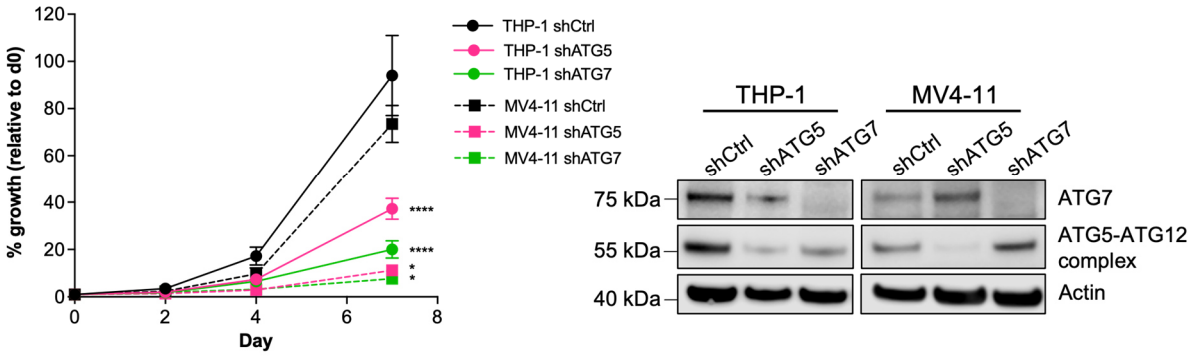

Figure 32. Metabolic alterations in AML cells upon ATG3 depletion using [U-$^{13}C_6$]-glucose. Growth analysis of shRNA-mediated depletion of ATG5 and ATG7 for 7 days. 1x10^5 cells were seeded in a 96 well plate and cell number was determined microscopically using trypan blue exclusion on the indicated days. Medium was changed after every counting. Western blot image shows depletion of ATG5 and ATG7 at day 7 of growth analysis. Student's t-test was performed. Error bars represent SEM. *p < 0.05, ****p < 0.0001.

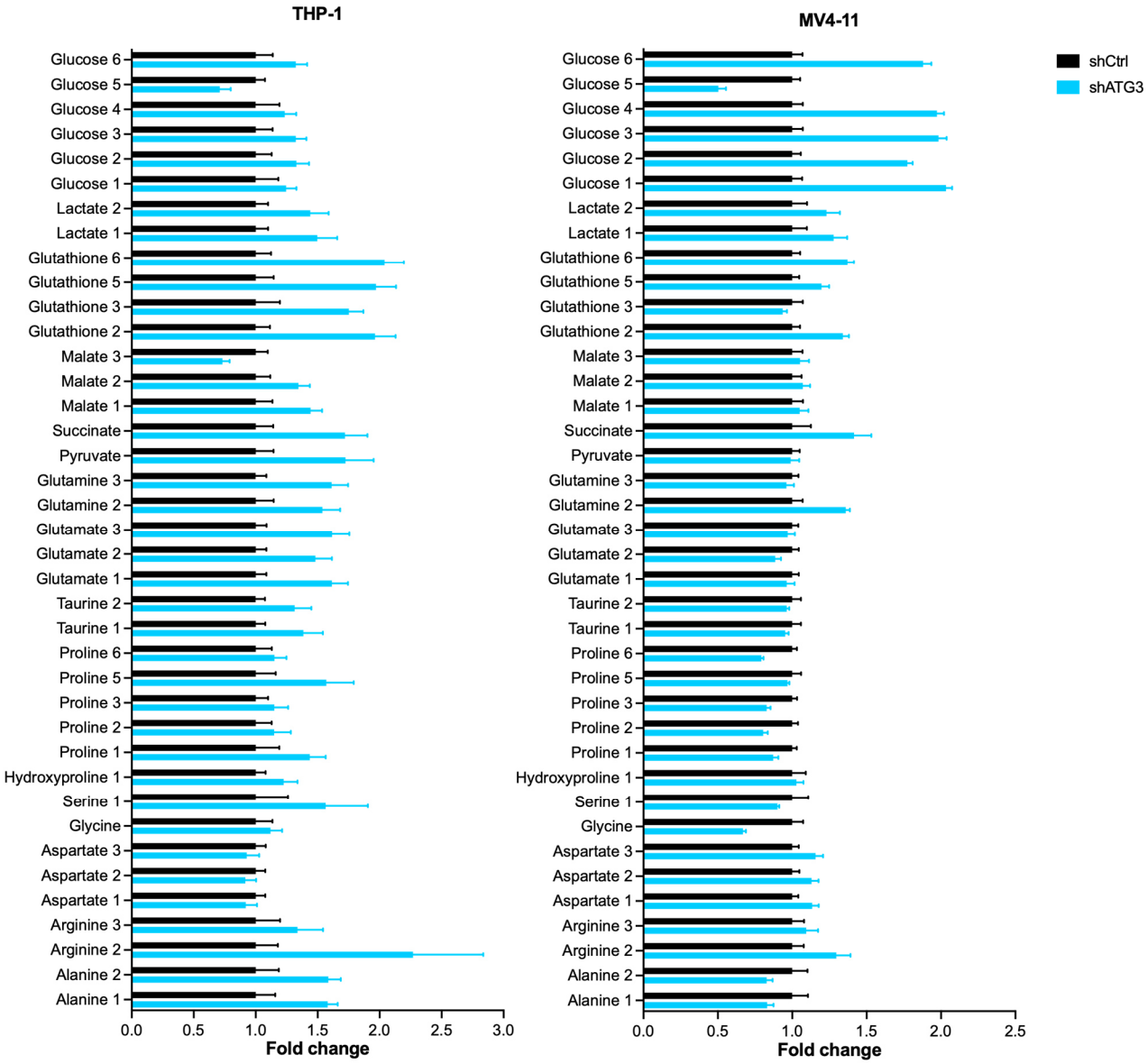

Figure 33. Metabolic alterations in AML cells upon ATG3 depletion using [U-$^{13}C_6$]-glucose. Fold change of the indicated metabolites normalized to control cells and analyzed by U-$^{13}C_6$]-glucose tracer-based NMR. Error bars represent SEM.

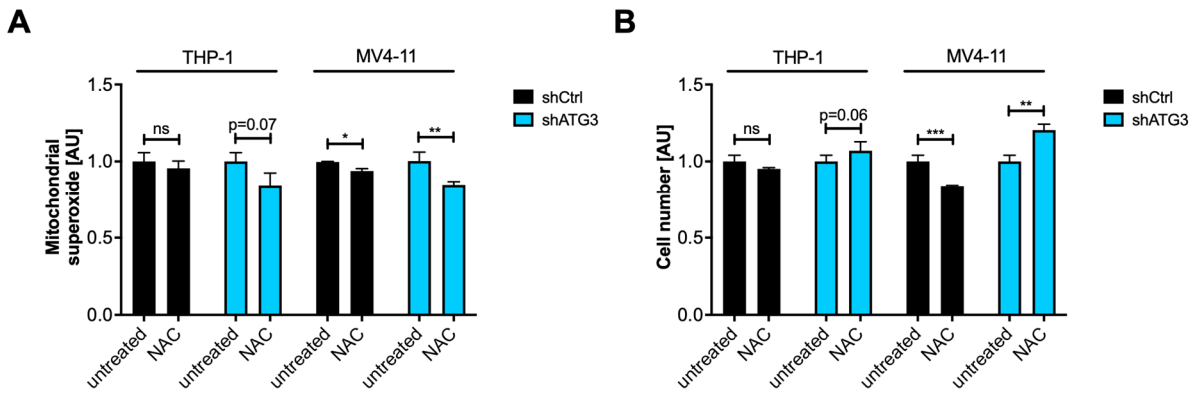

Figure 34. Cell survival of ATG3-depleted AML cells upon NAC treatment. Cells were treated with 5 mM NAC for 24 hours. (A) Mitochondrial superoxide was determined by MitoSOX™ staining and flow cytometry and normalized to untreated conditions. (B) Cell number was determined using trypan blue exclusion and normalized to untreated conditions. Student's t-test was performed. Error bars represent SEM. ns, not significant, *p < 0.05, **p < 0.01, ***p < 0.001.

9.2. Tables

Gene	THP-1	MV4-11
AMBRA1	-0,21631	-0,26313
ARF6	-0,86046	-0,42287
ATF4	-0,43119	-0,96271
ATG12	-0,27027	-0,74769
ATG16L2	-0,24731	-0,32446
ATG3	-0,22859	-0,35269
ATG9A	-0,58688	-0,56421
CUL3	-1,1211	-0,65467
CUL4A	-0,22789	-0,48651
DDB1	-1,3566	-0,90619
HSP90AB1	-0,31328	-0,46716
PEX13	-0,51176	-0,26722
RAB24	-0,26089	-0,41817
RAB7A	-0,27252	-0,37598
RHEB	-1,0812	-0,88027
SEC22B	-0,55519	-0,40238
SNAPIN	-0,38198	-0,29873
SPNS1	-0,235	-0,34462
STUB1	-1,236	-0,44057
USP15	-0,25182	-0,3026
USP8	-0,44653	-0,70789
WAC	-0,71382	-0,25579
ZFYVE1	-0,35312	-0,31107

Table 7. Log_2 fold change of the common dropout hits from CRISPR/Cas9 screening with a threshold of log_2 fold change ≤ -0.2.

Gene	THP-1	MV4-11
AMBRA1	2,1060	3,7346
ARF6	5,3028	2,7882
ATF4	5,3028	5,3028
ATG12	2,4330	5,3028
ATG16L2	2,4318	2,7151
ATG3	2,1060	2,7173
ATG9A	5,3028	5,3028
CUL3	5,3028	5,3028
CUL4A	5,3028	2,4135
DDB1	5,3028	4,8256
HSP90AB1	2,9467	5,3028
PEX13	3,7117	2,5371
RAB24	2,4318	4,0723
RAB7A	5,3028	3,7346
RHEB	5,3028	5,3028
SEC22B	5,3028	2,1740
SNAPIN	4,4577	3,2129
SPNS1	3,7117	2,7909
STUB1	5,3028	2,9544
USP15	2,9467	2,3647
USP8	3,7117	4,0723
WAC	4,8256	2,1740
ZFYVE1	4,4577	2,4123

Table 8. -$\log_{10}$ p-value of the significant common dropout hits from the CRISPR/Cas9 screening (-$\log_{10}$ p-value ≥ 2).

Core autophagy genes	Protein ubiquitination enzymes	GTPases	Autophagy regulators	Ubiquitin-specific proteases	Transcription factors	Autophagy receptors	Other
ATG3	CUL3	ARF6	AMBRA1	USP15	ATF4	-	SPNS1
ATG9A	CUL4A	RAB7A	PEX13	USP8			SNAPIN
ATG12	DDB1	RAB24	WAC				ZFYVE1
ATG16L2	STUB1	RHEB					SEC22B
							HSP90AB1

Table 9. Assignment of dropout hits from the CRISPR/Cas9 screen to the autophagy function.

10. Abbreviations

2-DG	2-deoxy glucose
7AAD	7-Aminoactinomycin D
α-KG	α-ketoglutarate
AA	Amino acid
Ac-CoA	Acetyl Coenzyme A
Ala	Alanine
AML	Acute myeloid leukemia
AMP	Adenosine monophosphate
AMPK	AMP-activated protein kinase
Arg	Arginine
Asn	Asparagine
Asp	Aspartate
ATG	Autophagy-related genes
ATP	Adenosine triphosphate
BSA	Bovine serum albumin
BM	Bone marrow
Baf	Bafilomycin A1
BrdU	Bromodeoxyuridine
Cit	Citrate
CR	Complete remission
CCCP	Carbonyl cyanide m-cholorophenylhydrazone
CLP	Common lymphoid progenitor

CMP	Common myeloid progenitor
COXIV	Cytochrome C oxidase subunit IV
CQ	Chloroquine
Cys	Cysteine
DFP	Deferiprone
ETC	Electron transport chain
ER	Endoplasmic reticulum
FBS	Fetal bovine serum
FCCP	Carbonyl cyanide-p-trifluoromethoxyphenylhydrazone
FR	Flexible region
Fum	Fumarate
G6P	Glucose-6-phosphate
GFP	Green fluorescent protein
GLS	Glutamine synthetase
GLUT	Glucose transporters
Gly	Glycine
GMP	Granulocyte macrophage progenitors
gRNAs	Guide RNAs
GSH	Glutathione
GTP	Guanosine triphosphate
H_2O_2	Hydrogen peroxide
HEK-293	Human embryonic kidney cell 293

His	Histidine
HR	Handle region
HRP	Horseradish peroxidase
HSC	Hematopoietic stem cell
IDH	Isocitrate dehydrogenase
Iso	Isoleucine
Lac	Lactate
LDH	Lactate dehydrogenase
Leu	Leucine
LIR	LC3-interacting region
LICs	Leukemia-initiating cells
LSC	Leukemic stem cell
Lys	Lysine
mTOR	Mammalian target of rapamycin
Mal	Malate
MEP	Megakaryocyte erythrocyte progenitor
Met	methionine
MPP	Multipotent progenitors
O_2•−	Superoxide radical
OAA	Oxaloacetate
OH•	Hydroxyl radical
OCR	Oxygen consumption rate
OXPHOS	Oxidative phosphorylation

PAS	Phagophore assembly site
PBS	Phosphate buffered saline
PBS-T	PBS and 0.1% Tween® 20
PEI	Polyethylenimine
Pen/Strep	Penicillin and streptomycin
Phe	Phenylalanine
Pro	Proline
Pyr	Pyruvate
R5P	Ribose-7-phosphate
ROS	Reactive oxygen species
RT	Room temperature
Ser	Serine
shATG3	shRNA against human ATG3
shCtrl	non targeting control shRNA
Succ	Succinate
Tau	Taurine
TCA	Tricarboxylic acid
Thr	Threonine
Trp	Tryptophane
Tyr	Tyrosine
Ub	Ubiquitin
Val	Valine

11. List of Figures

Figure 1. Schematic description of normal and malignant hematopoiesis. 2
Figure 2. Schematic description of autophagy. 5
Figure 3. Potential role of autophagy in malignant transformation and tumor progression. 6
Figure 4. Overview of main metabolic pathways involved in metabolic rewiring. 9
Figure 5. TCA cycle and OXPHOS are directly linked within mitochondria. 13
Figure 6. Function and structure of ATG3. 16
Figure 7. CRISPR/Cas9 dropout screen identifies certain autophagy genes that are important for leukemia cell proliferation. 34
Figure 8. CRISPR/Cas9 proliferation screen identifies 23 common dropout genes in AML cell lines. 37
Figure 9. CRISPR/Cas9 proliferation screen identifies core autophagy genes as dropout genes in two AML cell lines. 38
Figure 10. CRISPR/Cas9-mediated loss of the core autophagy genes ATG3, ATG9A, and ATG12 impairs AML cell growth. 39
Figure 11. Loss of the core autophagy genes ATG3, ATG9A, and ATG12 impairs autophagy. 40
Figure 12. Loss of ATG3 impairs proliferation and colony formation capacity of AML cells. 41
Figure 13. Loss of ATG3 impairs autophagy flux and LC3-lipidation. 42
Figure 14. Autophagosome formation is impaired upon loss of ATG3. 43
Figure 15. ATG3 depletion reduces S-phase in AML cells. 44
Figure 16. Loss of ATG3 induces apoptosis in leukemia cells. 45
Figure 17. Mitophagy is not altered in ATG3-depleted AML cells. 47
Figure 18. Mitochondrial membrane potential is not affected by loss of ATG3. 48
Figure 19. Mitochondrial mass is not altered upon ATG3 depletion. 49
Figure 20. Loss of ATG3, ATG5, and ATG7 increases cellular ROS and mitochondrial superoxide levels. 51
Figure 21. Loss of ATG3, ATG5, and ATG7 increases ATP levels per cell. 52
Figure 22. Oxidative phosphorylation is increased in ATG3-depleted AML cells. 53
Figure 23. Loss of ATG3 increases consumption of glucose and glutamine. 54
Figure 24. ATG3-depleted THP-1 and MV4-11 cells rewire their central carbon metabolism by activating their energy metabolism. 55
Figure 25. Autophagy is regulated by glycolysis. 56
Figure 26. Loss of ATG3 activates glycolysis. 57
Figure 27. Lactate is retained intracellularly in AML cells upon loss of ATG3. 59
Figure 28. Activation of TCA cycle and glutathione production in ATG3-depleted AML cells. 61

Figure 29. ^{13}C incorporation into different metabolites varies between AML cell lines upon loss of ATG3. 62
Figure 30. ATG3 depletion sensitizes leukemia cells to OXPHOS inhibition. 63
Figure 31. Metabolic rewiring in ATG3-deficient AML cells. 73
Figure 32. Metabolic alterations in AML cells upon ATG3 depletion using [U-$^{13}C_6$]-glucose. 95
Figure 33. Metabolic alterations in AML cells upon ATG3 depletion using [U-$^{13}C_6$]-glucose. 96
Figure 34. Cell survival of ATG3-depleted AML cells upon NAC treatment. 97

12. List of Tables

Table 1. List of reagents, cell culture media, and kits 21
Table 2. List of used antibodies for western blot 21
Table 3. List of used antibodies for immunofluorescence 22
Table 4. List of instruments, incubators, and microscopes 22
Table 5. MAGeCK count report of the CRISPR/Cas9 screen results in human AML cell lines. 33
Table 6. Significant dropout genes in THP-1 and MV4-11 cells from the focused CRISPR/Cas9 screen. 36
Table 7. Log_2 fold change of the common dropout hits from CRISPR/Cas9 screening with a threshold of log_2 fold change ≤ -0.2. 98
Table 8. $-log_{10}$ p-value of the significant common dropout hits from the CRISPR/Cas9 screening ($-log_{10}$ p-value ≥ 2). 99
Table 9. Assignment of dropout hits from the CRISPR/Cas9 screen to the autophagy function. 100

13. Publications and conferences

13.1. Publications

Fatima Baker, Ibrahim H. Polat, Khalil Abou-El-Ardat, Islam Alshamleh, Marlyn Thoelken, Daniel Hymon, Andrea Gubas, Sebastian E. Koschade, Jonas B. Vischedyk, Manuel Kaulich, Harald Schwalbe, Shabnam Shaid*, and Christian H. Brandts* (6 December 2021) '**Metabolic Rewiring Is Essential for AML Cell Survival to Overcome Autophagy Inhibition by Loss of ATG3**', Cancers 13(23):6142.

* Corresponding authors

Sebastian E. Koschade, Kevin Klann, Shabnam Shaid, Binje Vick, Jan A. Stratmann, Marlyn Thölken, Laura Meyer, The Duy Nguyen, Julia Campe, Laura M. Moser, Susanna Hock, **Fatima Baker**, Christian T. Meyer, Frank Wempe, Hubert Serve, Evelyn Ullrich, Irmela Jeremias; Christian Münch, and Christian H. Brandts (submitted Dec 2021) '**Translatome proteomics identifies autophagy as a resistance mechanism to on-target FLT3 inhibitors in acute myeloid leukemia**'.

The Duy Nguyen, Shabnam Shaid, Olesya Vakhrusheva, Sebastian E. Koschade, Kevin Klann, Marlyn Thölken, **Fatima Baker**, Jing Zhang, Thomas Oellerich, Duran Sürün, Anja Derlet, Isabella Haberbosch, Stefan Eimer, Heinz D. Osiewacz, Christian Behrends, Christian Münch, Ivan Dikic, and Christian H. Brandts (2019) '**Loss of the selective autophagy receptor p62 impairs murine myeloid leukemia progression and mitophagy'**, Blood 133(2): 168-179.

13.2. Conferences including talks and poster contributions

Frankfurt Cancer Conference (2021)
Frankfurt am Main, Germany

2nd Rhein-Main Cancer Retreat (2020)
Virtual Meeting

1st Rhein-Main Cancer Retreat (2019)
Königstein, Germany
Poster: Targeting autophagy to overcome cytarabine resistance in acute myeloid leukemia

Molecular Mechanisms in Signal Transduction and Cancer (2019)
EACR – FEBS Advanced Lecture Course
Spetses, Greece
Talk: The role of the selective autophagy receptors p62 and c-CBL in acute myeloid leukemia
Poster: The role of the selective autophagy receptors p62 and c-CBL in acute myeloid leukemia

9th UCT Science Day (2019)
Frankfurt am Main, Germany
Poster: Targeting autophagy to overcome cytarabine resistance in acute myeloid leukemia

Acute Myeloid Leukemia Retreat (2019)
Bad Kreuznach, Germany
Poster: Targeting autophagy to overcome cytarabine resistance in acute myeloid leukemia

SFB 1177 Retreat (2019)
Bad Kreuznach, Germany
Talk: Elucidating the role of c-CBL as an autophagy receptor in AML

Frankfurt Cancer Conference (2018)
Frankfurt am Main, Germany

4th Scientific Retreat, Partner Site Frankfurt/Mainz (2018)
Bad Homburg, Germany